# The University Of Sheffield.

**Modelling peak cooling demand and heat stress vulnerability of a city's dwelling stock in future climate: Seoul's high-rise apartment neighbourhoods 2014-2050s**

**By:**

Choo Yoon Yi

A thesis submitted in partial fulfilment of the requirements for the degree of
Doctor of Philosophy

The University of Sheffield
Faculty of Social Sciences
School of Architecture

July 2019

**ACKNOWLEDGMENTS**

All that I have done is only due to the people who are mentioned here. This PhD thesis would have not been accomplished without their guidance and assistance.

First and foremost, I feel deeply indebted to my supervisor, Dr. Chengzhi Peng for his continuous guidance, assistance and encouragement. Above all, he understood my personal circumstances and supported what he best can do in his place. Moreover, he gave me a way of thinking in all aspects of research as well as life. As an international student here, I feel he is always my family.

I would like to express my special thanks to all of my PhD colleagues on the 9th floor of the ArtsTower in the University of Sheffield. They were friends and supervisors who carefully listened my works. Especially, I am sincerely thankful to Jinvo and Jonathan for providing such a nice support as a friend. I am also grateful to my best friends, Kee-hoon, Sang-geun, Ja-young and Peter for providing special cheer-up.

Finally, I am grateful to my family, Seri, Jihyo and my little baby Chewon, who have provided me through emotional support in my life. During this PhD journey, they were the only place where I took a rest. Also, I would like to express a very special gratitude to my parents and parents-in-law. With a special mention to my mother because I owe it all to you.

**Abstract**

Cooling demand for indoor thermal comfort is expected to increase as hot days are increasing in temperature and becoming more frequent across the globe. As urban residential buildings and neighbourhoods are increasingly subject to such excessive heat events, urban dwelling can become vulnerable to heat stress if the cooling demand cannot be met for reasons such as power outages or summer fuel poverty. This thesis investigates how data-driven peak cooling energy demand modelling can be developed for assessing heat stress vulnerability (HSV) of a city's residential building (dwelling) stock in the future climate. The hypothesis is twofold: (1) that the predicted future indoor peak cooling demand (PCD, $kWh/m^2$) can serve as a heat stress vulnerability (HSV) indicator of a city's dwelling stock on the grounds that higher PCD demands will lead to higher HSV levels, (2) that potential HSV of the current stock composition can be assessed according to the predicted peak cooling loads required to restore the estimated indoor thermal conditions to acceptable thresholds. The purpose of subjecting a city's dwelling stock to the PCD-based HSV assessment is to identify segments of the dwelling stock with higher HSV levels that may require urgent actions of adaptation through renovation or replacement. The thesis presents a modelling framework and then applies it to Seoul's high-rise apartment stock using the multiple data sources available for 2014-2050 including Seoul's climate projections under RCP4.5 and RCP8.5. The HSV assessment outcome is presented as relative rankings among the six apartment archetypes in the 18 city-district residential neighbourhoods in Seoul. The implications of the findings are discussed as inputs to what, where and how adaptation and mitigation strategies could be developed for the neighbourhoods identified, leading to a significant reduction of peak cooling demands while remaining satisfactory to dwellers' thermal well-being as a priority.

**Table of Contents**

## List of Acronyms

| | |
|---|---|
| AMIS | Apartment Management Information System |
| AN | Apartment neighbourhood |
| AWS | Automatic weather station |
| CD | City district |
| CDDs | Cooling degree days |
| HDDs | Heating degree days |
| HSV | Heat stress vulnerability |
| HSV-A | Heat stress vulnerability assessment, based on referencing to a fixed threshold indoor temperature which is often recommended by a statutory authority on residential use of cooling systems |
| HSV-B | Heat stress vulnerability assessment, based on referencing to a city population's indoor heat acclimatisation (IHA) history as captured by the actual peak cooling energy use data over many years |
| HSV-A$_E$, HSV-B$_E$ | Cooling *Energy* Demand based heat stress vulnerability assessment |
| HSV-A$_T$, HSV-B$_T$ | Cooling *Temperature* Set Points based heat stress vulnerability assessment |
| HVAC | Heating, ventilation, and air conditioning |
| IHA | Indoor heat acclimatisation |
| IR | Increase rate of energy use for cooling |
| KMA | Korea Meteorological Administration |
| KOSIS | Korean Statistical Information Service |
| MAE | Mean absolute error |
| MAPE | Mean absolute percentage error |
| MDOP | Meteorological Data Open Portal |
| MK-PRISM | Modified Korean Parameter-elevation Regressions an Independent Slopes Model |
| MoLIT | The Ministry of Land, Infrastructure and Transport |
| MR | Mortality ratio |
| MSE | Mean square error |

| NWD | Non-weather-dependent |
| PCD | Peak cooling demand |
| $R^2$ | Coefficient of determination |
| RCP | Representative concentration pathways |
| RMSE | Root mean square error |
| SBR | Simple bivariate regression |
| Sqrt | Square root |
| UBEM | Bottom-up urban building energy model |
| UHI | Urban heat island |

## List of Figures

## List of Tables

# Chapter 1. Introduction

## 1.1. Research background

Facing warming temperatures and more extreme weather events, there is increasing concern about the likelihood of increasing cooling demand in urban dwelling leading to indoor thermal discomfort, heat-related illness and even mortality (McMichael et al., 2006; De Wilde and Coley, 2012). This is particularly important to urban dwellers, considering the compounding effects of ageing population, intensified urban heat islands, and increased frequency of urban heatwave episodes. It can be devastating for the urban population if peak-cooling demands cannot be met even for a short period of time.

Historically, many parts of the world have already experienced unexpected heat-related risks caused by events such as heatwaves, resulting in mortality and morbidity. The heatwave in Chicago in 1995 caused 700 excess deaths in only one week (Whitman et al., 1997), and 70,000 excess deaths were linked to the heatwave in Europe in 2003 (Robine et al., 2007), including 2,000 in the UK alone (Johnson et al., 2005) and 15,000 in France (Fouillet et al., 2006). In South Korea, about 4.1% of increased excess deaths were observed to be related to heatwaves across the seven major cities from 2000-2007 and it reached up to 8.4% in Seoul (Son et al., 2012).

Those irregular and extreme events are not that far removed from human activities. The latest global scientific consensus of climate change reported that the largest contribution to climate change is the increase of atmospheric $CO_2$ concentrations and it is mainly caused by anthropogenic activities since 1750, preindustrial condition (IPCC, 2013). Consequently, it was predicted a substantial increase of the global average surface temperature by 2100. Depending on model scenarios (i.e., representative concentration pathways, RCP), the range of temperature change for 2081-2100 relative to 1986-2005 was projected to likely be 0.3°C to 1.7°C (by RCP2.6), 1.1°C to 2.6°C (RCP4.5), 1.4°C to 3.1°C (RCP6.0) and 2.6°C to 4.8°C (RCP8.5). Moreover, the intensity, frequency and

length of heatwaves were predicted to increase (Meehl and Tebaldi, 2004; Jones et al., 2008; Perkins et al., 2012). Particular attention must be paid on a regional scale. Those estimates are not even over land regionally. For instance, in South Korea under the downscaled MM5 mesoscale model developed by Grell et al. (1994), the temperature for the summer period of 2071-2100 is predicted to increase up to 5.5°C relative to 1991-2000 (Boo et al., 2006). In the UK, the mean daily maximum temperature was predicted to increase by 5.4°C in Southern England and by 2.8°C in Northern Britain in 2080 according to the UKCP09 (Murphy et al., 2009). Furthermore, the regional specific land cover exacerbates the effect of global climate change. Urban heat island (UHI) is a good example. The effects of UHI were widely observed in many cities with the increased range of 5°C to 11°C when compared to the surrounding rural areas (Aniello et al., 1995; Knight et al., 2010; Tomlinson et al., 2012). Especially, in the urban context, the surface temperature of dark albedo materials such as asphalt pavement could reach up to 30-40°C higher than the immediate atmospheric temperature (Frumkin, 2002).

Under these circumstances, many researchers highlighted the need for better understanding of how climate change impacts human health (Patz et al., 2005; McMichael et al., 2006; O'Neill and Ebi, 2009; Portier et al., 2017). Patz et al. (2005) and McMichael et al. (2006) broadly reviewed the connected chain effects of climate change on human health, including direct and indirect heat related risks. Recently, Portier et al., (2017) reported around 11 broad health-related categories to be influenced by the change in climate including even heat-related mental stress disorders. Especially, Patz et al. (2005) highlighted that such studies must be carried out on a regional-scale of spatial resolution in early summer of temporal scope when people have not yet become accustomed to the increased temperature. O'Neill and Ebi (2009) identified a number of vulnerable subgroups to temperature extremes within the urban population of the U.S.A. under the existing climate change projections: the poor, the elderly, children and the

impaired. They also suggested the inclusion of a wide range of parameters in projecting future impacts on human health: i.e., estimates of length and strength of extreme temperature; nonfatal heat related sickness; the effect of UHI with urban planning.

Consequently, over the past few decades, many studies have been carried out to estimate how climate change impacts human health in the future regionally, as excess deaths were clearly related to extreme temperatures and the duration of the exposure (Hajat et al., 2002). In the UK, all regions were observed to have the potential to be exposed to heat-related risks and the related deaths were predicted to increase by about 257% by the 2050s relative to the current annual baseline of about 2000 deaths (Hajat et al., 2014; Hames and Vardoulakis, 2012). Across seven major cities in South Korea, the heat-related (temperature-attributable) mortality ratio (MR) was projected to increase by 1.53 (under RCP4.5, temperature rise by 2.83$^{o}$C) and by 3.30 (under RCP8.5, by 5.10$^{o}$C) by the 2090s relative to baseline of 1991-2015 deaths (MR=1.00) (Lee et al., 2018). In Canada, more than double the amount of casualties from the present level was predicted by 2050s and tripled by 2080s (Cheng et al., 2009). For other countries and cities, Huang et al. (2011) summarised the regional impacts of climate change on human health.

Although most heat-related risk projections were developed on the basis of epidemiological studies in the relationship between external temperature and excess deaths, there is lack of evidence in the link between the heat related deaths and indoor thermal environment (Vardoulakis et al., 2014; 2015). Moreover, those heat-related risk projections encompass a wide range of risk factors leading to mortality. Thus, better understanding of the process of heat risk and the factors is crucial in order to identify the specific point for establishing intervention of potential heat risk in future years. The "casual chain" from heat exposure to heat death is well-documented by Kovats and Hajat (2008). For instance, the "casual chain" is composed threefold: "Heat" affects "Heat

stress" with factors affecting exposure; then, "Heat stress" leads to "Heat illness" with factors affecting sensitivity to given heat exposure; finally, "Heat illness" results in "Heat death" with factors affecting access to treatment. This shows that the starting point in assessing potential heat risk on human health must be "heat stress".

Moreover, the factors of heat-related risk on human health include a large number of determinants. Kovats and Hajat (2008) also summarised the determinants of heat-related mortality and morbidity with six categories as following:

- Age and Aging: heat vulnerability to old age by rapid changes in thermoregulatory system (i.e., Flynn et al., 2005; Grundy, 2006; Thomas and Soliman 2002)

- Clinical or Pathophysiological factors: i.e., people with depression (Stafoggia et al., 2006) and with diabetes (Schwartz, 2005)

- Living in Institutions: i.e., the elderly (+75) living in retirement homes in France (Fouillet et al., 2006) and people living in nursing homes and care homes in the UK (Hajat et al., 2007)

- Housing characteristics and air-conditioning: i.e., poor thermal envelop and inefficient natural ventilation system in residential building (Mirchandani et al., 1996; Vandentorren et al., 2006); lack of air-conditioning (Klinenberg, 2002)

- Socio-economic factors: i.e., deprivation in cities, such as low-income groups (Michelozzi et al., 2005)

- Urban Heat Islands: i.e., Kunkel et al., 1996; Watkins et al., 2002

Heat itself is a known source of present and future environmental hazards. Looking beneath those factors of heat-related risk as described above, all of them cannot be separated to populations who live in urban areas. People spend the majority of their life indoors: over 90% in developed countries alone (Harrison et al., 2002; Lat et al., 2004; Vardoulakis, 2009; Vardoulakis et al., 2015) and 66% of their time is spent in their homes

in particular (i.e. UK, Schweizer et al., 2007). Especially, the proportion of vulnerable groups staying in their homes could be much higher (Torfs et al., 2008). Moreover, public awareness of extreme heat occurrence and the related risks were shown to be insufficient in a recent survey in New York (Lane et al., 2014), which may worsen the adversary effects of heat-related risk on the urban population. Therefore, it is important to investigate urban dwelling's indoor thermal environment in the future as one of the key interventions of any potential heat risk (Hacker et al., 2005; Vardoulakis et al., 2015).

Different from other building sectors, household's end-use energy consumption is highly user-specific, determined by multiple factors such as residents' socio-economic circumstances, indoor thermal conditions resulting from interaction with urban microclimates, and energy use behaviours. For instance, as shown in the characteristics of urban dwelling's cooling energy use presented later, there appeared to be clear spatial variations in the metered residential cooling energy uses during the summer period of previous years across Seoul's city districts, and such variations were predicted to widen over the timeframe of climate change projections (see Chapter 4 for more detail). The cooling energy use data suggests that there can be substantial differences in individual households' indoor thermal conditions and therefore, there can be varying levels of indoor heat exposure experienced by the residents. As urban residential buildings and neighbourhoods are increasingly subject to excessive heat events, urban dwelling can become vulnerable to heat stress if cooling demand cannot be met for reasons such as power outage or summer fuel poverty. Thereby, this thesis defines "Heat stress vulnerability" as an indicator in assessing urban dwellings' potential heat-related risk according to the predicted peak cooling loads required to restore the temperature thresholds of indoor thermal conditions which are acceptable and agreeable to dwellings' populations.

## 1.2. Aims and objectives

- **Research aims**

This thesis investigates how data-driven peak cooling energy demand modelling can be developed for assessing heat stress vulnerability (HSV) of a city's residential building (dwelling) stock in the future climate. The hypothesis is twofold: (1) that predicted future indoor peak cooling demand (PCD, kWh/m$^2$) can serve as a heat stress vulnerability (HSV) indicator of a city's dwelling stock on the grounds that higher PCD demands will lead to higher HSV levels, (2) that potential HSV of the current stock composition can be assessed according to the predicted peak cooling loads required to restore the estimated indoor thermal conditions to acceptable thresholds.

The question therefore is how indoor thermal conditions and peak cooling demands of a city's dwelling stock in future climate might be modelled, assuming no housing stock adaptation. If the indoor thermal conditions of dwelling units could be estimated through empirical data modelling combined with contextual building energy simulation, the peak cooling demands could be estimated in terms of the amount of cooling energy required to bring the indoor thermal conditions down to some threshold cooling temperature set points agreeable or acceptable to the dwelling population.

The purpose of subjecting a city's dwelling stock to the PCD-based HSV assessment is to identify neighbourhoods of the dwelling stock with higher HSV levels that may require urgent actions of adaptation through renovation or replacement. The expectation is that sustainable urban dwelling stock management will take well-informed measures to reduce peak cooling energy demands while meeting the population's thermal well-being requirements and hence lowering heat stress vulnerability. The city of Seoul was chosen as a test case study. The goal is to be able to quantify the potential heat stress

vulnerability of Seoul's dwelling stock over the timeframe of climate change projections. To achieve the research aims, multiple objectives are further carried out as presented:

- **Research objectives**

*Objective 1*

The first objective is to investigate characteristics of historical residential cooling energy use through several statistic relational analyses within different temporal and spatial resolutions to understand its' relationship with other relevant multiple factors (*Chapter 4*).

Unlike other building sectors, residential cooling energy use highly depends on household-related factors such as socio-economic circumstances and energy use behaviours for cooling under the interaction with building thermal environments. This represents that the knowledge of dwellers' cooling energy use behaviour is essential in housing stock energy modelling. However, obtaining such user-related information through a completed survey in an urban context is challenging. In the absence of this reliable knowledge, this thesis investigates the characteristics of historical cooling energy use to explore possible knowledge of households' user-related information.

The hypothesis is that the datasets of households' cooling energy use contains their historical cooling energy use behaviours determined by their own circumstances in responding to external and internal climates. To confirm this, several statistic relational analyses between residential cooling energy use and other relevant multiple factors are carried out in different summer months (July – September) and different spatial scales (city vs. neighbourhood). The expectation is that if a certain spatial resolution of neighbourhood can capture the homogenous datasets of multiple factors (energy flow pathways) affecting peak cooling energy use, the housing archetype can be developed

within that boundary scale with reduction of uncertainties in terms of representativeness to housing stock. Hence, the urban housing stock energy modelling will take well-informed knowledge that enables one to outline detailed modelling techniques for the purpose of assessing heat stress vulnerability.

*Objective 2*

The objective here is to develop archetypes of a city's dwelling stock for estimating present indoor thermal conditions of residential neighbourhoods (*Chapter 5*).

Given the derived modelling ideas from the literature review in Chapter 2, a bottom-up housing stock energy modelling framework is proposed for assessing potential heat stress vulnerability of a city's dwelling stock (Chapter 3). To estimate likely peak cooling demand of a dwelling unit for assessing heat stress vulnerability of an urban dwelling stock, the knowledge of a possible range of indoor air temperatures under such conditions is essential. However, to obtain such knowledge through field survey campaigns for a city's entire dwelling stock would be cost-prohibitive if not impossible. In the absence of reliable city-wide measurements of indoor thermal conditions, archetype is first developed within a neighbourhood scale of microclimate boundary for building physics. Then, the detailed data requirements of neighbourhoods' archetypes are analysed to be applied into a model calibration process of peak cooling energy use proposed for estimating archetypes' present indoor thermal conditions.

*Objective 3*

The following objective is to assess potential heat stress vulnerability (HSV) of a city's dwelling stock in the coming years (*Chapter 6*).

The potential HSV of a city' dwelling stock under climate change projections is assessed in two perspectives: (1) in terms of future indoor thermal conditions; and (2) in terms of future peak cooling demands. The indoor thermal condition perspective points to implications for dwellers' health and welling under the "no change of peak cooling energy use behaviour" scenario. On the other hand, the peak cooling demand perspective points to implications for cooling energy supply and demand over the timeframe of climate change projections under the "no stock change" scenario.

In both approaches, the HSV assessment outcomes are summarised as the distances between estimated set points and base reference points. It follows that neighbourhood archetypes further away from the reference points present higher heat stress vulnerability. Finally, the quantified distances are sorted as relative ranking among a city's neighbourhood archetypes.

However, in both assessments, the base reference points of indoor thermal conditions are crucial. Therefore, the question is what suitable base reference points can be considered in assessing HSV of a city' dwelling stock under climate change projections. This thesis introduces two types of reference points. One is based on referencing to a fixed threshold indoor temperature which is often recommended by a statutory authority on residential use of cooling systems. Another is based on referencing to the population of a city's indoor heat acclimatisation (IHA) history as captured by the actual peak cooling energy use data over many years. The outcomes derived from each of these assessments will be compared to each other and the implications will consequently be discussed.

## 1.3. Thesis structure

To achieve the research aims and objectives described above, this thesis is composed of a preliminary study section and three main bodies of results (Figure 1-1). The preliminary study (Chapter 2) provides a key body of knowledge in establishing a methodological framework for assessing potential heat stress vulnerability of a city's dwelling stock (Chapter 3). Chapter 4 in particular gives fundamental ideas on archetype-based stock energy modelling. Applying the methodological framework, the results are presented and discussed in Chapters 5 and 6. The brief introduction of each chapter is described as below:

*Chapter 1* – "Introduction" introduces the research background on potential heat-related risk on human health in urban dwellings and provides the needs for assessing potential heat stress vulnerability of a city's dwelling stock. This chapter ends with a detailed reference to research aims and objectives, including research questions.

*Chapter 2* – "Literature review" explores the possible approaches to the main research question, "how might peak cooling demands (PCDs) of a city's dwelling stock be modelled to maintain indoor thermal conditions agreeable and acceptable to urban populations in future years". This chapter reviews previous studies in relation to the urban building energy model and climate change impacts on heat stress vulnerability of indoor dwelling environments. It subsequently identifies the key body of knowledge in addressing research aims and objectives.

*Chapter 3* – "Methodology" presents a bottom-up stock energy modelling framework for assessing potential heat stress vulnerability of a city's dwelling stock, given the body of knowledge identified and modelling ideas in literature review (Chapter 2). This chapter also describes the key constituent methods, including EnergyPlus model calibration

process to estimate indoor thermal conditions and details of stock energy modelling process for the purpose of assessing potential heat stress vulnerability.
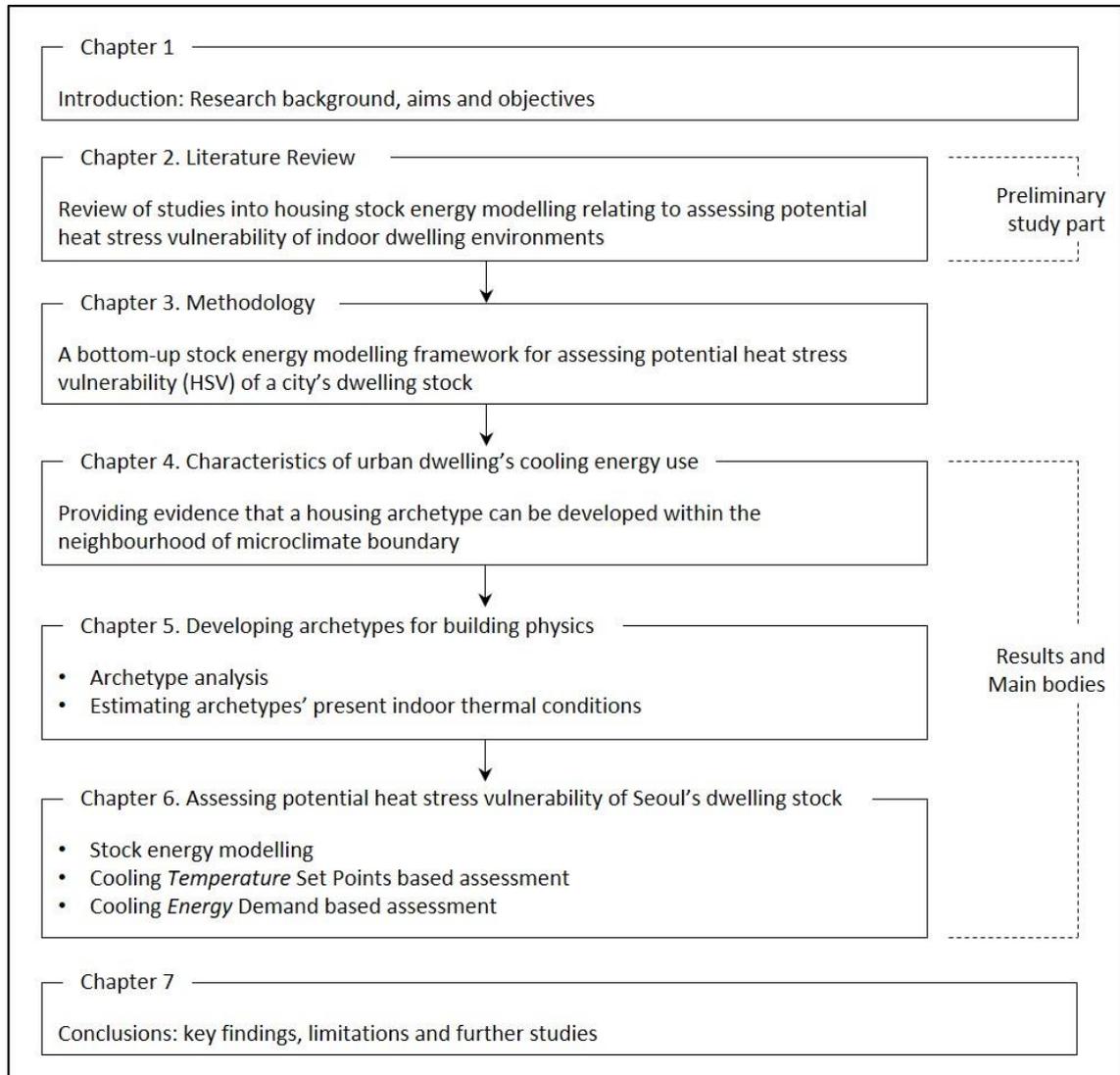


Figure 1-1. Overall thesis structure

*Chapter 4* – "Characteristics of urban dwelling's cooling energy use" presents a data analysis of Seoul's open heterogeneous datasets to investigate characteristics of historical cooling energy use through several statistic relational analyses within different

temporal (summer months, July – September) and spatial resolutions (city to neighbourhood scale). The statistic relational analyses include Pearson-correlation, analysis of variance (ANOVA) and regression analysis. Those analyses are mainly to characterise the residential peak month (August) cooling energy use behaviour in responding to external climates (i.e. temperature) on a neighbourhood scale. This chapter provides evidence that a housing archetype can be developed within the neighbourhoods of a microclimate boundary for the purpose of modelling the peak month (August) cooling energy use of a city's dwelling stock.

*Chapter 5* – "Developing archetypes for building physics" presents how urban dwelling archetypes can be developed for building physics underpinning the Seoul Study. It includes Seoul's collected data and the analysis required for archetype developments into building physics, EnergyPlus model calibration process. In the absence of reliable field measurements of dwellings' indoor thermal conditions in the city context, the possible approach to obtaining a replaceable indicator of indoor thermal measurements can be found in developing archetypes. Then, each archetype can be specified with known sources of building and occupancy information as input requirements for EnergyPlus model calibration process to estimate indoor thermal conditions. Finally, the estimated indoor thermal conditions in each archetype neighbourhood are presented. There are six archetypes developed in the 18 city-district neighbourhoods in this study.

*Chapter 6* – "Assessing potential the heat stress vulnerability of Seoul's dwelling stock" describes Seoul's neighbourhood dwelling stock modelling and the outcomes of heat stress vulnerability (HSV) assessment. Applying the methodological framework presented in Chapter 4, the potential HSV is assessed in two perspectives: (1) in terms of Cooling *Temperature* Set Points based; and (2) in terms of Cooling *Energy* Demand based. Consequently, the stock energy modelling is presented into two types for the purpose of each of the HSV assessments: hence, (1) modelling indoor thermal conditions

and (2) modelling peak cooling demands. In both approaches, the HSV assessment outcomes are summarised as the distances between estimated set points and base reference points. It follows that neighbourhood archetypes further away from the reference points present higher heat stress vulnerability. Finally, the quantified distances are sorted as a relative ranking among a city's neighbourhood archetypes.

*Chapter 7* – "Conclusions" gives key findings from this study and finally, concluding remarks. This chapter also discusses the implications of the findings as inputs to what, where and how adaptation and mitigation strategies could be developed for the neighbourhoods identified.

# Chapter 2. Literature review

To explore how peak cooling demands (PCDs) of a city's dwelling stock might be modelled to maintain indoor thermal conditions agreeable and acceptable to urban populations in future years, this chapter intensively reviews recent studies into building stock energy modelling relating to assessing potential heat stress vulnerability of indoor dwelling environments. Section 2.1 first accounts for the limited applicability of current building energy simulation methods into quantifying urban dwellings' PCDs associated with indoor thermal environments for future years. As an alternative approach, section 2.2 introduces statistical methods of a building energy model on a large scale and also addresses the required body of knowledge in using such a statistical model, (i.e. the knowledge of households' present indoor thermal conditions). Section 2.3 covers a possible approach to obtaining the addressed knowledge requirements at neighbourhood scale: hence, archetype in segmented building physics. Section 2.4 finally illustrates the need for addressing adaptive capacity in bottom-up urban building energy model (UBEM) for assessing dwellings' potential heat stress.

## 2.1. The limit in application of building simulation in potential heat stress assessment

Most residential buildings in heating-dominant countries may not be equipped to alleviate extreme heat stress. Overheating has been observed in central London (Mavrogianni et al., 2015) and even across England as a whole (Beizaee et al., 2013; Symonds et al., 2017). Investigating the problems of overheating has been mostly limited to free running buildings in the European context. However, in Seoul, clear overheating has been detected in even mechanically cooled households during peak summer periods (Bae and Chun, 2009; Lee and Lee, 2015).

In response to the changing climate on buildings, the risk of overheating in residential buildings has been identified as one of the key source areas of any potential heat threat (Vellei et al., 2017; Lomas and Porritt, 2017). However, few studies have been carried out in quantifying potential heat stress risk (or vulnerability) of a city's residential building stock with sufficient spatial-temporal resolutions corresponding to the stock composition. Such studies may be difficult as it is rare that a large number of households' indoor thermal environmental measurements are collected readily for analysis; also fine-grained on-site future weather data required for dynamic building energy performance modelling (e.g., Guan, 2009) is not yet widely available below the city-scale.

In the absence of data availability for the future, most potential heat related studies in residential buildings tend to estimate cooling energy demands to maintain certain levels of indoor thermal comfort based on energy modelling. This approach assumes that the estimated cooling energy demands may be met by power suppliers or be paid by dwellers. Otherwise, the heat stress would occur in terms of occupants' indoor thermal environment. A number of previous studies used fixed cooling temperature set points to estimate peak cooling loads in future years. For instance, 27$^{o}$C was used as a fixed threshold temperature of cooling set point for calculating future cooling loads in the UK (Gaterell and McEcoy, 2005). Others suggested that 26$^{o}$C should be the cooling set point for summer acclimatisation in the UK (Collins et al., 2010); 29$^{o}$C as an acceptable point for a short term under the external hot climates in Switzerland (Frank, 2005); and 25.5$^{o}$C in Hong Kong (Chan, 2011). Consequently, all projections showed a certain level of increase in cooling energy demands in future years but dynamic variations appeared in the amount of the increment regionally. More detailed regional climate change impacts on built environment was summarised by Li et al. (2012). They also highlighted that the largest energy demands would occur in warm winter and hot summer climates owing to high demands for cooling energy. For instance, in South Korea, cooling degree days

(CDDs) by the year of 2099 from 1980 were predicted to increase up to 160% while heating degree days (HDDs) would be reduced up to 63%, implying a substantial increase of energy demands in cooling potentially (Lee and Levermore, 2010).

Those indoor overheating criteria based studies largely rely on building energy simulation. One important body of knowledge emerging in such climate impact studies is a definition of the future climates as the starting point (De Wilde and Coley, 2012). The importance of on-site weather input is widely understood in building simulation (Chan, 2011) and therefore, the needs in such studies are obvious (Guan, 2009). In previous decades, great efforts have been made to generate climate change projection datasets applicable in this area. UKCP09 and UKCIP02 in the UK are good examples, projected by UK Met Office's HadRM3 regional models (Met Office). Those projections can be applied into a building simulation model (i.e., Kolokotroni et al., 2012) and even statistical model (i.e., regression model, Braun et al., 2014) to predict future energy consumption in the UK. Further development in specific weather variable such as solar radiation has been carried out by Tham et al. (2011). Moreover, a specific type of future weather input readily accessible on building simulation was developed by PROMETHEUS project of the University of Exeter Centre for Energy and Environment, which is the probabilistic future reference year weather datasets using UKCP09. Many researchers applied the probabilistic climate change projections into their climate impact studies (i.e., Kershaw et al., 2011; Tian and de Wilde, 2011; Jenkins et al., 2011). Similarly, Du et al. (2012) developed design reference years. However, those efforts were limited to the UK.

For other regional contexts, Belcher et al. (2005) developed a method, which is called "morphing" to generate future regional climates. The tools, CCweatherGen (Jentsch et al., 2008) and CCWorldWeatherGen (Jentsch et al., 2013) are well-known examples applied the morphing method, developed by Sustainable Energy Research Group in the University of Southampton (SERG). Using the morphing method, Crawley (2008)

estimated the future energy demands in world-wide and Chan (2011) in Hong Kong. However, the limitations of morphing method were widely discussed: uncertainties of high spatial-temporal resolutions (de Dear, 2006); lack of interactions among weather variables (Guan, 2009); limited consideration of geographic conditions (Eames et al., 2011). Recently, the Korea Meteorological Administration (KMA) developed a regional model, MK-PRISM (Modified Korean Parameter-elevation Regressions an Independent Slopes Model) (Kim et al., 2012; Kim et al., 2013) to project future climates at the city district level (see section 3.2.4 for more detail). However, the data availability is limited to temperature and precipitation. In the absence of the detailed hourly future weather input for a building simulation, the impacts of changing climate on urban dwelling's indoor environment cannot be assessed only by building energy simulation, representing that other approaches must be explored.

## 2.2. Statistical methods of residential energy model on a large scale

### 2.2.1. Overview of techniques to building energy modelling

There is a fundamental difficulty and complexity in predicting building energy use as a large number of factors have an influence on the energy performance, such as ambient climates, building thermal characteristics, geometric configurations, building sub-level component service systems and user-related aspects which dynamically vary in residential buildings in particular. Moreover, such factors are more dynamic in high spatial resolutions of urban contexts. Building energy model is a function to quantify energy demands determined by input parameters, such as energy associated major drivers. The modelling method can be subdivided into two categories, depending on the modelling purpose and the level of details of input: top-down and bottom-up (Swan and Ugural, 2009; Li et al., 2017).

The top-down approach is typically used to estimate energy supply requirements on a regional or national scale based on a long-term relationship between historical energy use and the associated key drivers, such as gross domestic product (GDP), economic indices, climate, housing population rate, etc. Thus, the method of top-down tends to rely on statistical approaches. For instance, one early top-down model was introduced by Hirst et al. (1977). They modelled residential annual energy consumption in the U.S. based on econometric regression model with econometric parameters. Nesbakken (1999) assessed how socio-economic variables affect the housing end-use energy by econometric model in Norway. This simple regression model was also applied within Denmark by Bentzen and Engsted (2001). Closely relating to this study, climatic variables were used into the multiple linear regression energy model as an independent variable. In the UK, Summerfield et al. (2010) found that for every 1$^\circ$C increase for heating period, the average residential energy use was estimated to drop by about 1MWh/year. In China, Zhang (2004) analysed the relationship between annual energy use per household and heating degree days (HDDs) and then, compared it to other countries, the U.S., Canada and Japan. One distinctive advantage of top-down model is the model applicability within the limited level of details of input: hence, it only needs aggregated data (i.e., total national households' end-use energy data). However, owing to the aggregated inputs on model, the downscaled variations in individual households or neighbourhoods can be easily ignored.

On the other hand, the bottom-up model allows to identify the households' energy associated drivers at the downscaled spatial resolutions, such as individual households or neighbourhood scale and then, aggregates each of them to a certain level of stock composition. Thus, the bottom-up model is able to account for the energy use at the spatial resolution where the data is collected. Especially, the statistical method of bottom-up model uses the relationship between households' end-use energy data (i.e. billing

data) collected from a sample, which can vary in terms of spatial scope, and the associated determinants, such as socio-economic factors, climates, etc.: hence, a similar approach to top-down. However, a distinctive characteristic that is different from the top-down is to use a deeper level of detail of inputs in terms of spatial resolution and consequently, to have the more detailed model representative. For instance, the statistical bottom-up model allows one to reflect dwellers' behavioural aspects into residential energy model (Lutzenhiser, 1992; Emery and Kippenhan, 2006), which can be ignored in top-down.

### 2.2.2. Statistical methods in residential energy modelling

Typically, several statistical techniques are widely used in the bottom-up modelling area depending on model applicability within data availability. There are three well-informed statistical methods in residential energy modelling: regression, conditional demand analysis (CDA) and neural network (NN) (Swan and Ugural, 2009).

Firstly, regression model can be achieved by regression analysis which can explore the relationship between one dependent variable (energy use data) and several independent variables (other factors affecting energy use), and finally determine the model coefficients. The key idea of the regression model is to identify major determinants on energy use. For instance, climatic variables were identified as a key determinant such as HDD (Hirst et al., 1986; Jones and Harp, 1982). Similarly, Raffio et al., (2007) examined the relationship between utility bills and weather data within multiple residential areas. They identified different coefficients in each of the residences as "energy signature", also termed to "fingerprints" (Hirst et al., 1986), which represents unique metred energy occurrences determined by weather only for that specific residence (Swan and Ugural, 2009). This fingerprint is particularly important in energy modelling of

the residential sector as it can represent dwellers' energy use behaviours corresponding to the key driver.

Secondly, conditional demand analysis (CDA) is also run by regression. However, the data source and type required in CDA tends to be individual households' belongings, such as end-use appliances, their ownership (i.e. usage ratio) and the details of building characteristics (i.e. details of users and building service systems at conditioned zones) (Li et al., 2017). The model coefficients are determined by regression of the total energy use on the collected ownership lists of home appliances (or other relevant data lists) as this technique uses the presence of appliances' ownership to account for the level of usage (Swan and Ugural, 2009). Therefore, the model accuracy of CDA method largely relies on the sample size and the number of variables. This shows us that the CDA method requires large sampling based on comprehensive survey data for households' home appliances in order to achieve model reliability on large scale energy modelling. For instance, Parti and Parti (1980) used 5,286 households survey data, including appliance ownership and house characteristics such as the floor area and demographic components, to determine individual usage level of appliances through the regression method in San Diego. Also, Aigner et al. (1984) used 100 households' dataset based on a very high resolution of time interval (15 min). The largest sample, about 100,000 in total in Quebec has been used by LaFrance and Perron (1994), including climate indicators and heating sources and finally, the model coefficient of determination ($R^2$) was reached up to (.700). The primary benefit in CDA enables to reflect occupancy behavioural factors (i.e. appliances' ownership and their usage rate) into modelling, while the sampling large enough can be challenging at city scale modelling.

Thirdly, neural network (NN, also called artificial neural network, ANN) is typically used in case that the relationship between the independent (i.e. dwelling characteristics in energy modelling as input parameters) and the dependent (i.e. end-use energy data as

output parameters) is non-stationary due to the capability of NN model to find hidden parameters which enable to interconnect neural structures between the parameters (Swan and Ugural, 2009). Aydinalp et al. (2002) employed the ANN technique for modelling energy use in the Canadian residential sector by components, such as modelling energy use of appliance, lighting and space cooling. For the input parameters, they used a number of housing characteristics datasets collected from 988 households (741 for training datasets and 247 for testing). Thus, $R^2$ of the model was reached at .909. In a Korean apartment housing context, Suh and Chang (2012) developed ANN model for estimating energy demand. They introduced eight key indicators affecting energy and water usage, which can be considered substantially reduced input parameters in ANN, and the model reliability was reached at 4.5% - 7.3% of MAPE (mean absolute percentage error) in error statistics for electricity model. However, despite such high reliability in ANN model performance, several parameters required as inputs for estimating residential energy demands in future years can be challenging.

Thus, the regression model can be considered as a suitable statistical modelling technique in this thesis taking into account the modelling purpose, predicting peak cooling demands within limited data availability for future years (i.e., daily temperature climate change projections in Seoul's city-districts). If certain parameters are clearly identified as key determinants to do with historical peak cooling energy use, which are also available for the future, the regression model allows one to estimate the likely peak cooling demand of urban dwellings.

### 2.2.3. Microclimate as a key determinant on residential cooling energy use

In regression modelling, it is important to understand the factors affecting residential cooling energy use. Yu et al. (2011) documented major determinants affecting residential

energy use and they can be classified into three categories: (a) climates including urban heat island; (b) building physical characteristics, i.e. thermal property of building envelope, geometric configurations and service systems; and (c) user-related aspects, i.e. occupants' behaviours and socio-economic circumstances. In relation to cooling energy use, this study adds climate (microclimate) change as an additional important factor taking into account the likely impacts of rising external temperature on cooling loads.

It is widely understood that climate is one of the most influential factors affecting building thermal and energy performance. Of the wide range of climatic variables, air temperature (dry-bulb), humidity, wind pattern (speed and direction) and solar radiation are considered as the most significant parameters (Flor and Domınguez, 2004). Especially, dry-bulb temperature is one of the most influential climatic variables and thus, it is largely used in measuring heating and cooling degree days (HDDs and CDDs) (Lee & Levermore, 2010), which is a key indicator of building weather dependent energy use.

In detail, the impacts of the ambient climates (i.e., microclimate) on building energy performance was clearly investigated by Flor and Dominguez (2004) throughout modifying weather variables on the basis of an integrated outdoor and indoor computational model. Allegrini et al. (2012) investigated the effect of microclimate influenced by neighbouring buildings of street canyon on building heating and cooling loads based on building physics. Especially, Moonen et al. (2012) broadly reviewed in this area and highlighted the importance of urban microclimate in assessing building energy demands. Many authors suggested an outdoor and indoor integrated or coupling computational building energy model as assessment methods to improve building energy performance and the assessing model accuracy (He et al., 2009; Bouyer et al., 2011; Yang et al., 2012; Yi and Peng, 2014).

In spite of the importance of microclimate in assessing building thermal and energy performance, very few field studies have been carried out to investigate the interrelations between microclimate and building weather dependent energy use (heating and cooling), including actual field measurements in residential sector in particular (Asimakopoulos et al., 2001). Santamouris et al. (2001) examined the impacts of urban microclimate on building energy consumption based on climatic field measurements from 30 urban and suburban weather stations but it was carried out into one representative office building for all locations. For residential buildings, other related studies used alternative inputs instead of on-site weather measurements, i.e. city-wide HDDs and CDDs for energy modelling studies (Aydinalp et al., 2002) and weather normalization process on the basis of line-of best fit between HDDs (and CDDs) and energy use measurements for the correlational study (Touchie et al., 2013).

The importance of microclimate consideration on building energy modelling is owing to diversity of urban climates such as an urban heat island (UHI). UHI can be considered as the representative example of urban anthropogenic climatic modifications, influenced by the energy and heat interactions between urban surfaces and the ambient atmospheric layers (Arnfield, 2003; Rizwan et al., 2008). The effects of UHI were widely observed in many cities. In New York city, the seasonal UHI magnitude was observed to be about 4°C in summer and autumn, and 3°C in winter and spring but the hourly based was over 8°C on nights (Gedzelman et al., 2003). In London, as hourly results for summer monitoring (June – August, 1999), the UHI was characterised into a nocturnal phenomenon and the UHI intensity was observed up to 7°C (Watkins et al., 2002). Also, in Birmingham (UK), the summer surface diurnal UHI magnitude under the heatwave event (18 July 2006) was observed up to 7°C (in city centre) compared to a city park (Tomlinson et al., 2012). In Seoul between 1999 and 2002, it was found that the maximum daily UHI during non-precipitation days (and precipitation days) was observed

to be 4.5°C (2.6°C) in spring, 3.5°C (2.4°C) in summer, 4.8°C (3.2°C) in autumn and 4.5°C (3.2°C) in winter (Lee and Baik, 2010). Moreover, in the perspective of micro-urban heat islands (MUHIs), defined as isolated urban locations that produce "hot spots" within a city (Aniello, 1993), the diurnal temperature differentiations in MUHIs were much large with the range of 5°C to 11°C warmer than surrounding areas in the U.S (Dallas in Texas) by mid-morning in October (Aniello et al., 1995).

At an individual building or neighbourhood level, the effect of UHI generates on-site microclimate conditions (i.e. MUHIs) and then, they have an influential impact on building weather dependent energy use, especially cooling loads. Santamouris et al. (2001) and Kolokotroni et al. (2006) investigated the effect of UHI on cooling energy use in office buildings in Athens and London respectively: in Athens, where the mean UHI intensity exceeded 10°C, the urban cooling load was estimated to be double that of rural buildings; in London, the cooling energy demand of rural reference buildings was 84% of urban areas and there was no cooling demand predicted in the optimised rural building in order to maintain indoor temperature below 24°C. In improving the model accuracy in building energy assessment, Chan (2011) highlighted the use of on-site weather input (i.e. typical meteorological year, TMY) modified based on on-site measurements. The author applied the modified on-site TMY weather input into the Hong Kong study and found that there was about 10% of increased cooling loads compared to the application of existing TMY in both office and residential buildings. Similarly, Salvati et al. (2017) reported the effects of UHI on residential cooling energy use in Barcelona, where the maximum UHI intensity at street level was 4.3°C: the cooling demands was predicted to increase of 18%-28% due to the effect of on-site UHI.

Furthermore, in the residential sector, the energy use largely depends on the user-related aspects, such as the occupants' behaviour (Yun and Steemers, 2011), occupant age (Chen et al., 2013) and socio-economic circumstances (Schuler et al., 2000).

However, the influence of those factors varies according to location and the type of energy use (i.e. heating or cooling). Occupants' behaviour was more significant for cooling energy use in the US (Yun and Steemers, 2011), and the age of occupants was more influential than their income for both heating and cooling in Hangzhou, China (Chen et al., 2013). Socio-economic circumstances were investigated as significant factors but less dominant than building physical configurations for heating in Western Germany (Schuler et al., 2000). Similarly, in the Netherlands, the user characteristics and the behaviours explained only 4.2% variation for heating, while the building physical characteristics explained 42% (Santin et al., 2009).

However, even though the literature has shown that user-related aspects could play an important role in residential energy use, such influence might be inconclusive depending on the location and energy type. This implies that the application of such diversity into stock energy modelling can be challenging. Therefore, this thesis (Chapter 4) intensively investigates the characteristics of historical residential cooling energy use through several statistic relational analyses within different temporal and spatial resolutions. As described later, the spatial resolution of residential neighbourhood within microclimate boundary (1km radius neighbourhood) could capture a set of homogeneous user behaviours in terms of cooling energy use responding to the external climates.

Consequently, as this study aims at assessing urban dwellers' potential heat stress vulnerability, the knowledge of households' present indoor thermal conditions city-wide is essential and it should be explored in relation to peak cooling energy use. The challenging body of knowledge is the collecting of such data for an entire city is cost-prohibitive, even if possible at all. In the absence of reliable measurements of urban dwellings' indoor thermal conditions, this study seeks the solution at the idea of archetype in building physics to obtain a replaceable indicator of indoor thermal measurements, such as HVAC cooling temperature set points.

## 2.3. Archetype in building physics

Over the past decades, there have been two approaches in building energy modelling according to the purpose and the scale: individual building energy model (simulation) for a building designer and building stock energy model on a large scale (i.e., regional and national scale) for policy makers. However, recently they have been merged into hybrid methods such as the bottom-up urban building energy model (UBEM) for the scale of the neighbourhood (Reinhart and Davila, 2016). The basic idea of UBEM is the extended capacity of individual building energy simulation model, which is a physical and thermodynamics model used to predict energy use as well as indoor thermal environments, to a large scale of building stock. Hence, UBEM is also called to bottom-up building physics (Kavgic et al., 2010).

As an essential element in UBEM, the definition of an *archetype* can be either sample building (i.e. a documented real building) or virtual building (i.e. a hypothetical building synthesised through statistical building data and/or expert opinions) (Reinhart and Davila, 2016). Archetype is widely used to classify building (housing) stock based on building type, envelop fabric, geometry, size etc. and consequently, to be a representative building within certain levels of spatial resolutions (Swan and Ugursal, 2009).

### 2.3.1. Methods in developing archetypes

Reinhart and Davila (2016) summarised the two key processes in developing archetype for UBEM: segmentation and characterisation. The segmentation is a step for grouping within whole building stock, classified by building form, year of construction, climate and system (i.e., Dascalaki et al., 2011; Filogamo et al., 2014). In turn, the characterisation is a phase to define the detailed thermal properties within each of the identified segments. Parekh (2005) outlined more detailed characterisation method through introducing three

basic criteria in developing archetype of housing stock for building energy simulation: building thermal characteristics, geometric configuration and operation parameters. In studying the Hellenic building stock, Dascalaki et al. (2011) reported the link of residential building topologies to energy performance assessment. In Osaka (Japan), Shimoda et al. (2004) developed 20 virtual housing archetypes based on households' characteristics (i.e. family type and activities of housewife), housing building type (i.e. detached house and apartment house) and floor area. A classification of residential building stocks using 12 sample building typologies was proposed by Filogamo et al. (2014), which was applied to the whole residential building sector of Sicily. More recently, Sandberg et al. (2017) developed a segmented dynamic stock modelling approach to scenario analysis of future energy demand of the Norwegian dwelling stock towards 2050. The segmentation parameters for archetype definitions in other cities have been summarised by Reinhart and Davila (2016): typically based on building typological factors, i.e., shape, area and system.

However, those building typological classifications were limited in accessing the actual measurements of individual energy use, which may poorly reflect an occupants' behaviours into UBEM. Thus, Famuyibo et al. (2012) identified key parameters (one key determinant and eight supplementary variables) affecting energy use data by using multiple regression analysis and then, developed 13 Irish residential archetypes by using clustering statistics. The noticeable value of this Irish study is an attempt to show how historical residential energy use data is used in defining archetypes to improve model reliability.

Furthermore, it appears that the aspect of urban climatic diversity, such as a micro-urban heat island has been paid much less attention in developing archetypes at city scale modelling, while in national scale, climate was commonly used as a segmentation parameter (i.e. Ballarini et al., 2014; Dascalaki et al., 2011; Mata et al., 2014). Sensitivity

analysis is often used in urban building energy modelling to quantify sensitivity of each segmentation input parameter on the model results. This enables determination of a set of key parameters within a number of variables for developing archetype. Kavgic et al. (2013) investigated the sensitivity of 14 parameters on predefined dwelling archetypes' $CO_2$ emission model and found that the highest normalized sensitivity coefficients occurred at external air temperature. Therefore, it is important to consider both climates and residential energy use characteristics in developing housing archetypes for housing stock energy modelling on the city scale along with building typology.

### 2.3.2. Seoul's apartment housing stock

As Seoul was chosen as a test case study in this thesis, it is necessary to understand housing typological characteristics in the Seoul context first. Seoul is the capital city of South Korea and it is composed of 25 "*gu*" (city district) (see also Figure 4-1). According to the Korea Meteorological Administration (KMA, 2018), Seoul is located in the temperate zone (middle latitudes of the Northern Hemisphere geographically) and there are four distinct seasons. Seoul's annual temperature is 12.5°C: the lowest monthly temperature is -2.4°C in January while the highest is 25.7°C in August. About 61% of annual precipitation occurs in the summer months (June, July and August), while only 5% in winter periods (December, January and February). Therefore, Seoul's energy use can be characterised into both heating and cooling. However, the distribution of the monthly heating and cooling degree days (HDDs and CDDs) shows that the heating is more dominant than the cooling (see Figure 5-5). Due to the high temperature and humidity climatic conditions during the summer months, Seoul's housing stock can be considered a mechanically cooled dwelling. Households' air conditioning (AC) penetration rate supports this. According to the Korea Power Exchange (KPX, 2012), the household AC

penetration rate per household is 0.61, as counted by outdoor heat rejection unit nationally. However, as this penetration rate was surveyed at national scale including other types of residential building, it can be limited to represent Seoul's apartment housing stock. Another survey which has been carried out in apartments (Seo and Hong, 2014) showed the rate was increased to 0.85. This suggests that the number of household AC units cannot be above one but serving one or more zones for cooling (e.g., a multi split AC system driven by one outdoor unit).

Seoul's total population in 2016 was 9,805,506 (KOSIS, 2017) and the total number of households was 2,830,857 of which about 58% (1,641,383) are apartments. As the dominant housing type in Seoul, Apartment neighbourhood (AN, multi-family housing complex and also named *Danji* in Korean) has unique features distinguished from other countries' housing context (Figure 2-1). Thus, AN is often called Korean-style apartment complex (Suh and Chang, 2012). Similar to Hong Kong and other Asian mega cities, the usual type of residential buildings in Seoul are high-rise apartment buildings (KOSIS, 2013): about 84% of apartments are tall buildings over 10 floors high. The background of such high-density and high-rise apartment neighbourhoods is not apart from the Korean modernising history, which experienced extreme rapid economic growth during a short modernisation period, since the 1970s (Kim and Park, 2005). Also, between 1965 and 1991, Seoul's total population was rapidly increased: increase of about 286,000 per year (representing increase of 780 per day) (Kim, 2013). This led to very high demands in the housing market, since the 1970s. Therefore, the neighbouring ANs at certain areas were developed contemporarily (see also Table 5-4).

| (a) 1960s | "Naksan Simin" apartment | Floor plan at building level | 25.6m² floor plan |

"Naksan Simin" apartment     Floor plan at building level     25.6m² floor plan

"Yeoido Sibeom" apartment neighbourhood (Slab type)     117m² floor plan

"Garak Geumho" apartment neighbourhood (Tower type)     84m² floor plans: 1980s (left); 1990s (right)

"Jamsil Parkrio" apartment neighbourhood (bottom) redeveloped from the aged "Jamsil Siyoung" (up)     Typical 84m² floor plan of "Jamsil Parkrio" apartment building

Figure 2-1. Changes in Seoul's apartment neighbourhoods (ANs) between 1960s and 2000s (Source: Park et al., 2005; Kim, 2012; Choi et al., 2004)

In 1960s, the first large-scale apartment neighbourhoods were supplied by the central government for the labour class in Seoul's selected 32 districts in order to solve the housing shortage problem (Park et al., 2005). Thus, the floor area per apartment unit was less than 30m$^2$ mostly (See Figure 2-1 (a)). One distinctive feature of 1960s' apartments is the sharing toilets located in the middle of each floor and the form of the building is typically "slab" type.

In 1970s, the supply of apartment was extended to the middle class. *Yeoido* district (about 8.48 km$^2$) housing development project was carried out in *Yeongdungpo* city-district located in the riverside of *Han* River. Especially, *"Yeoido Sibeom"* apartment neighbourhood (built in 1971 in this area) is one of the iconic apartment neighbourhoods historically, due to the fact that it contains commercial area and public park within the neighbourhood of 1,790 apartment households (Kim, 2012) (See Figure 2-1 (b)). From this project, a single apartment neighbourhood has formed its' own community district.

In 1980s and 1990s, the housing market was led by private developers commercially and as a result, user demands were reflected into the planning of housing development. According to a study into changes in Korean apartment floor plans (Choi et al., 2004), various floor plans were experimented in 1980s and they were standardised into a few typical floor plans based on the occupants' preferences and popular floor area size (i.e. 84m$^2$) in 1990s (see Figure 2-1 (c)). Also, the form of apartment buildings was changed to "tower" type from "slab" type: about 70 – 80% of new apartment developments built in 1990s were tower type (Choi et al., 2004), representing that there appeared high-rise apartment neighbourhoods.

In 2000s, the housing market can be characterised into "Hosing redevelopment", which contains the complete demolishment of existing buildings first and then new development in the same site, owing to the poor liveability of the aged apartments built in early 1970s

(Choi et al., 2013). As seen in Figure 2-1 (d), the aged "Jamsil Siyoung" (built in 1971) apartment neighbourhood (5563 apartment households and slab type buildings with 5 story-tall) was fully redeveloped to "Jamsil Parkrio" (6864 apartment households and tower type buildings with up to 36 story-tall) in 2008. The building form became various but the placement and layout of housing components were not significantly different the 1990s'. Furthermore, super high-rise apartment buildings appeared in 2000s, i.e. "Mokdong Hyperion Tower", 256m of 69 story-tall and built in 2003 (Choi et al., 2013).

To investigate potential housing archetype developments in the Seoul context, it is necessary to understand the typological characteristics at a single apartment neighbourhood level first. In terms of geometric configurations, the building type of AN can typically be classified into two: *Slab type and Tower type* (Choi et al., 2012). As seen in Figure 2-1 (b), the form of slab type apartment building is horizontally linear such as *"I"* where the core (lift and stairs) is located in the side areas across the several apartment housings linearly attached. On the other hand, tower type in Figure 2-1 (c) is vertically linear where the core is placed in the middle of the surrounded a few number of apartments (typically 2-4 apartments in each floor equally). The difference between slab type and tower type is the number of external walls exposed to external climate in apartments: 2 sides in slab type; 3 sides in tower type. Also, shading effects of one apartment building on other neighbouring buildings can be different. Therefore, energy loads required for cooling and heating can probably be differentiated in each type of AN. However, according to a recent study into energy load variations by the location of apartment units, taking into account the number of exposed walls and shading effects, there was no significant locational differences in cooling loads while heating loads were sensitive to both parameters (Kim et al., 2015). This suggests that the consideration of building type and height can be minimised in developing archetypes for Seoul's cooling model.

A single AN tends to be built upon the same construction assembly profiles (Tae et al., 2011) according to insulation criteria of building regulation (see Table 4-9). This is due to the fact that the apartment neighbourhood is a single development of several apartment buildings built by one housing developer (or a consortium of several developers as a main housing supplier). The number of households in each apartment neighbourhood citywide can vary significantly from the hundreds to the thousands depending on housing development projects. Also, the floor area of apartment units is multiple, usually from 59.4 $m^2$ to 148.4 $m^2$ according to KOSIS (2013), indicating diverse family sizes. However, in a single apartment neighbourhood, about 89% of similarity in the floor area of apartment units was observed (Choi et al., 2012). Therefore, apartments within each AN can be considered architecturally homogeneous in terms of not only geometric configurations but also thermal characteristics (Choi et al., 2012; Tae et al., 2011).

Furthermore, the architectural homogeneity has also formed unique socio-economic characteristics. For instance, there is no significant difference in property price of each apartment household within a single apartment neighbourhood (KAB, 2015b). Also, according to a recent survey derived from the selected four ANs in Seoul (Choi et al., 2012), similarity of characteristics in family member were found: over 60% of similarity in the age of a housewife, about 90% in educational level of housewife, 90% in employment of housewife (i.e. full-time housewife), 75% in family composition (i.e. nuclear family) and up to about 90% in monthly income.

However, beyond the architectural and socio-economic homogeneity at a single apartment neighbourhood level, investigating typological characteristics of the combined apartment neighbourhoods (as the apartment housing stock at large scale) is further required in archetype developments for the purpose of housing stock energy modelling at a city scale. TABULA (Typology Approach for Building Stock Energy Assessment)

project can be a good example, which is developed for building typology definitions in 20 European countries (Loga et al., 2016). The building typological classifications have been widely used for building stock energy modelling at large scale in European context (Ballarini et al., 2014; Ballarini et al., 2011; Vimmr et al., 2013; Kragh and Wittchen, 2014).

As this study is the first attempt to develop housing archetypes in a certain level of spatial resolution for city scale modelling, such details of housing typology are not yet readily accessible at present. In the absence of reliable measurements of urban dwellings' typological characteristics, this study seeks the solution to the idea of "typical apartment floor plan" proposed by the "guideline for evaluating design and performance of green houses" established by a central government of the Ministry of Land, Infrastructure and Transport (MoLIT, 2009) in Korea (see also Figure 5-4). The purpose of establishing typical floor plans is to be used for assessing "green home certification" for new apartment development projects as the base reference floor areas and plans and they were developed based on the existing and potential trends of apartment floor plans (Tae et al., 2011). Thus, the MoLIT's typical floor plans have been applied into assessing apartments' life cycle $CO_2$ emissions (Shin et al., 2011; Tae et al., 2011) and into evaluating the embodied environmental impacts of apartment buildings (Roh et al., 2017).

Finally, as described later in section 4.4.2.1, one distinctive characteristic of residential cooling energy use is that only within each residential neighbourhood (city-district microclimate boundary setting), there are high internal consistency and similarity in terms of the distribution of households' monthly cooling energy use. Moreover, there are a set of dominant thermal characteristics and geometric configurations identified in neighbourhood of microclimate boundary. Therefore, it is reasonable to assume that the archetype can be defined within microclimate boundary (segment) potentially for this study. Once an archetype is developed in each segmentation, the thermal modelling can be performed using dynamic building simulation tools (i.e. DOE-2, Huang and Broderick,

2000). Especially, the estimation of archetypes' indoor thermal conditions (i.e. HVAC cooling temperature set points) can be achieved by model calibration methods (Raftery et al., 2011a) on the basis of metred cooling energy use (see chapter 3 for more detail).

## 2.4. Addressing adaptive capacity in UBEM for assessing dwellings' potential heat stress

### 2.4.1. Bottom-up urban building energy model (UBEM) associated with indoor dwelling environments

Over the past decade, research into building stock energy modelling on large scales (city, regional, or national) has intensified in response to policy-making to reduce building-related end-use energy demand and $CO_2$ emissions. Pittam et al. (2014) reported how a bottom-up approach for local authority housing in Cork City, Ireland was developed for stock modelling in the absence of a detailed housing database. Using GIS, climate, buildings and dwellings statistics datasets, Buffat et al. (2017) developed and validated a bottom-up heating energy demand model based on 1,845 buildings in two Swiss municipalities. To achieve segmented dynamic dwelling stock model energy analyses, stock renovation probability functions have been developed for realistic estimates for a nation's renovation activity (Sandberg et al., 2017), which were applied to model future Norwegian dwelling stock energy demand towards 2050. For the housing stock energy models developed and deployed in the UK throughout the past 25 years, a comprehensive review and evaluation of 29 such models have identified several areas for improvement including transparency, accuracy, sensitivity and updatability (Sousa et al., 2017). As the model-theoretical frameworks and large urban datasets are set to grow, there will be a demand for practical computational tools and platforms to be developed. TEASER (Tool for Energy Analysis and Simulation for Efficient Retrofit), for instance, is

an open framework for urban energy modelling of building stocks to perform dynamic building performance simulation on urban-scale (Remmen et al., 2018). TEASER's usability was shown to be applicable to building, neighbourhood and urban scales.

However, it appears that the aspect of cooling energy demand has been paid much less attention in urban dwelling stock modelling research. Moreover, even though internal temperature was identified as the most dominant parameter in residential energy use (Famuyibo et al., 2012), it is hardly found the UBEM encompassed with indoor thermal conditions in statistical approaches. Furthermore, dynamic building physics cannot be practical in predicting cooling energy demands owing to limited applicability of future weather input. Under these circumstances, this study attempts to develop an urban dwelling stock modelling framework for predicting archetypes' peak cooling energy demands taking into account indoor thermal conditions, such as threshold cooling temperature set points agreeable and acceptable to the dwelling populations. Thus, the specific threshold of indoor thermal environment can be key reference point to estimate peak cooling energy demands in future years. Back to the related cooling loads studies in building physics (in section 2.1), they used various fixed cooling temperature set points regionally. Those thresholds set points stipulate overheating criteria for achieving regulated cooling energy uses mechanically. However, these thresholds may not correspond to dwellers' actual thermal preferences (tolerances) borne out of outdoor-indoor heat acclimatisation. As shown in this study of Seoul, the cooling temperature set points estimated through empirical data modelling and building energy model calibration are higher than the statutory 26°C and moreover, the indoor temperature was significantly different in each neighbourhood (spatially) and by year (temporally) (see section 5.4). The implication is clearly that such variations cannot be explained by any single comfort model.

**2.4.2. Addressing adaptive capacity in assessing dwellings' potential heat stress**

In the energy modelling, the reference point of indoor thermal condition (comfort or discomfort) is crucial to estimate the energy demands. For instance, there is an assumption for the UK, if the winter dwellings' indoor temperature is raised by 1°C, the energy requirements would be increased by 10% (Humphreys and Hancock, 2007). There have been on-going debates between static (Fanger, 1970) and adaptive thermal comfort models (Humphreys and Nicol, 1998), due to the limitations of steady state approaches in field studies (Humphreys and Nicol, 2002; Stoops, 2004; Jokl and Kabele, 2007). More recently, further adaptive thermal models have been developed, ranging from context-specific residential building energy simulation (Peeters et al., 2009), global households' indoor neutral (comfort) temperatures responding to the outdoor prevailing mean temperature (Humphreys et al., 2013), and climate change impact on comfort standards (Kwok and Rajkovich, 2010).

However, the perception of thermal comfort or discomfort ultimately lies with the subjects, and any attempts at assessments for the future will contain large uncertainties, leading to over- or underestimation. In fact, a recent field study showed that the European adaptive model, BS EN 15251 (BSI, 2007), underestimated dwellers' discomfort in the UK (Vellei et al, 2017). Such discrepancy was also found in other field studies (i.e., Humphreys and Hancock, 2007; Tweed et al., 2014). This may be accounted for by the complexity of human thermal sensation and adjustments through behavioural (voluntary), physiological (involuntary) and psychological adaptations as summarised by de Dear and Brager (1998). In reality, there can be voluntary adaptive behaviours other than just turning on or off the air-conditioning such as the changing of clothing level, using a fan or drinking cold liquids (Kwok and Rajkovich, 2010). Therefore, not all household's indoor thermal environments can be neatly characterised into some kind of uniformity. For instance, a past field survey of sampled indoor temperatures of Seoul's households

showed substantial variations even within each season, ranging from 21.3°C and 33.2°C in summer; 16.0°C – 31.5°C in autumn; 17.1°C – 28.3°C in winter (Bae and Chun, 2009).

There appears to be a wide range of comfort variations associative with environmental variables relating to different behavioural and cognitive level of adaptation (Nikolopoulou, 2011). Therefore, it is important not to disregard the element of "adaptive opportunities" in assessing potential heat stress, which is do with dwellers' adaptability to their surrounding thermal environments (Baker and Standeven, 1995; Nicol and Humphreys, 2002). However, it would be problematic to deduce some fixed points of adaptive discomfort for the purpose of heat stress assessment. Instead, as argued by Chappells and Shove (2005), "comfort is a highly negotiable socio-cultural construct", the concept of comfort can be reproduced. As Brooks and Adger (2005) suggested that adaptive capacity may be best revealed from the dwellers' past experiences of living with effects of external climates on indoor thermal conditions over time. In mechanically cooled dwellings, households' actual cooling energy use could contain such histories of dwellers' cooling energy use behaviours afforded by adaptive opportunities (Bae and Chun, 2009; Yun and Steemers, 2011). However, the question here is about the potential impact of a changing climate on the extent of population adaptability constrained by limited energy supply and/or socio-economical affordability (Kim and Joh, 2006; Maller and Strengers, 2011).

## 2.5. Conclusions

It is evident that the possible approach to predicting peak cooling demands (PCDs) associated with urban dwelling's indoor thermal environment in the coming years is a bottom-up urban building energy model (UBEM) on the basis of statistical approach. Especially, regression model can be considered as a suitable statistical modelling technique in this thesis. If certain parameters are clearly identified as key determinants on historical peak cooling energy use, which are also available for future years, the regression model allows one to estimate the likely peak cooling demand of urban dwellings.

However, one challenging body of knowledge in generating the regression model is how to obtain the data requirement of dwellings' present indoor thermal conditions at an urban scale, of which collecting city-wide data is cost-prohibitive and almost impossible to achieve. In the absence of reliable measurements of urban dwellings' indoor thermal conditions, this study seeks the solution to the idea of archetype in building physics to obtain a replaceable indicator of indoor thermal measurements, such as HVAC cooling temperature set points. If a certain spatial boundary can capture a set of homogenous characteristics in terms of thermal property, geometric configurations and cooling energy use, the archetype can be defined within the dwelling stock of the identified spatial resolution in urban contexts. Then, archetypes' present HVAC cooling temperature set points can be estimated through empirical data modelling combined with contextual building physics.

Once the PCDs energy model is generated, the reference point for indoor thermal condition (comfort or discomfort) is crucial in estimating PCDs. However, the perception of thermal comfort or discomfort ultimately lies with the subjects. Moreover, the HVAC cooling temperature set points does not represent any details of occupants' thermal

perceptions as there can be a number of occupants' voluntary adaptive behaviours. Thus, this study seeks out the possible reference points for estimating PCDs in the future into investigating the dwellers' historical experiences of living with the effects of external climates on indoor thermal conditions over time.

# Chapter 3. Methodology

## 3.1. A bottom-up stock energy modelling framework

From the literature, the possible approach to predicting peak cooling demands associated with indoor thermal conditions was concluded to be the statistical regression model owing to the limited applicability of future weather inputs into building physics. Moreover, to assess heat stress vulnerability (HSV) of an urban dwelling stock, it is essential to obtain measurements of the stock's indoor thermal conditions during peak cooling months. However, obtaining such large-scale field measurements to cover the interiors of a city's housing stock extensively both in space and time will be prohibitively expensive if not impossible. Therefore, a bottom-up energy modelling framework (Figure 3-1) is proposed for estimating indoor thermal conditions of a city's dwelling stock during peak cooling demand. The methodological framework was built on the basis of the data requirements for the purpose of assessing heat stress vulnerability.

Here the main idea is to identify and develop a system of dwelling 'archetypes' in stock composition and placement modelling. Each archetype is then specified with known sources of building and occupancy survey information for EnergyPlus model calibration based on publicly available urban microclimate data and metered energy usage data. From the model calibration process, the HVAC cooling temperature set-point of an archetype can be extracted as a key indicator of the archetype's present indoor thermal condition which is then taken as the basis for potential heat stress vulnerability assessment in present and future climate. The methodology presupposes a "business as usual" scenario assuming no major dwelling stock retrofit or replacement to take place into the coming years.

The potential HSV is assessed in accordance to two approaches: (1) in terms of Cooling *Temperature* Set Points based (HSV-A$_T$, HSV-B$_T$); and (2) in terms of Cooling *Energy* Demand based (HSV-A$_E$, HSV-B$_E$). Consequently, the stock energy modelling is divided

into two types for the purpose of each of the HSV assessments: hence, (1) modelling indoor thermal conditions and (2) modelling peak cooling demands.
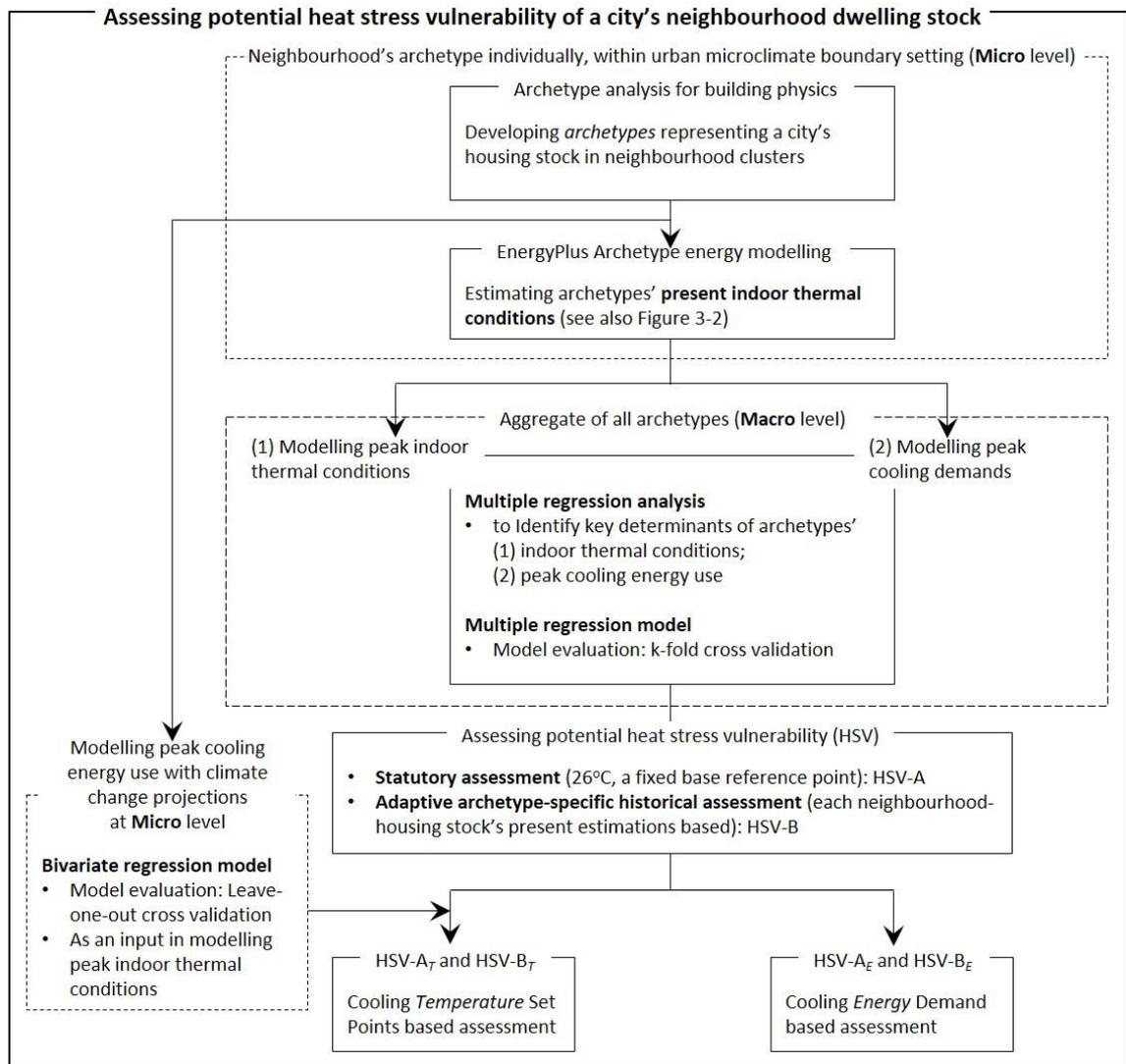


Figure 3-1. A bottom-up stock energy modelling framework for assessing potential heat stress vulnerability of a city's dwelling stock through combined micro building energy modelling and macro statistical modelling

In both modelling process, multiple regression model is employed. In both modelling types, key determinants are identified by multiple regression analysis and then, a multiple

regression model is generated. The model accuracy is evaluated by k-fold cross validation. To predict archetypes' indoor thermal condition in future years, peak cooling energy use is required as an input for modelling indoor thermal condition. Therefore, modelling for archetypes' peak cooling energy use is carried out at Micro level responding to external climates. A more detailed account of the components of the modelling framework is provided in the following sections.

## 3.2. Developing neighbourhood dwelling archetypes for building physics

Recent research in building stock energy modelling has shown identification and specification of archetypes at different spatial scales to represent the composition of a building population (i.e., building archetype definitions summarised by Reinhart and Bavila (2016). Arguably, residential buildings present a highest level of uncertainty in quantitative modelling. Hence, it is of an interest to reduce uncertainty by maximal use of empirical data where available.

Here a bottom-up approach to housing stock modelling is considered by developing archetypes at the spatial resolution of urban neighbourhood. This method is particularly pertinent if field measurement data such as energy use, local weather, and building construction information are readily accessible. Another rationale is the correspondence between urban neighbourhoods and urban microclimate boundary (as defined by a 1km radius of a city-district automatic weather station).

For the purpose of archetype building energy modelling, this spatial resolution and empirical data availability could reflect more closely to variations in local environmental and building conditions as well as in the contingency of residents' energy use decision-making. In this thesis, methods on how the residential neighbourhood archetypes can be developed for building physics in City of Seoul is presented in chapter 5.

## 3.3. Estimating present indoor thermal conditions of neighbourhood archetypes

Based on the identification and specification of an archetype building, building energy modelling can be performed with inputs reflecting in its urban and user context. A workflow is developed to estimate archetypes' present-day indoor thermal conditions through a peak cooling energy model calibration process (Figure 3-2). The goal is to obtain the HVAC cooling temperature set points as estimated ranges of indoor temperatures, which for the purpose of this study reflects a certain level of dwellers' indoor heat acclimatisation determined under adaptive opportunities (see section 6.2.4 for more details). In turn, this present-day estimates are used in developing neighbourhood specific models for estimating archetypes' indoor conditions in line with climate projections.

The archetype cooling energy model calibration follows an iterative process (Raftery et al., 2011a). As there are no field measurement data available for internal loads of household equipment, the calibration process consists of two phases: (1) initial archetype non-weather-dependent (NWD) energy model calibration to estimate internal heat gains of household NWD equipment, and (2) archetype peak cooling energy model calibration to estimate present-day indoor thermal conditions expected during the hottest month of the year.

As shown in the upper section of Figure 3-2, an initial step is required to obtain estimates of internal heat gains from household equipment usage (i.e., lighting, cooking, machinery and others), which are then taken as inputs to peak cooling energy model calibration for each neighbourhood archetype (see the lower part of Figure 3-2). For the initial non-weather dependent (NWD) energy model calibration, three types of inputs (by measurement or by inference) are required: (a) physical properties in terms of 3D

geometry and thermal property of building material assembly profile; (b) urban microclimate boundary specific TMY weather data; and (c) NWD energy usage data including NWD household equipment use profiles.
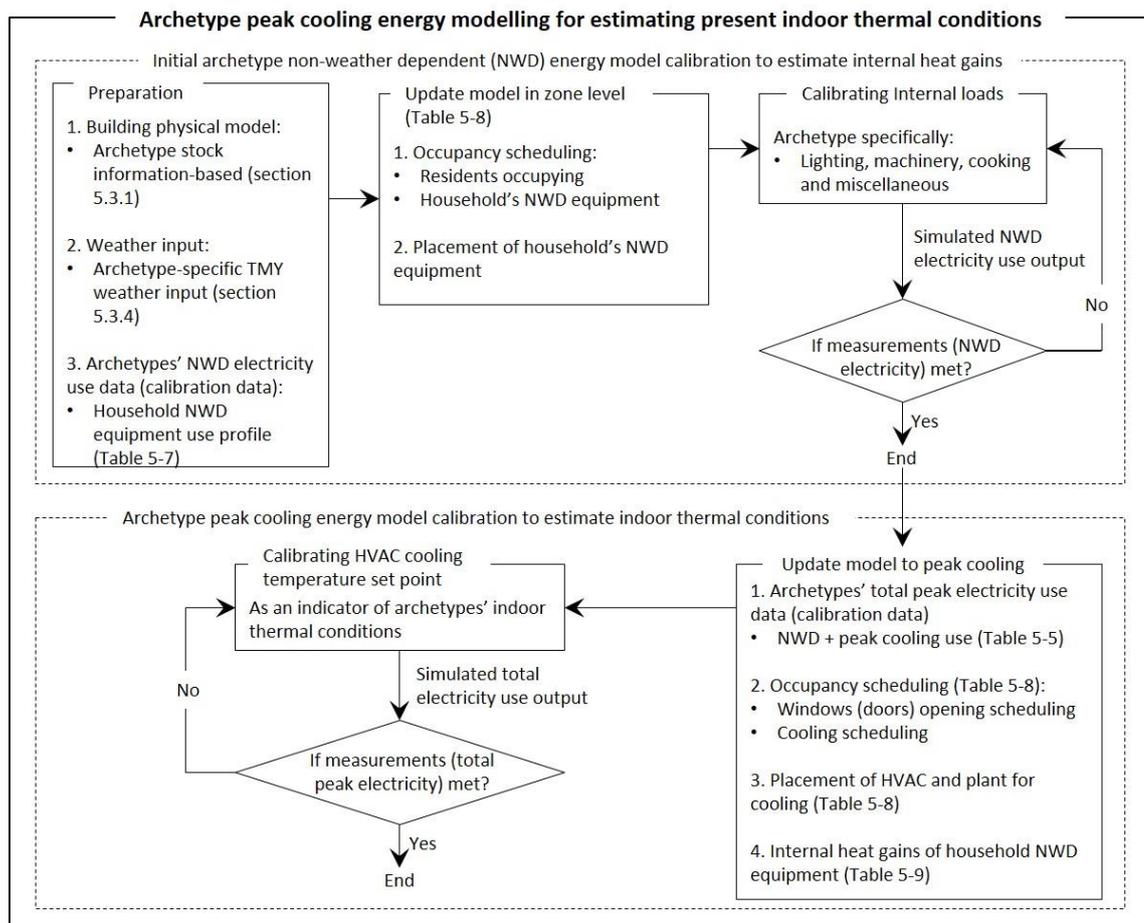


Figure 3-2. Model calibration process of peak cooling energy use for estimating an archetype's present indoor thermal conditions

Given the initial preparation, the archetype model can be updated at the zone level to include operating parameters of occupancy scheduling and placement of household NWD equipment. The application of a certain standard profile of household operation parameters in the zoning level should be adjusted or calibrated for the neighbourhood

model specifically through the iterative model calibration process based on the actual field measurements, i.e. hourly based especially. However, due to the limited data availability of residential neighbourhoods' profiles in more detail, the selection of standard occupancy profile is carried out by empirical data analysis, of which the spatial resolution of hourly residential electricity use profile is on the national scale. Considering that the occupancy profile plays a key role in residential energy use (which then, affects indoor thermal environments at high resolution of time scale), such normalisation may lead to uncertainty in reflecting neighbourhood-specific circumstances into the model. However, the question is how this national scale data may differ from Seoul. In the stock energy modelling, the definition of archetype building contains uncertainty. Instead, it is important to point out the differences of the estimated indoor thermal conditions in each neighbourhood under the even inputs. However, different from other NWD dependent energy uses, lighting can probably be classified into seasonal use. Therefore, seasonal circumstances must be considered in the occupancy scheduling (see Table 5-8 for more details).

Through iteration until the simulated NWD energy use outputs meet the measured NWD energy usage data, the internal loads for each archetypes' NWD energy use can be obtained. The calibrated internal loads then are used to estimate internal heat gains of NWD equipment use, such as lighting, machinery, cooking and miscellaneous.

Based on the initial NWD model obtained, peak cooling energy model calibration can be further performed by: (1) replacing the calibration data from NWD to total peak cooling energy use data; (2) updating operating parameters of occupancy scheduling and HVAC placement for cooling; and (3) inputting the internal heat gains of NWD household equipment use estimated previously. Finally, peak cooling temperature set points are derived from the iterative calibration process against the measured total amount of peak energy use (i.e., NWD + peak cooling).

## 3.4. Identifying key determinants for multiple regression models

In theory, peak indoor thermal conditions (and/or peak cooling demands) of a city's housing stock in future years can be modelled in a way similar to the present-year modelling as described above (section 3.3). However, future TMY/DSY weather data required for EnergyPlus modelling are not available at city-district level to be comparable to the present-year modelling. Therefore, statistical modelling techniques are employed for extrapolating future indoor thermal conditions (and peak cooling demands) of a city' housing stock based on past and present conditions, presupposing no occurrence of major stock and other urban changes. It starts with estimating present indoor thermal conditions (and peak cooling energy use) as a dependent variable; the task here is to identify the key determinants via multiple regression analysis at the macro level, i.e., the aggregate of all the neighbourhood archetypes developed previously to ensure a largest possible training dataset.

In this study, independent variables considered potential determinants of an archetype's indoor thermal condition during peak cooling demand include: (1) the highest monthly external average temperature, (2) highest monthly cooling energy use, (3) property price as a socio-economic factor in cooling energy use decision-making, (4) floor area ratio (FAR) of residential neighbourhoods as a morphological density indicator, (5) non-weather dependent energy use, and (6) U-value of building envelop. For the modelling for peak cooling demands, the dependent variable can be swapped from the estimated cooling temperature set points to peak cooling energy use. Using Seoul's available data in current case study, it was found that the August average external temperature and August archetypes' cooling energy use were identified as the key determinants of present indoor thermal conditions (see section 6.2.1). On the other hand, August average external temperature and HVAC cooling temperature set points temperature were

identified as the key parameters of peak cooling energy use (see section 6.3.1). These two determinants may not be applicable to other cities without city-specific analyses.

## 3.5. Modelling archetypes' peak indoor thermal conditions and peak cooling demands

Based on the key determinants of indoor thermal conditions (and peak cooling energy use) identified, archetypes' peak indoor thermal conditions (and peak cooling demands) are modelled by further multiple regression analyses. The statistical model is subject to $k$-fold cross validation to assess how the model predicts against an independent test dataset, taking into account yearly based sample characteristics. For example, in this Seoul study, four folds were used as there were four years' annual datasets (2014-17) available for analysis; hence, for the cross evaluation: $k$=1, 2017 as the testing case (while $k$=2, 2016; $k$=3, 2015; $k$=4, 2014). Moreover, five criteria are used in error statistics: mean absolute error (MAE); mean square error (MSE); root mean square error (RMSE); mean absolute percentage error (MAPE); coefficient of determination ($R^2$).

Notably, as this is a bottom-up approach using all inputs derived from the micro level, the resultant regression model can be applicable to predict the future peak indoor thermal conditions (and peak cooling demands) of each neighbourhood archetype given its projected monthly average external temperatures based on city-wide climate change projections and peak cooling energy of future (and HVAC cooling temperature set points required).

## 3.6. Modelling archetypes' peak cooling energy uses

To predict the housing archetypes' indoor thermal conditions during peak cooling periods in future years, the model needs an input, estimates of the archetypes' peak cooling energy uses in future years, along with climate change projections for Seoul at the city-district level. To obtain such estimations, the modelling archetypes' peak cooling energy uses is carried out at the Micro level, under the "no change of peak cooling energy use behaviour" scenario.

According to the correlational study of monthly external temperatures and cooling energy uses in Seoul's residential neighbourhoods (Chapter 4), the correlation coefficients found at the city-district neighbourhood level were positive and exceptionally strong during the hottest month of the year (August). Moreover, there appear significant spatial variations in the strength of the coefficients, implying that peak cooling energy uses aggregated at the neighbourhood complex level is location-specific and closely related to urban microclimate boundary. In this study, assuming no major housing stock renovation or replacement will take place into the future, bivariate regression models are developed to estimate archetypes' future peak cooling energy uses in accordance with the latest climate change projections. This statistical modelling should take place at the micro level to reflect historical energy use behaviours of the housing stock residents, which may carry some degree of continuity onto future years.

To avoid overfitting training datasets with regard to testing datasets when the sample size is relatively small, peak cooling energy regression models should be subject to statistical checks such as the leave-one-out cross validation (LOOCV). The assumption of no stock renovation/replacement involved in the modelling can still produce results to inform likely consequences of "business as usual" scenarios; hence, in virtual retrospect,

what measures could be taken now to undertake innovative and purposeful housing stock management over a timeframe allowed by a city's latest climate projections.

## 3.7. Assessing potential heat stress vulnerability

Finally, given the indoor thermal condition model and the peak cooling demands model, the potential heat stress vulnerability (HSV) of a city's dwelling stock is assessed in two approaches labelled as HSV-A and HSV-B. The HSV-A assessment is based on referencing to a fixed threshold indoor temperature which is often recommended by a statutory authority on residential use of cooling systems. For example, the Ministry of Land, Infrastructure and Transport of South Korea recommends 26ºC as the threshold temperature for domestic HVAC use (MoLIT, 2017). On the other hand, the HSV-B assessment is based on referencing to a city population's indoor heat acclimatisation (IHA) history as captured by the actual peak cooling energy use data over many years. The rationale behind HSV-B is that urban dwellers may adapt to indoor heat conditions over time (i.e., indoor heat acclimatisation), hence an individual household's decision on cooling energy use may deviate significantly from the fixed statutory set point. As an alternative reference point, here this study uses the Max value of cooling temperature set points inferred from historical cooling energy use data for HSV-B assessment.

Furthermore, within HSV-A and HSV-B, two methods are introduced: Cooling *Temperature* Set Points based (HSV-A$_T$, HSV-B$_T$), and Cooling *Energy* Demand based (HSV-A$_E$, HSV-B$_E$). Both sub-methods assume that future peak cooling energy demand will be met by energy suppliers and affordable by dwellers to maintain the statutory set point temperature (HSV-A$_T$) or the historical IHA level (HSV-B$_T$). Hence, the peak cooling energy demand based HSV assessment is carried out over two strands: (1) HSV-A$_E$ peak cooling loads estimated according to a statutory cooling temperature set point for all

neighbourhoods; and (2) HSV-B$_E$ peak cooling loads estimated according to each neighbourhood archetype's present Max cooling set point temperature as the vulnerability threshold.

In both approaches, the HSV assessment outcomes are summarised as the difference between estimated set points and base reference points. It follows that neighbourhood archetypes further away from the reference points present higher heat stress vulnerability. Finally, the quantified differences are sorted as relative ranking among a city's neighbourhood archetypes. Applying this methodological framework, this study presents an assessment of potential heat stress vulnerability of Seoul's dwelling stock in Chapter 6.

# Chapter 4. Characteristics of urban dwelling's cooling energy use

The content of this Chapter has been published in a peer-reviewed journal under the title:

## 4.1. Introduction

The main idea of the proposed modelling framework (Chapter 3) is to identify and develop a system of housing archetypes representative to the dwelling stock population. Especially, as the framework was developed by a bottom-up approach to modelling a dwellings' peak (August) cooling demands (PCDs) at the city scale, it is important to identify a possible spatial boundary (as a "bottom" level) of housing stock, which can capture key components of households' cooling energy pathways in developing housing archetypes. As the principal elements in archetype developments, not only building physical configurations (i.e. geometric form and thermal characteristics) but also households' cooling energy use behaviour during the peak months must be considered for the purpose of modelling PCDs of a city's dwelling stock. This represents that the knowledge of a dwellers' cooling energy use behaviour is essential in energy modelling.

However, obtaining such user-related information through a completed survey in an urban context is cost-prohibitive. Even if possible, the diversity of individual household's energy use behaviours would be poorly abstracted into the urban energy model. In the absence of this reliable knowledge, this chapter first investigates the characteristics of historical cooling energy use to explore possible knowledge of households' user-related information. The hypothesis is that the datasets of households' cooling energy use contain their historical energy use behaviours determined by their own circumstances in responding to external and internal climates. It was developed on the grounds that residential cooling energy use highly depends on household-related factors such as economic circumstances and energy use behaviours under the interaction with building thermal environments.

Therefore, several statistic relational analyses between energy use data and other multiple factors are introduced (see Figure 4-5). Also, they are carried out within different

temporal (summer months, July-September) and spatial resolutions (city and neighbourhood scale). To account for building interaction with the urban microclimate, this thesis defines urban area as being within a 1 km radius of urban weather stations as the spatial location and boundary in sampling a city's housing stock: hence, the neighbourhood scale. This is considered an acceptable spatial scale reflecting climatic variation in an urban climate zone (Oke, 2004; 2006). Therefore, this thesis considers that there could be similar climate (particularly dry-bulb temperature) conditions affecting residential neighbourhoods within a sub-urban spatial resolution.

The expectation is that if the residential neighbourhood of microclimate boundary can capture the homogenous datasets of multiple factors (energy flow pathways) affecting peak cooling energy use, the housing archetype can be developed within that boundary scale with reduction of uncertainties in terms of representativeness to housing stock. Hence, the urban housing stock energy modelling will take well-informed knowledge that enables one to outline detailed modelling techniques.

The city of Seoul has been identified as the case study site where the datasets required to address the above issues are available in the public domain under the country's open data and protection law - Article 23 in "Multi-family Housing Management Act" (MoLIT, 2016). The goal in this chapter is to investigate characteristics of residential peak month (August) cooling energy use to outline housing archetype developments for the purpose of assessing heat stress vulnerability of a city's dwelling stock.

To achieve the primary aim of this chapter, section 4.2 first presents the collected Seoul's open data based on the literature of factors affecting residential cooling energy use. Section 4.3 on methods analyses the collected data and introduces a statistic relational analysis framework to understand the characteristics of the urban dwelling's cooling energy use. The results are presented and discussed in section 4.4. Finally, chapter 4.5

concludes with the key findings and presents limitations and further developments in stock energy modelling.

## 4.2. Seoul's open data

The city of Seoul is made up of 25 "*gu*" (city district, CD) and each CD has its own automatic weather station (AWS). Seoul's open data is first analysed to look for potential correlations between (a) the actual residential cooling energy use extracted from the energy bill data from the apartment neighbourhoods, and (b) the actual location-specific microclimate urban weather data as measured from the CD AWS.

By the Article 23 in "Multi-family Housing Management Act" (MoLIT, 2016), apartment neighbourhoods (ANs, multi-family housing complex) with at least 300 households (or 150 with specific article under the Act) are subject to "compulsory management", meaning to make their neighbourhood aggregate monthly utility energy use available on the Apartment Management Information System (AMIS, see section 4.2.2 for more detail). As in 2018, there are 2,343 apartment neighbourhoods registered on AMIS, and 16,464 apartment buildings, 1,419,808 apartment households, about 87% of the total, are registered with AMIS (2018a). Each apartment neighbourhood is composed of about seven apartment buildings and each apartment building contains about 86 households arithmetically. In the Seoul study, the boundary of 1km radius of a city-district automatic weather station (CD-AWS) is used as the microclimate boundary in sampling the city's high-rise apartment neighbourhoods.

**4.2.1. Urban microclimate data**

The urban microclimate data collected at the AWS of each city district in Seoul are open to the public (KMA, MDOP). However, the scope of AWS data is restricted to temperature (dry-bulb), wind direction/speed and precipitation (above 0.5mm). As dry-bulb temperature is the most influential weather variable affecting building thermal regulations and energy use, it was chosen to represent the urban weather data in this study. Figure 4-1 shows the locations and boundaries of the 19 city areas identified, considering the sample size for statistical analyses (see section 4.2.3 for more detail). The boundary of 1km radius within the AWS location is chosen according to the spatial scale of urban microclimate (Oke, 2004; 2006). Thus, a total of 98 apartment neighbourhoods are identified across the 19 district sites.
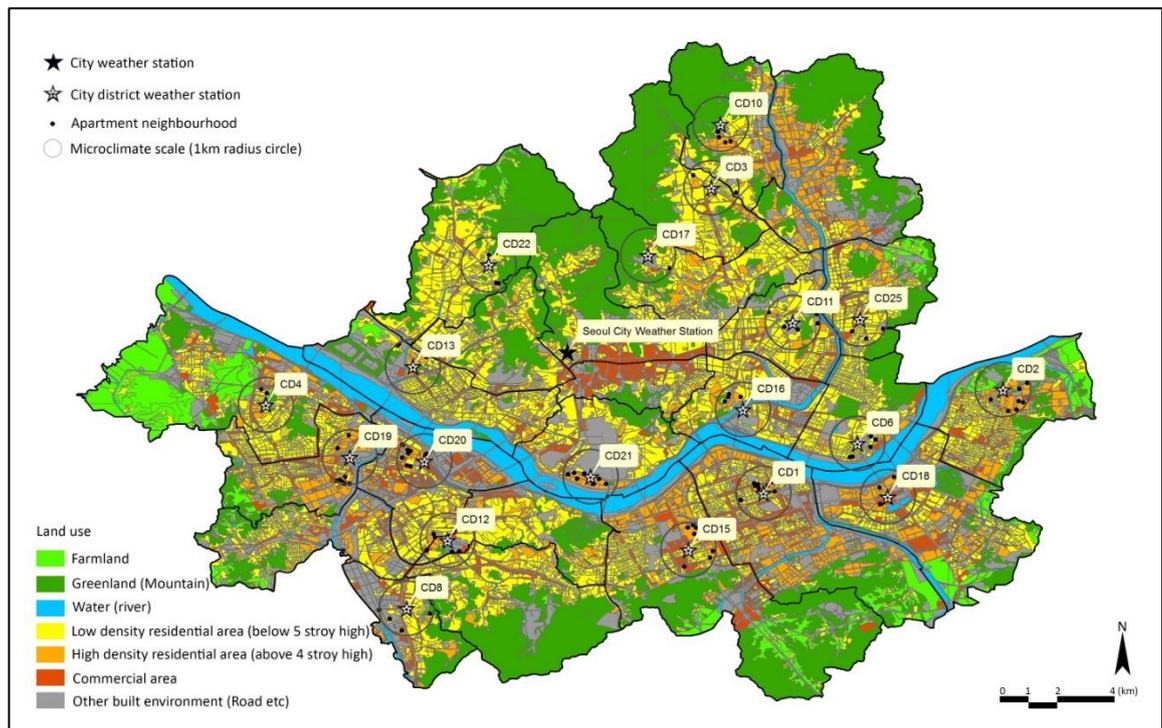


Figure 4-1. Locations of the 98 apartment neighbourhoods (ANs) within 1km radius of the 19 city district (CD) automatic weather stations (AWS) in Seoul highlighted for the study.

Table 4-1. The location information of Seoul's 19 City District (CD) Automatic Weather Station (AWS), and height and size information of the Apartment Neighbourhood (AN) within each CD-AWS 1km boundary (Source: KMA; AMIS, 2018b)

| | CD AWS info. | | | | | AN info. | | | |
|---|---|---|---|---|---|---|---|---|---|
| | Location | | Height info. | | | | | | |
| | Lat. | Long | Sea lv. (m) | Street lv. (m) | Roof lv. (Stories) | Avg. Top floor lv. | Avg. Min floor lv. | No. Apt. Building | No. Apt. |
| CD1 | 37.5134 | 127.0470 | 59.6 | 50.6 | 3 | 21 | 13 | 59 | 4193 |
| CD2 | 37.5555 | 127.1450 | 56.9 | 47.9 | 3 | 17 | 12 | 61 | 4977 |
| CD3 | 37.6397 | 127.0257 | 55.7 | 34.7 | 7 | 17 | 12 | 15 | 1517 |
| CD4 | 37.5499 | 126.8425 | 79.1 | 64.1 | 5 | 20 | 13 | 64 | 3519 |
| CD6 | 37.5336 | 127.0853 | 38.0 | 38.0 | 0 | 19 | 11 | 16 | 1692 |
| CD8 | 37.4655 | 126.9001 | 41.5 | 29.5 | 4 | 21 | 15 | 30 | 2156 |
| CD10 | 37.6661 | 127.0295 | 55.5 | 43.5 | 4 | 14 | 11 | 47 | 4862 |
| CD11 | 37.5846 | 127.0604 | 49.4 | 34.4 | 5 | 21 | 11 | 47 | 3387 |
| CD12 | 37.4937 | 126.9181 | 33.8 | 33.8 | 0 | 19 | 15 | 17 | 2049 |
| CD13 | 37.5655 | 126.9027 | 25.0 | 13.0 | 4 | 16 | 10 | 18 | 1192 |
| CD15 | 37.4889 | 127.0156 | 35.5 | 26.5 | 3 | 17 | 10 | 67 | 6565 |
| CD16 | 37.5472 | 127.0388 | 33.7 | 18.7 | 5 | 17 | 10 | 25 | 2065 |
| CD17 | 37.6117 | 126.9994 | 125.9 | 107.9 | 6 | 19 | 11 | 37 | 3033 |
| CD18 | 37.5115 | 127.0967 | 53.6 | 29.6 | 8 | 18 | 15 | 105 | 11276 |
| CD19 | 37.5296 | 126.8782 | 9.7 | 6.7 | 1 | 18 | 9 | 119 | 7892 |
| CD20 | 37.5271 | 126.9070 | 24.4 | 12.4 | 4 | 21 | 15 | 52 | 3980 |
| CD21 | 37.5204 | 126.9761 | 32.6 | 20.6 | 4 | 21 | 13 | 52 | 4681 |
| CD22 | 37.6077 | 126.9338 | 65.0 | 56.0 | 3 | 16 | 8 | 34 | 1976 |
| CD25 | 37.5855 | 127.0868 | 40.2 | 28.2 | 4 | 18 | 12 | 11 | 1087 |

Table 4-1 shows the locations of the 19 AWS, including height above sea level, estimated street and building roof level and the associated neighbourhood facts such as apartment building height and size. However, as the AWS data contains only location and height above sea level, the street level of each AWS was estimated from the sea level information given in KMA with 3m for each floor. For instance, CD1 AWS is placed on the top of a three-story building and thus, the likely street level is 50.6m (=59.6m-9.0m). Arguably, there are vertical variations in the distribution of air temperature observed in urban context regionally, seasonally, and diurnally (Jayamurugan et al., 2013). However, as most of the CD AWS are placed on building roof tops, the collected temperature data could be thought of as an influential weather variable affecting cooling energy use of the associated neighbourhoods. It should be highlighted here that the CD AWS datasets encompass urban heat island (UHI) effects wherever and whenever present in the district neighbourhoods.

**4.2.2. Cooling energy use data**

Due to the very high ratio of apartment buildings in South Korea, the Ministry of Land, Infrastructure and Transport (MoLIT) set up the Apartment Management Information System (AMIS) in 2010, under the country's open data and protection law - Article 23 in "Multi-family Housing Management Act" (MoLIT, 2016).

The AMIS was constructed to inform the monthly energy bill of each apartment neighbourhood including aggregate monthly utility bill for gas, electricity and water (Korean Won per square meter, KRW/m$^2$) and the amount of monthly electricity use (kWh/m$^2$, available since 2014). In order to withdraw cooling energy use data from the AMIS, the electricity "bill" data was chosen, especially for this study within chapter 4, as only the electricity bill mirrors energy use for summer cooling in Seoul (i.e. uses of household air-conditioning and electric fans). Notably, the spatial resolution of the AMIS energy bill data is an average monthly energy bill of each apartment neighbourhood not a single residential household's monthly energy bill. Therefore, the collected electricity bill data from each apartment district (Korean Won per square metre, KRW/m$^2$) reflects collective energy use for summer cooling specific to the placement of a neighbourhood.

The Korea Electric Power Corporation (KEPCO, 2016) have stated that the only electric power supplier in South Korea, currently 95% of total apartments in South Korea have their metres read on the same day (the18$^{th}$ of each month). It is therefore assumed that 95% is satisfactory for all apartments in this preliminary statistic relational study to have the same metre reading day. Bearing in mind their sample sizes, city districts containing fewer than 3 apartment neighbourhoods were not included in this paper. Thus, 19 city districts and a total of 98 apartment neighbourhoods (approx. 72,000 apartment households) were chosen for the study, each of which is within 1 km radius of the city-district weather station. Furthermore, considering the fact that the AMIS only started in

2010, going through the system testing period 2010-2013, 2012-14 were selected as the temporal range for the AMIS energy (electricity) bill data. Finally, the locations of the 98 apartment neighbourhood (AN) sites coupled with the 19 city-district weather station sites selected for the relational study are identified (Figure 4-1).

### 4.2.3. Property price data

The AMIS data portal also provides apartment property cost data by joining the information service of publicly noticed value (PNV) of real estate price (KAB, 2015a), which is preserved by the Korea Appraisal Board (KAB, 2017) under the MoLIT. Therefore, the apartment property price data in this study is not of market price, but of PNV for deciphering the household's property tax. Like energy use data, the unit of the property price is shown in Korean Won per square metre (KRW/m$^2$) and the length of time to collect was 2012-14.

### 4.2.4. Seoul's climate change projection data

First set up by the Korea Meteorological Administration (KMA), Seoul's Climate change datasets, projected by MK-PRISM (Modified Korean Parameter-elevation Regressions an Independent Slopes Model) (Kim et al., 2012; Kim et al., 2013a), are available at present at the Climate Information Portal (CIP). The future climate data available is daily maximum, minimum and mean temperature and rainfall up to Year 2100 at the city district level. The MK-PRISM model was engineered on the basis of the 2000-2010 weather data collected from the CD AWS sites with 1km horizontal resolutions taking into account topographic influence and data histogram.

There are four climate change scenarios used in this projection: Representative Concentration Pathways (RCP) 2.6, 4.5, 6.0, 8.5, representing $CO_2$ concentration touching 420, 540, 670 and 940 ppm in 2100 respectively. The RCP4.5 and RCP8.5 scenarios were selected in this study. Also, the projected daily mean temperature data for August was used to create a future peak monthly average temperature on the basis of the same metre reading day for electricity use data.

## 4.3. Methods

The first survey of the above open datasets from the 19 city districts suggests a need for a systematic approach to analysing the data in accordance to the research question. Hence, a data mining method was created in three steps in section 4.3.1: (1) extracting summer cooling energy use data (see also section 5.3.2 for the further developed analysis based on metred electricity use data, kWh/m$^2$), (2) identifying the summer cooling period and (3) data normalisation. Furthermore, to analyse the open data fairly, a statistic relational analysis framework and the workflow were developed in section 4.3.2, which allows to understand characteristics of residential cooling energy use with other multiple factors in diverse temporal and spatial resolutions.

### 4.3.1. Data mining

First of all, in searching for potential correlations between energy use (electricity bill) and urban weather data (air temperature etc.), it is essential to minimize inclusion of the non-weather-dependent electricity bill (Asimakopoulos et al., 2001). In this study, the rise (IR) of the monthly electricity bill during summer period was proposed as a cooling energy use index which can be calculated by the increment of electricity bill of each summer

month based on the non-weather-dependent electricity bill of the year. The non-weather-dependent bill can be thought of as the minimum electricity bill of the year, because it could potentially contain the operating costs of lighting and home appliances not affected by the external thermal conditions (Bronson et al., 1992). The equation for working out the monthly IR of an apartment neighbourhood is simply as follows (Equation 1), where $B_{sm}$ is the summer monthly electricity bill and $B_{min}$ is the non-weather-dependent electricity bill:

$$IR\ (\%) = \frac{(B_{sm} - B_{min})}{B_{min}} \times 100 \qquad\qquad (1)$$

It may be contentious whether the minimum electricity month excludes any cooling and heating energy use or not. In a real situation, it is difficult to be sure of this differentiation due to the complexity of user behaviour and circumstances in residential energy use. Here it was presumed that the month where the minimum electricity bill occurs was non-weather-dependent or, at least, it was minimal in cooling and heating energy use.
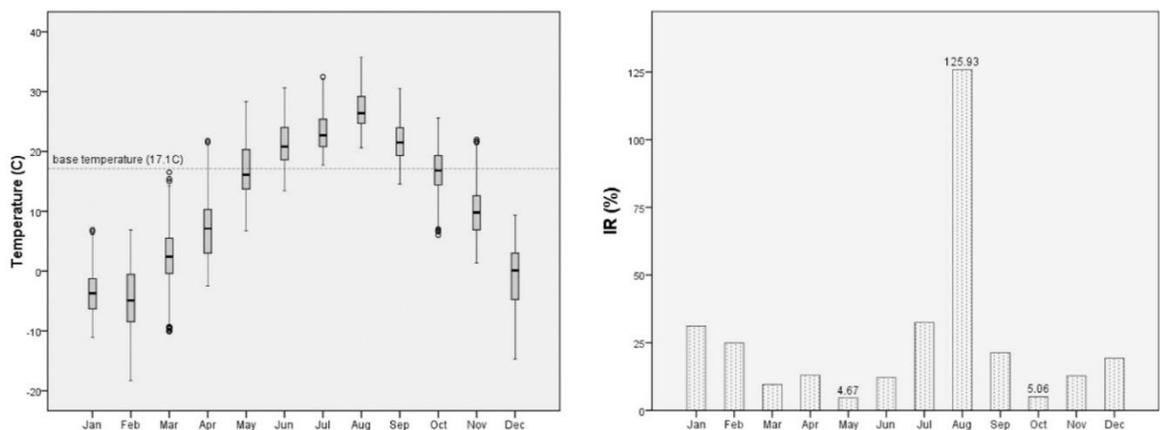


Figure 4-2. Monthly temperature distribution based on hourly dataset from city weather station for 2012 (left) and monthly IR data of aggregate of all 98 ANs across the 19 CD's boundaries

Figure 4-2 backs up this assumption, showing that monthly temperature distribution and the monthly IR in 2012 as an example. For Seoul, the base temperature for HDD and CDD was set at 17.1°C as a transition point of electricity demand from heating to cooling (Lee et al., 2014). As seen in monthly temperature distribution, May and October are placed on near the base temperature and therefore, about 60% of 98 ANs displayed that the minimum electricity bill occurred in May (28%) and October (29%). Furthermore, the minimum IR occurred in both months with only 4.67% and 5.06% respectively. More detailed analysis for identifying non-weather-dependent electricity use is presented in section 5.3.2.
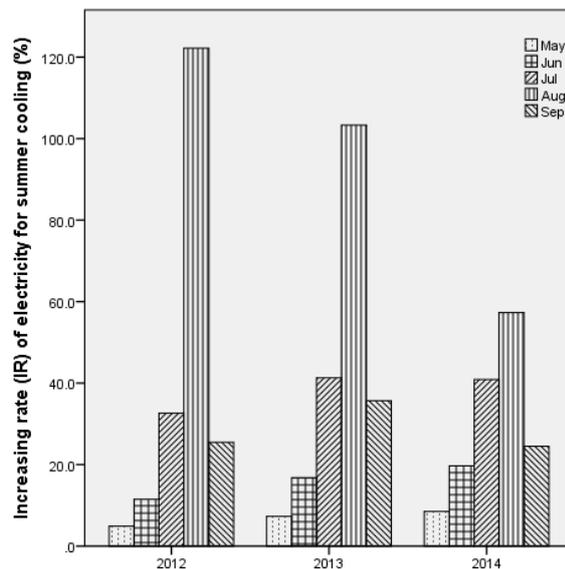


Figure 4-3. Distribution of the monthly mean IR indexes of the aggregated 98 apartment neighbourhoods in Seoul over May-September 2012-14

Secondly, the summer cooling period in Seoul was recognised by the monthly IR distribution (Figure 4-3). The Korean Meteorological Administration (KMA) currently states that June, July and August as the official summer months (KMA, 2014). However, it was proposed to look once more at the summer months in Seoul according to the distribution of the IRs during May and September 2012-2014 as Lee and Levermore

(2010) broadly defined the summer period by excluding winter period (Oct-Apr) in their previous study of the cooling degree days (CDDs) in South Korea. The lay out of the monthly IRs was calculated as the mean of monthly IR of the aggregated 98 apartment neighbourhoods in Seoul. Notably, the time unit (day) in the IR-based analysis is set to the metre reading day of electricity billing: the 18th of each month, which is also applied to the city-district weather station datasets.

Figure 4-3 shows that the summer cooling period in Seoul could be July-September rather than June-August as the KMA previously thought. Even though cooling energy use (IR) happened in May and June, the levels were significantly lower than the other months, which may be a sign of climate change. Through the monthly IR distribution analysis, July-September was identified as the summer cooling period in Seoul 2012-14, which was attached to the corresponding AWS datasets.

Table 4-2. Normality distribution of IR (increase rate of energy use for cooling) of the 98 apartment neighbourhoods (ANs) by each of the summer months and the summer period 2012-2014. * Values in () are square root transformed IR

|  | N | Mean | Std. D | Skewness | Kurtosis | Kolmogorov-Smirnov Sig. |
|---|---|---|---|---|---|---|
| Jul IR | 294 | 37.94 | 23.62 | .942 | .508 | .000 |
|  | (98ANs x 1mon x 3yr) | (5.86) | (1.90) | (.270) | (-.449) | (.077) |
| Aug IR | 294 | 96.02 | 48.77 | .803 | .446 | .002 |
|  | (98ANs x 1mon x 3yr) | (9.49) | (2.46) | (.254) | (-.519) | (.004) |
| Sept IR | 294 | 24.43 | 20.67 | 1.898 | 5.301 | .000 |
|  | (98ANs x 1mon x 3yr) | (4.44) | (2.17) | (-.015) | (.662) | (.000) |
| Summer Period IR (Jul–Sept) | 882 | 52.80 | 45.65 | 1.484 | 2.299 | .000 |
|  | (98ANs x 3mon x 3yr) | (6.60) | (3.05) | (.393) | (.017) | (.000) |

Finally, as the main statistical method of this study would be parametric statistics (e.g. Pearson correlation and analysis of variance), normality of the IR values was checked first. Also, it was performed by each summer month (July, August, and September)

during 2012-2014 due to the monthly time base of each parametric analysis. The output of normality distribution of the IR is shown in Table 4-2.
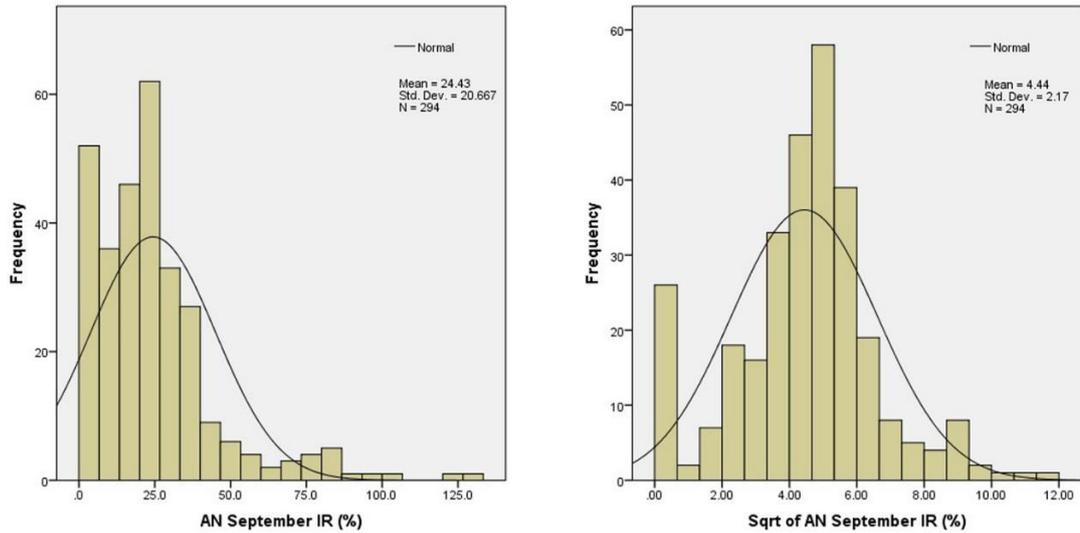


Figure 4-4. Normality distribution of original (left) and Sqrt transformed (right) September IR of the 98 apartment neighbourhoods (ANs).

The normality of July and August IR was primarily accepted as each value of skewness (the symmetry of the distribution) and Kurtosis (the 'peakedness' of the distribution) was less than 1. Although Sig. of Kolmogorov-Smirnov was less than .05 in all cases, this was normal in a larger sample (N>30) (Pallant, 2010, pp. 63). Nevertheless, as the September IR and the Summer Period IR did not meet normality condition, which skewness and Kurtosis were 1.898 (1.484) and 5.301 (2.299) respectively, the IR data was converted using square root (Sqrt) transformation recommended by Tabachnick and Fidell (2007, pp. 87). Considering the coherence of data transformation, all IR data was subsequently Sqrt transformed. Figure 4-4 shows the normality distribution of original (left) and Sqrt transformed (right), taking the September IR as an example.

## 4.3.2. A statistic relational analysis framework

A statistic relational analysis framework and the workflow are created for correlating cooling energy use with urban microclimate and property price data (Figure 4-5). Here the statistic relational studies are performed at two spatial scales: (a) at the macro-level, aggregating the 98 apartment neighbourhoods (ANs) within the AWS 1km boundaries across the 19 city districts, and (b) at the micro-level, aggregating only the ANs within each CD-AWS 1km boundary individually. The results from the correlational analyses provide a basis for estimating future summer peak energy demands given the climate change projections made available at the city-district level.
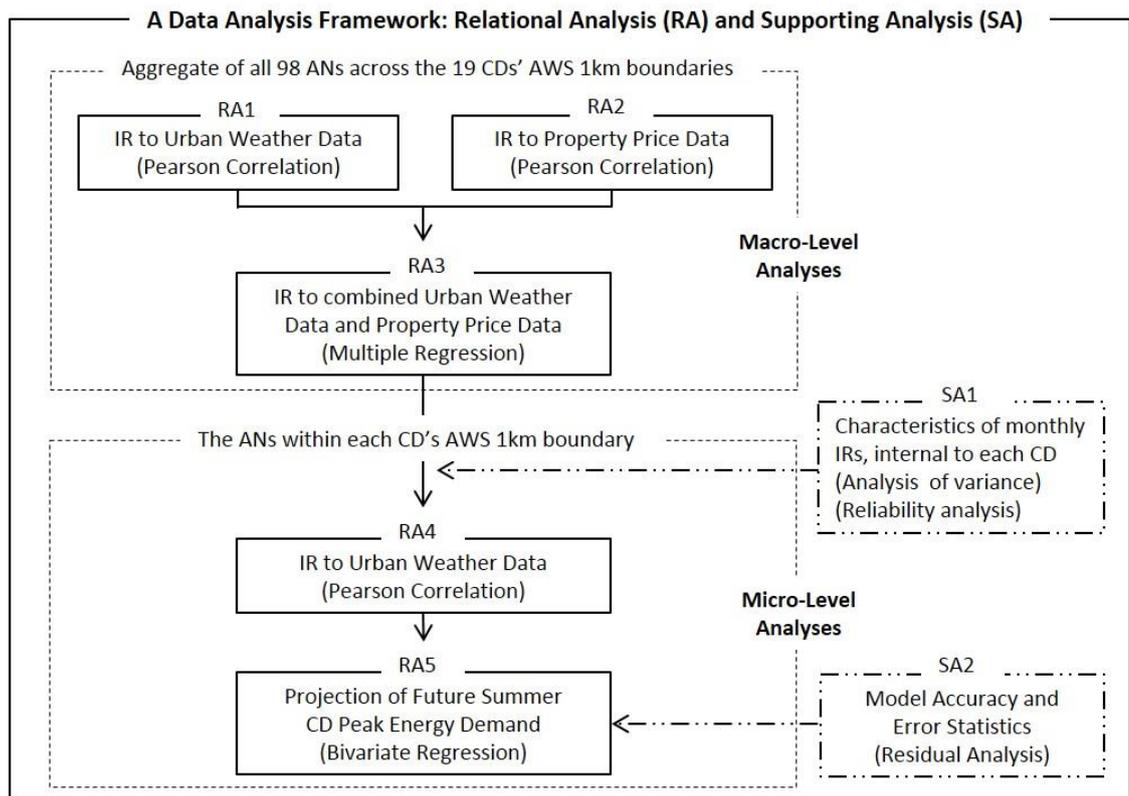


Figure 4-5. A statistic relational analysis framework for correlating cooling energy use with urban weather and property price data as a basis for projecting future summer peak energy demand

Firstly, at a macro-level, for the aggregated 98 apartment neighbourhoods (AN) chosen from the 19 CDs' AWS 1km boundaries, the relationships between cooling energy use (IR) and the two variables (urban weather and property price data) were investigated by Pearson correlation analyses (RA1, RA2). Then, a multiple linear regression analysis was completed to compare the impact of the two variables on IR (RA3). The purpose of the aggregation analyses at macro level is to investigate which parameter is the key deriver of residential cooling energy use in different summer months (July – September) overall. For instance, as described later (Section 4.4.1), the impact of urban weather on cooling energy use is much stronger than that of property price data in August (the hottest month of the year), while it is opposite in July (under milder summer month relative to August). This enables one to outline detailed micro-level analysis to understand the characteristics of residential cooling energy use responding to external temperature.

Secondly, at a micro-level, travelling into each CD's AWS 1km boundary individually, the number of apartment neighbourhoods varies from 3 to 10, the interaction between cooling energy use and urban weather data were examined in two aspects: (1) The huge range of IR by analysis of variance (SA1); (2) the relationship between IR and AWS data by Pearson correlation (RA4). Then, due to the varying strength of correlation in summer months and exceptionally strong relationship coefficients discovered in August (the hottest month of the year), a straight forward bivariate regression (SBR) model was derived for each of the 19 city district AWS boundaries (RA5). The SBR models were evaluated by residual analysis (SA2). Finally, the SBR models were applied to predict future peak energy demands of each city district using the climate change projection data for South Korea.

## 4.4. Results and discussions

In this section, the results of the proposed statistic relational analysis framework are offered and discussed. In accordance with the key steps presented in Figure 4-5, section 4.4.1 shows macro-level outputs (including RA1, RA2 and RA3) and section 4.4.2 displays micro-level outcomes (RA4 and SA1). Finally, given the results of RA4 and SA1, the estimating future peak cooling energy demands is presented in section 4.4.3 (RA5 and SA2).

### 4.4.1. Correlating cooling energy use with air temperature and property price at macro-level

### 4.4.1.1. Correlating cooling energy use with air temperature (RA1)

The relationship between the cooling energy use (Sqrt IR) and the urban weather (monthly average temperature) of the 98 apartment neighbourhoods within the 19 CDs' AWS 1km boundaries was scrutinised by Pearson correlation analyses. To confirm no violation of the assumption of normality, linearity and homoscedasticity, a preliminary analysis was performed for the whole summer period, and July, August and September of 2012-2014 (Figure 4-6).

Table 4-3 shows that there was an extremely strong and positive correlation between the two variables for the whole summer period (r=.770). For individual months, July (r=.574) and August (r=.749) show strong or very strong positive correlations but September (r=-0.009) shows negative, no correlation and no real significance.
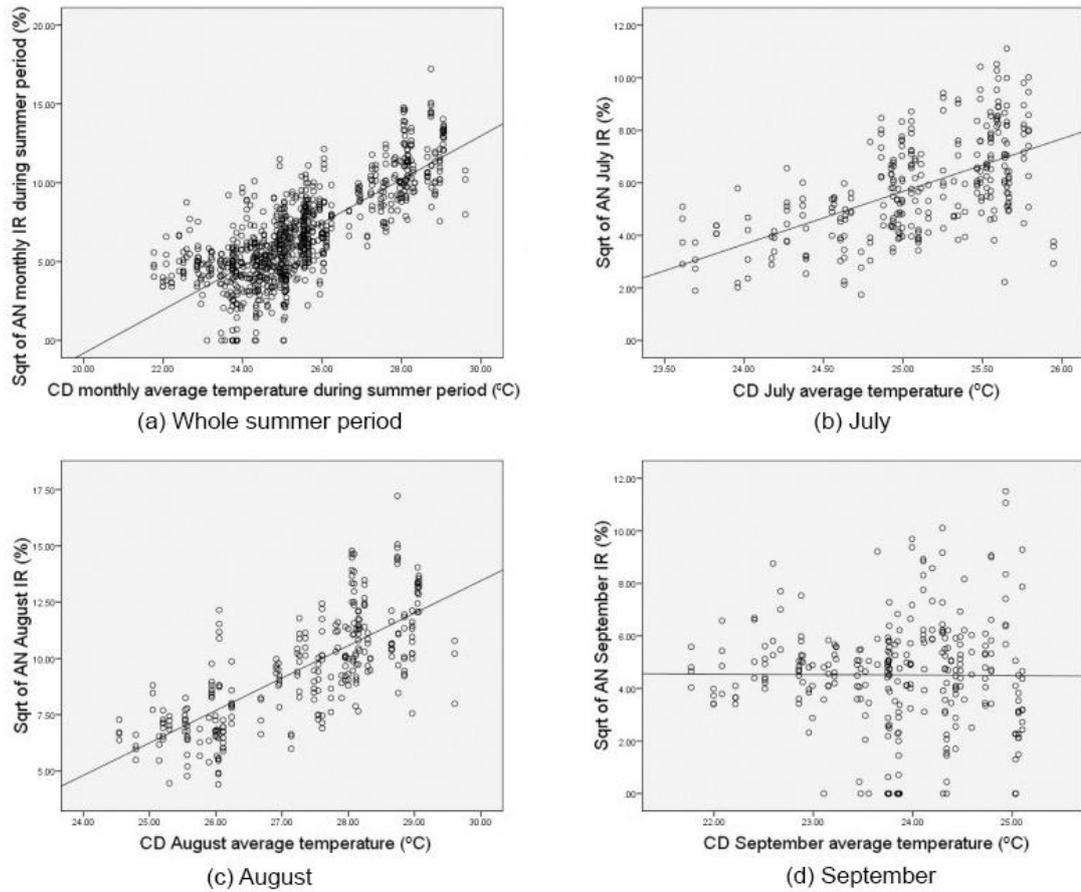
Figure 4-6. Scatterplot between cooling energy use (Sqrt IR) and monthly average temperature

Table 4-3. Correlation coefficients between cooling energy use (Sqrt IR) and monthly average temperature. **. $p < 0.01$ and *. $p < 0.05$

|  |  | Sqrt of AN monthly IR (Whole Summer) | Sqrt of AN monthly IR (July) | Sqrt of AN monthly IR (August) | Sqrt of AN monthly IR (September) |
|---|---|---|---|---|---|
| monthly average temperature | Pearson-C | .770** | .574** | .749** | -.009 |
|  | Sig. | .000 | .000 | .000 | .882 |
|  | r squared | .593 | .329 | .561 | .000 |
|  | N | 882 (98ANs*3Mon *3Yr) | 294 (98ANs*1Mon* 3Yr) | 294 (98ANs*1Mon* 3Yr) | 294 (98ANs*1Mon* 3Yr) |

To discover what might have contributed to the differences in the Pearson correlation coefficients seen in Table 4-3, another possible urban weather parameter, changes in humidity was looked into as the role of an air-conditioning system is to maintain not only

indoor air temperature but also humidity. However, as no humidity data was present at the AWS portal, the monthly temperatures were grouped into 2 types: monthly average temperature during Precipitation and Non-precipitation days (Table 4-4). It could be discussed if the humidity change can be simplified in those two temperature types. However, under the complexity of urban weather and limited data availability, it is assumed that the humidity situation in non-precipitation days is definitely drier than in precipitation days.

Table 4-4. Correlation coefficients between cooling energy use (Sqrt IR) and monthly average temperature in precipitation and non-precipitation days. **. $p < 0.01$ and *. $p < 0.05$

| | | Sqrt of AN monthly IR (Whole Summer) | Sqrt of AN monthly IR (July) | Sqrt of AN monthly IR (August) | Sqrt of AN monthly IR (September) |
|---|---|---|---|---|---|
| Precipitation monthly average temperature | Pearson-C | .738** | .443** | .693** | .027 |
| | Sig. | .000 | .000 | .000 | .647 |
| | r squared | .545 | .196 | .481 | .001 |
| | N | 882 (98ANs*3Mon *3Yr) | 294 (98ANs*1Mon* 3Yr) | 294 (98ANs*1Mon *3Yr) | 294 (98ANs*1Mon *3Yr) |
| Non-Precipitation monthly average temperature | Pearson-C | .762** | .525** | .746** | -.059 |
| | Sig. | .000 | .000 | .000 | .317 |
| | r squared | .580 | .276 | .556 | .003 |
| | N | 882 (98ANs*3Mon *3Yr) | 294 (98ANs*1Mon* 3Yr) | 294 (98ANs*1Mon *3Yr) | 294 (98ANs*1Mon *3Yr) |

Firstly, the cooling energy use over the whole summer phase (N=882, 98ANs*3Mon*3Yr) had a stronger correlation with non-precipitation average temperature (r=.762) than precipitation (r=.738), showing that air temperatures in non-precipitation days may have been more influential on residential cooling energy use. This was also ratified in the monthly correlation analysis: in July and August (N=294, 98ANs*1Mon*3Yr), the non-precipitation average temperature was more strongly linked with IR than precipitation. Secondly, comparing the two correlations in Table 4-3 and Table 4-4, the cooling energy use was more strongly correlated with monthly average temperature in the whole

summer period. Therefore, the left over relational study was carried out using only the monthly average temperature. However, the September case still showed no link, suggesting that under the mildest summer condition, other parameters such as solar radiation may be more influential than temperature.

**4.4.1.2. Correlating cooling energy use with apartment property price data (RA2)**

To give an explanation for possible human behavioural factors of cooling energy use (i.e., factors associated with decision on using cooling energy or not and how much), it was probed to see if cooling energy use was correlated to apartment property price data (Figure 4-8. c). However, physiological and psychological factors are not considered in this study due to the data limitation and complexity of those involuntary factors in the analysis. Here, it is assumed that the apartment property price is an overall gauge of the socio-economic circumstances of households, affecting residents' cooling energy use decisions. Since the property price data was circulated as the average price of 2012-2014, the correlation analysis was carried out based on total cooling energy use (IR) of the whole summer period and each summer month during 2012-2014; thus, the number of elements in all cases was 98. The property price data was also Sqrt transformed for data normalization. A one-way between-groups analysis of variance (ANOVA) was conducted to explore the difference of Sqrt of property price in each of the districts. The ANOVA output shows that the difference in the mean scores on the property price variable for 19 city districts is statistically significant: the sig. ($p$) was .000, less than .05.

Table 4-5. Correlation coefficients between cooling energy use (Sqrt IR) and Sqrt of property price 2012-2014. **. *p*<0.01

|  |  | Sqrt of total AN monthly IR (Whole Summer) | Sqrt of total AN monthly IR (July) | Sqrt of total AN monthly IR (August) | Sqrt of total AN monthly IR (September) |
| --- | --- | --- | --- | --- | --- |
| Sqrt of AN property price | Pearson-C | .712** | .698** | .708** | .101 |
|  | Sig. | .000 | .000 | .000 | .324 |
|  | R-squared | .507 | .487 | .501 | .010 |
|  | N | 98 | 98 | 98 | 98 |

Table 4-5 shows that the two variables had positive and very strong coefficient during the entire summer (r=.712). Nevertheless, the strength of the monthly coefficients varied, July (r=.698), August (r=.708), September (r=.101), suggesting higher cooling energy use correlated with higher apartment property prices. Surprisingly when comparing the two correlations in Table 4-3 and Table 4-5, the July correlation coefficient of property price (r=.698) was much more significant than that of average temperature (r=.574). This could be due to the fact that under milder weather conditions (July in this case), the socio-economic factor, as mirrored in the apartment property price data, can be more influential than the external weather conditions on cooling energy use. To go into more depth, a multiple regression analysis was carried out to investigate the combined effect of urban weather data and property price data on cooling energy use in the next section.

### 4.4.1.3. Effect of combined air temperature and property price on cooling energy use (RA3)

In the first place, the multi-collinearity was assessed using tolerance and VIF (Variance inflation factor) in collinearity statistics. The tolerance and VIF in 4 cases were not below .10 and not higher than 10 respectively, so the multi-collinearity assumption was not violated (Pallant, 2010, pp.157): whole summer period (.969 and 1.032), July (.751 and 1.332), August (.951 and 1.052) and September (.820 and 1.220). Also, a preliminary analysis for regression model was performed to check outliers, normality,

linearity, homoscedasticity and independence of residuals through inspecting the normal

probability plot (P-P) of the regression standardised residual and the scatterplot (Figure

4-7).
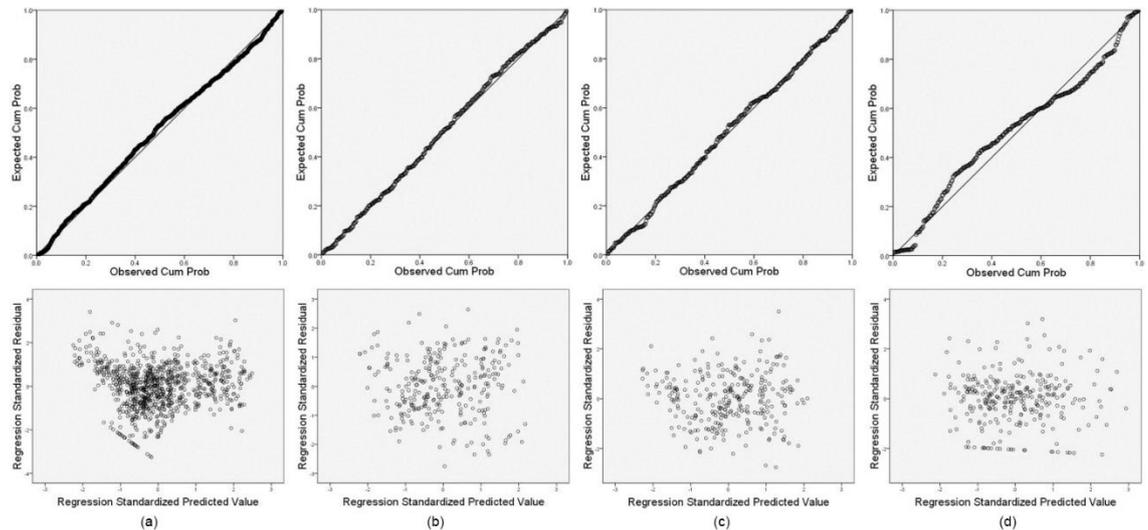


Figure 4-7. Normal P-P plots of regression standardized residual and the scatterplots for summer period, July, August and September. * Dependent variable: Sqrt of apartment neighbourhood (AN) monthly IR for whole summer period (a); for July (b); for August (c); for September (d)

The probability plot shows all the times reasonably placed in the straight diagonal line

except September (slightly biased): therefore, no large deviations from normality were

found in all cases. Moreover, in the scatterplot, there were no significantly great number

of points of more than 3.3 or less than -3.3: hence, no presence of outliers (Tabachnick

and Fidell, 2007, pp.125). This was also confirmed by looking closely at the Mahalanobis

distances, comparing to critical chi-squared value, that is, the distance must be less than

13.82 in case of 2 numbers of independent variables (Pearson and Hartley, 1958;

Tabachnick and Fidell, 2007): maximum Mahalanobis distance for whole summer (8.936); for July (8.866); for August (8.573); for September (8.611).

Table 4-6. Multiple regression analyses to investigate effect of combined monthly average temperature and Sqrt of property price on cooling energy use (Sqrt IR)

| Case regression model | Dependent | Independent | $B$ | Std. error | Beta | Sig. |
|---|---|---|---|---|---|---|
| Whole Summer Period<br><br>$R^2 = .613$,<br>$p = .000$ | Sqrt of AN monthly IR for whole summer months | (Constant) | -29.656 | .973 | | .000 |
| | | Monthly average temperature | 1.332 | .038 | .744 | .000 |
| | | Sqrt of AN property price | .001 | .000 | .146 | .000 |
| July<br><br>$R^2 = .506$,<br>$p = .000$ | Sqrt of AN monthly IR for July | (Constant) | -28.245 | 3.964 | | .000 |
| | | July average temperature | 1.162 | .167 | .331 | .000 |
| | | Sqrt of AN property price | .002 | .000 | .485 | .000 |
| August<br><br>$R^2 = .655$,<br>$p = .000$ | Sqrt of AN monthly IR for August | (Constant) | -30.282 | 1.808 | | .000 |
| | | August average temperature | 1.304 | .068 | .679 | .000 |
| | | Sqrt of AN property price | .002 | .000 | .314 | .000 |
| September<br><br>$R^2 = .007$,<br>$p = .224$ | Sqrt of AN monthly IR for September | (Constant) | 6.422 | 3.839 | | .095 |
| | | September average temperature | -.129 | .172 | -.048 | .453 |
| | | Sqrt of AN property price | .001 | .000 | .094 | .147 |

Table 4-6 displays the result from the regression analysis. Firstly, the regression model explained 61.3%, 50.6% and 65.5% of the variance in the Sqrt of neighbourhood monthly IR for whole summer period, July, and August 2012-2014 respectively; the statistical meaning in all 3 models was .000 (p<.0005). Secondly, evaluating each of the stand-alone variables, the impact of each variable on cooling energy use was different. In the entire summer period model, the impact of microclimate temperature (the standardised coefficient, Beta, .744) on cooling energy use was much higher than the property price (.146). This implies that the microclimate conditions (as reflected by the monthly average

temperature) are more of a dominant influence on residential cooling energy usage during the summer period overall.

However, comparing the Beta values between July and August, while the bearing of average property price (.485) was higher than that of monthly average temperature (.331) in July, the temperature (.679) was more influential on cooling energy use than the price (.314) in August. This suggests that only under the high temperature of August, the influence of the weather on cooling energy use is more dominant than that of the socio-economical (as reflected by the property price). However, under the lower temperature of July, the socio-economic factor appears more dominant.

### 4.4.2. Correlating cooling energy use with air temperature at micro-level (RA4)

Following the three relational analyses above at the macro-level (RA1-RA3 in Figure 4-5), the characteristics of residential cooling energy use (SA1) were investigated and then, further correlational analysis (RA4) was performed at the micro-level, looking into the apartment neighbourhoods within each city district's AWS 1km boundary.

### 4.4.2.1. Characteristics of monthly cooling energy use (SA1)

Firstly, the characteristics of the residential cooling energy use were investigated with external temperature and property price. Figure 4-8 (a) displays the August average air temperatures (19 Jul – 18 Aug, 2012) recorded at each city district AWS in Seoul, the hottest period during 2012-2014. The highest average August cooling energy use came up also in 2012 (Figure 4-8. b). However, at that time the average temperatures varied, and the gap between the highest and lowest was about 2.65°C (the highest 29.61°C occurred at CD25, while the lowest 26.96°C at CD22).
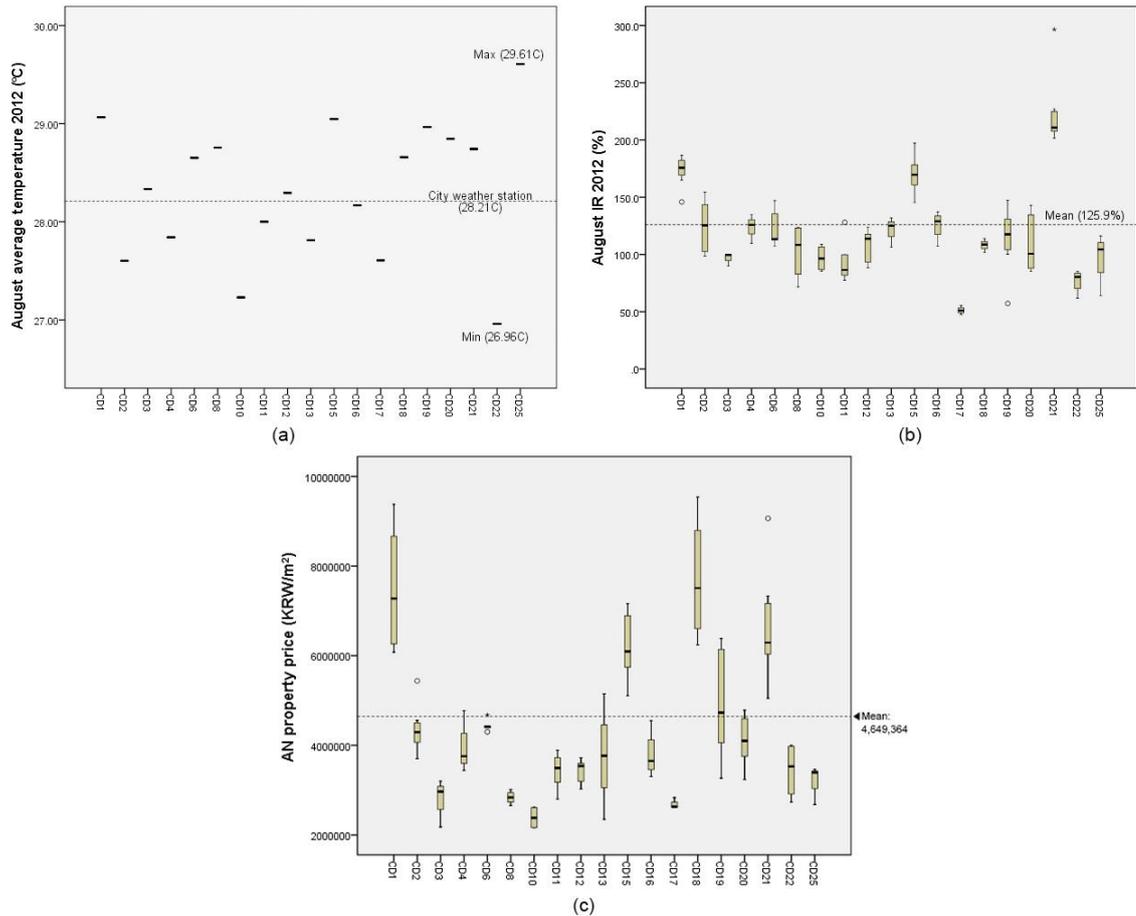
Figure 4-8. The August average temperature (a) and August ANs' IR (b) in 2012, and ANs' property price (c) within each of the 19 CDs' AWS 1km boundary

Furthermore, a number of city district temperatures differed significantly from the Seoul City Weather Station temperature (28.21°C). The August IR for cooling energy use also shows noticeable differences across the 19 city districts. However, these two measurements are not always in agreement with our instinct that higher air temperatures correspond to higher IRs and vice versa. As shown by the macro analyses above, socio-economic factor (reflected in the property price, Figure 4-8. c) could also affect cooling energy use massively. For instance, CD25 is an example: low IR, high temperature, and low property price band. The highest IR happened at CD21 (high temperature, high property price band), while the lowest IR occurred at CD17 (low temperature, low

property price band). Arguably, there can be other factors in determining residential cooling energy use, such as building characteristics (age, glazing ratio and air-conditioning penetration rate). If those on-site measurements in more detail are available, the relationship between cooling energy use and building characteristics can be further investigated.
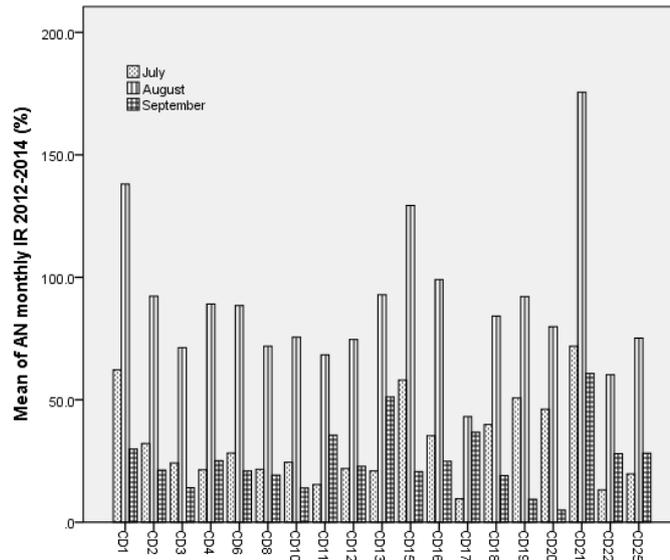


Figure 4-9. Mean of apartment neighbourhoods (ANs') monthly IR of each city district by July, August and September of 2012-14

Table 4-7. Analysis of variance (ANOVA) of monthly IR of July, August and September, 2012-2014, across the 19 city districts

|  | F | Sig. ($p$) |
| --- | --- | --- |
| Sqrt July IR | 26.308 | .000 |
| Sqrt August IR | 9.285 | .000 |
| Sqrt September IR | 14.708 | .000 |

Secondly, as shown in Figure 4-9, the mean of apartment neighbourhood's IRs of each individual city district during the summer period varied. For example, CD21 had the highest IR for all the 3 months during 2012-14, while CD17 had the lowest IR for July

and August and relatively large for September. The difference in cooling energy use across the 19 CDs was looked into by a one-way between-groups analysis of variance (ANOVA). As the climate conditions of each summer month were not the same, the ANOVA was carried out monthly for July, August, and September, 2012-2014. The ANOVA result in Table 4-7 displays that the difference in the monthly IR of the 19 CDs is statistically significant ($p < .05$)

Table 4-8. Cronbach's alpha coefficients and correlation coefficients between inter-items of monthly cooling energy use (IR) in each city district's AWS 1km boundary: () standardised Cronbach's alpha

|  | Cronbach's alpha coefficients | Correlation coefficients between inter-items (N=9, Jul to Sep 2012-14) |  |  |  |  |  | No. of ANs |
|---|---|---|---|---|---|---|---|---|
|  |  | Avg. | Min | Max | Range | Max/Min | variance |  |
| CD1 | .982 (.985) | .893 | .741 | .996 | .255 | 1.344 | .007 | 8 |
| CD2 | .986 (.992) | .945 | .876 | .994 | .118 | 1.135 | .001 | 7 |
| CD3 | .948 (.949) | .860 | .742 | .922 | .180 | 1.243 | .008 | 3 |
| CD4 | .990 (.993) | .978 | .960 | .992 | .032 | 1.034 | .000 | 3 |
| CD6 | .989 (.995) | .977 | .952 | .991 | .038 | 1.040 | .000 | 5 |
| CD8 | .922 (.941) | .799 | .554 | .962 | .408 | 1.737 | .018 | 4 |
| CD10 | .992 (.993) | .973 | .959 | .998 | .039 | 1.041 | .000 | 4 |
| CD11 | .953 (.968) | .860 | .693 | .953 | .260 | 1.375 | .008 | 5 |
| CD12 | .985 (.991) | .958 | .912 | .975 | .063 | 1.069 | .000 | 5 |
| CD13 | .974 (.978) | .936 | .890 | .991 | .101 | 1.114 | .002 | 3 |
| CD15 | .984 (.985) | .892 | .638 | .997 | .359 | 1.562 | .011 | 8 |
| CD16 | .986 (.990) | .961 | .931 | .989 | .058 | 1.062 | .001 | 4 |
| CD17 | .839 (.880) | .710 | .453 | .916 | .462 | 2.022 | .044 | 3 |
| CD18 | .965 (.972) | .896 | .779 | .981 | .202 | 1.260 | .008 | 4 |
| CD19 | .990 (.994) | .946 | .737 | .999 | .262 | 1.355 | .003 | 10 |
| CD20 | .990 (.993) | .946 | .810 | .996 | .186 | 1.230 | .003 | 8 |
| CD21 | .988 (.989) | .928 | .828 | .995 | .167 | 1.202 | .003 | 7 |
| CD22 | .959 (.960) | .857 | .731 | .984 | .253 | 1.345 | .007 | 4 |
| CD25 | .947 (.974) | .927 | .882 | .962 | .080 | 1.090 | .001 | 3 |

Moreover, it was looked at that there appears a close similarity of monthly IR distribution within each CD boundary in Figure 4-8 (b). To confirm this with figures, the internal consistency and the similarity was examined using Cronbach's Alpha and correlation coefficients between inter-items (monthly IR of each AN) respectively. As seen in Table 4-8, the Cronbach's alpha coefficients in all CDs were above 0.9 except CD17, but even CD17 was above 0.8. Furthermore, the average of correlation coefficients between inter-

items was above 0.7 in all examples. This means high internal consistency and similarity in terms of the layout of AN's monthly cooling energy use within each CD-AWS 1km boundary. Therefore, it is sensible to assume that the apartment buildings are mostly surrounded with homogeneous parameters of multiple factors affecting residential cooling energy use beyond microclimate conditions, such as building physical characteristics. The detailed apartment building information was explored in the following subsection.

### 4.4.2.2. Apartment building information

Holistically speaking, energy use for cooling in the context of this study can be thought of as a human comfort and economic decision in response to the result of dynamic interaction between building envelope and surrounding urban microclimate. The differences or similarities of physical thermal properties of the apartment buildings play a specific role in the characteristics of cooling energy use seen at the city district level. Nevertheless, here in Chapter 4 of this study, one adopts an "all in the energy bill" approach as a wrapper encompassing some aspects of the complex physical interactions. Nonetheless, some key building evidence is presented in this subsection.

First of all, the building insulation criteria (U-value) according to the year of building regulation applied (Table 4-9) was collected. Figure 4-10 (a) shows that there is one dominant insulation regulation type in each CD boundary although some CDs are not the same (e.g. CD8 & 15). However, even those 2 CDs can be put into one dominant insulation type because the adjacent insulation criteria have similarity in terms of the U-value (see Table 4-9). Secondly, as seen in Figure 4-10 (b), there appears to be a similarity in the size of a household within the given categories of floor area collected from AMIS.
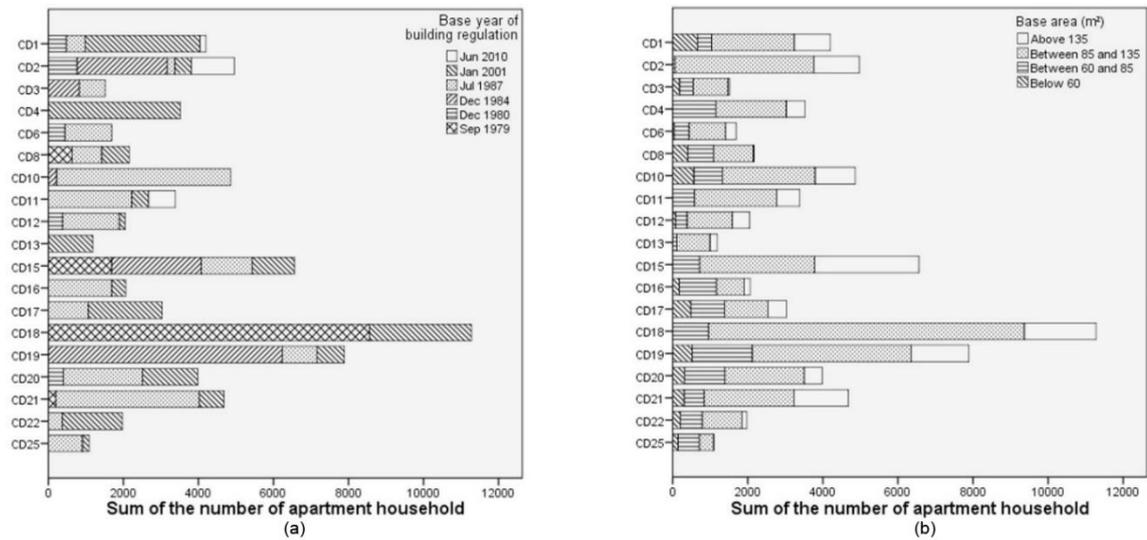
Figure 4-10. The number of apartment households (units) within each CD-AWS boundary according to the building insulation criteria applied in certain built years (a) and the ranges of floor area (b)

Table 4-9. Insulation criteria for Seoul's housing stock according to the year of building regulation applied (U-value, $W/m^2*K$). (Source: Kim et al., 2013b) *Side wall represents the external wall without opening area, such as glazing

| Building regulation | Base year | External wall | External/ Ground Floor | External Roof | Side wall | Window |
|---|---|---|---|---|---|---|
| R1 | Sep 1979 | 1.05 | 1.05 | 1.05 | - | 2.56 |
| R2 | Dec 1980 | .58 | 1.16 | .58 | - | 3.49 |
| R3 | Dec 1984 | .58 | .58 | .58 | .47 | 3.49 |
| R4 | Jul 1987 | .58 | .58 | .41 | .47 | 3.37 |
| R5 | Jan 2001 | .47 | .35 | .29 | .35 | 3.84 |
| R6 | Nov 2008 | .47 | .35 | .29 | .35 | 3.0 |
| R7 | Jun 2010 | .36 | .30 | .20 | .27 | 2.1 |

Thirdly, an apartment building's glazing ratio and its orientation can affect its internal solar gain to a large degree. However, the cost of collecting such thorough building information is prohibitive given the large sample size (72,104 apartment buildings in total). Here this study referred to a previous paper on glazing ratio (Kim et al., 2010) and assume that the 98 ANs may have similar glazing ratios (Table 4-10). However, given

this restricted information, the characteristic of glazing ratio within each CD boundary remains inconclusive.

Table 4-10. Average glazing ratio (%) of the apartment building by type of apartment building. (Source from Kim et al., 2010)

| Faced orientation | Tower type | Slab type | Total (Tower +Slab) |
|---|---|---|---|
| South | 61.48 | 34.98 | 41.91 |
| East | 48.57 | 22.00 | 28.80 |
| West | 70.19 | 25.65 | 36.10 |
| North | 56.49 | 46.30 | 49.48 |

### 4.4.2.3. Correlating cooling energy use with air temperature within microclimate boundary (RA4)

When the characteristics and internal consistency of monthly cooling energy use in each CD are looked at, a relational study between cooling energy use (Sqrt IR) and urban weather data was performed within each CD-AWS 1km boundary. Shown in Table 4-11, for the whole of the summer stage, there were positive and very strong correlation coefficients between Sqrt IR and monthly average air temperature in most CDs (r>.700 and even r>.900 in some cases). Nonetheless, several city districts stand out with relatively smaller correlation coefficients (r<.700), for example, CD11, CD13, CD17 and CD22.

Amongst the monthly correlation coefficients, the August correlations were the strongest and most measurable, while July varied and September were the weakest, showing no relation or even negative. Moreover, the August coefficients increased hugely even in the aforementioned four city districts, compared to whole summer correlation coefficients. This suggests that under extreme weather conditions, such as August (being the hottest month in Seoul), the outside temperature can be the key parameter in affecting

residential cooling energy use in most CDs. Though under relatively milder weather conditions (i.e. July or September), there may be other parameters affecting cooling energy use.

Table 4-11. Correlation coefficients between cooling energy use (Sqrt IR) and monthly average temperature within each CD-AWS 1km boundary. **. $p<0.01$ and *. $p<0.05$

| | Whole summer months (Jul – Sept inclusive) | | | July | | August | | September | | |
|---|---|---|---|---|---|---|---|---|---|---|
| | Pears-C | Sig. | N | Pears-C | Sig. | Pears-C | Sig. | Pears-C | Sig. | N |
| CD1 | .883** | .000 | 72, 8ANs | .306 | .146 | .913** | .000 | .143 | .504 | 24, 8ANs |
| CD2 | .890** | .000 | 63, 7ANs | .523* | .015 | .877** | .000 | -.114 | .624 | 21, 7ANs |
| CD3 | .850** | .000 | 27, 3ANs | .323 | .397 | .959** | .000 | .043 | .912 | 9, 3ANs |
| CD4 | .909** | .000 | 27, 3ANs | .863** | .003 | .937** | .000 | .001 | .997 | 9, 3ANs |
| CD6 | .928** | .000 | 45, 5ANs | .691** | .004 | .918** | .000 | .100 | .723 | 15, 5ANs |
| CD8 | .819** | .000 | 36, 4ANs | -.055 | .865 | .836** | .001 | .118 | .716 | 12, 4ANs |
| CD10 | .942** | .000 | 36, 4ANs | .742** | .006 | .972** | .000 | .069 | .831 | 12, 4ANs |
| CD11 | .628** | .000 | 45, 5ANs | .509 | .052 | .738** | .002 | -.088 | .755 | 15, 5ANs |
| CD12 | .891** | .000 | 45, 5ANs | .552* | .033 | .943** | .000 | .006 | .984 | 15, 5ANs |
| CD13 | .649** | .000 | 27, 3ANs | .869** | .002 | .870** | .002 | -.084 | .830 | 9, 3ANs |
| CD15 | .881** | .000 | 72, 8ANs | .283 | .180 | .931** | .000 | .415* | .043 | 24, 8ANs |
| CD16 | .932** | .000 | 36, 4ANs | .802** | .002 | .948** | .000 | .385 | .217 | 12, 4ANs |
| CD17 | .267 | .178 | 27, 3ANs | -.282 | .462 | .684* | .042 | -.432 | .246 | 9, 3ANs |
| CD18 | .896** | .000 | 36, 4ANs | .263 | .408 | .960** | .000 | .401 | .196 | 12, 4ANs |
| CD19 | .848** | .000 | 90, 10ANs | -.136 | .475 | .838** | .000 | .702** | .000 | 30, 10ANs |
| CD20 | .829** | .000 | 72, 8ANs | -.339 | .106 | .909** | .000 | .213 | .317 | 24, 8ANs |
| CD21 | .898** | .000 | 63, 7ANs | .696** | .000 | .883** | .000 | -.210 | .361 | 21, 7ANs |
| CD22 | .616** | .000 | 36, 4ANs | -.045 | .890 | .726** | .007 | .004 | .990 | 12, 4ANs |
| CD25 | .739** | .000 | 27, 3ANs | -.861** | .003 | .774* | .014 | -.328 | .388 | 9, 3ANs |

The results of the monthly correlation coefficients discovered at the micro-level are similar to those found at the macro-level (see section 4.4.1.1, Table 4-3): August (strongest, r=.749); July (strong, r=.574); September (negative and no correlation, r=-.009). However, looked at the micro-level, the strength of correlation coefficients varies among the CDs. It can be understood that there are not only temporal variations in relationship between residential cooling energy use and urban microclimate data, but also spatial variations.

### 4.4.2.4. Other parameters affecting residential cooling energy use

Why did the 4 CDs (CD11, CD13, CD17 and CD22) demonstrate relatively smaller correlation coefficients (Table 4-11)? Firstly, usual to these CDs is a relatively small sample size (3 to 5 ANs). As the statistical approaches performed in this study are parametric, the output can be sensitive to sample size. For example, the internal consistency and the correlation coefficients between inter-items of those 4 CDs are relatively minor (see Table 4-8), especially, the minimal coefficient in CD17 was only .453. With a slight sample size, such a weak internal consistency could result in a weak relationship.

Secondly, there may be other variables (e.g. solar radiation) affecting cooling energy usage in such CDs. As recent studies have discovered that air temperature and solar radiation play a significant role in residential cooling energy use at the same time (Flor & Domınguez, 2004; Salvati et al., 2017), the probability of solar radiation on these 4 CDs was investigated, through deciphering floor area ratio (FAR) and site coverage ratio (SCR) as a density indicator (Figure 4-11). Here both the FAR and SCR are the percentage ratios actually used in the 98 existing ANs, not inferred from the building regulation of land use.

Intriguingly, there appears to be characteristics in the FAR of the four CDs: one or two ANs had massively different FAR values. The different density may affect non identical internal solar gains and in turn, lead to different cooling energy use, resulting in fragile internal consistency, and finally, it results in smaller correlation coefficients within a little sample size. However, the SCR plot is not clear. This implies that those four CDs, showing relatively poorer correlation coefficients, may need to take solar radiation into account in correlating cooling energy use. Finally, there may be socio-economic factors (e.g. property price) usual to these CDs that belong to a relatively lower property price

band (see Figure 4-8. c). Here the socio-economic issue as represented by property price may be more influential than the external temperature even in August.
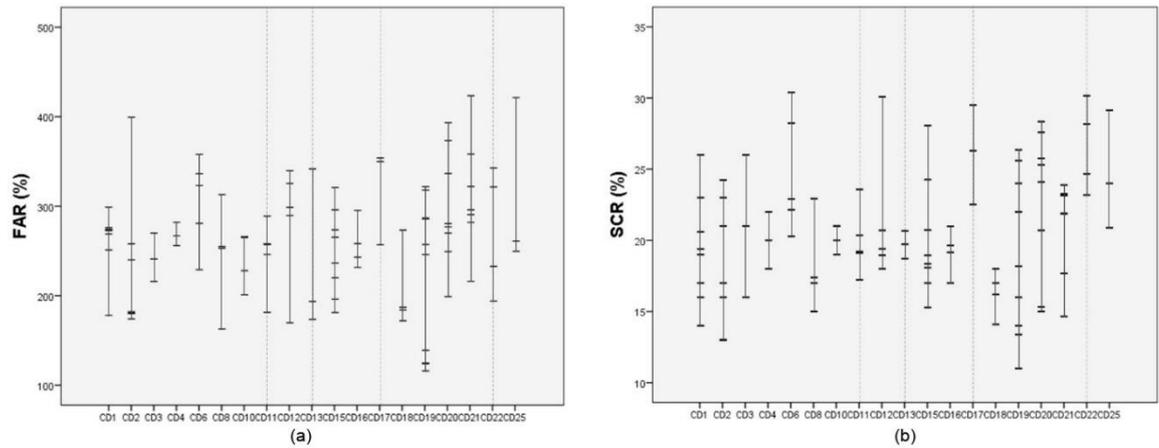


Figure 4-11. The actually applied floor area ratio (FAR) (a) and site coverage ratio (SCR) (b) of ANs within each CD-AWS boundary

### 4.4.3. Estimating future peak cooling energy demands

Given the outcome of the Pearson correlation analysis of IR to monthly average temperature (RA4), which was corroborated by ANOVA and Cronbach's alpha coefficients analyses (SA1), city-district specific energy models are resultant in estimating future peak cooling energy demands according to the latest climate change projection for Seoul. This is attained by a bivariate regress analysis (RA5, section 4.4.3.1) checked by model accuracy and error statistics (SA2, section 4.4.3.2). The peak demand presumptions for each city district are then presented in section 4.4.3.3.

**4.4.3.1. Simple bivariate regression (SBR) models (RA5)**

As the cooling energy use (IR) shows a very strong link with the external temperature in August, a simple cooling energy use model for estimating peak cooling demand for each CD boundary can be derived from bivariate regression. The reason for this modelling exercise is to estimate cooling energy use for each city district (within the AWS 1 km boundary), not for a single apartment neighbourhood. Hence, the dependent variable (Sqrt IR) must be the sum or an average of all ANs' IR within each CD boundary as its peak cooling energy use.

Table 4-12. Coefficients of simple bivariate regression (SBR) models for estimating each CD's peak cooling demand within its AWS 1km boundary

| Sqrt of AN Aug IR of | Constant | | CD Aug Avg. temp | | R | $R^2$ | Adjusted $R^2$ | Sig. | N |
|---|---|---|---|---|---|---|---|---|---|
| | $B$ | $p$ value | $B$ | $p$ value | | | | | |
| CD1 | -30.126 | .000 | 1.505 | .000 | .913 | .834 | .827 | .000 | 24 (8 ANs) |
| CD2 | -34.159 | .000 | 1.632 | .000 | .877 | .769 | .757 | .000 | 21 (7 ANs) |
| CD3 | -27.637 | .000 | 1.315 | .000 | .959 | .919 | .908 | .000 | 9 (3 ANs) |
| CD4 | -31.872 | .001 | 1.526 | .000 | .937 | .878 | .860 | .000 | 9 (3 ANs) |
| CD6 | -31.228 | .000 | 1.466 | .000 | .918 | .843 | .831 | .000 | 15 (5 ANs) |
| CD8 | -23.132 | .005 | 1.148 | .001 | .836 | .699 | .669 | .001 | 12 (4 ANs) |
| CD10 | -33.680 | .000 | 1.603 | .000 | .972 | .945 | .940 | .000 | 12 (4 ANs) |
| CD11 | -18.437 | .017 | .985 | .002 | .738 | .544 | .509 | .002 | 15 (5 ANs) |
| CD12 | -31.226 | .000 | 1.463 | .000 | .943 | .889 | .880 | .000 | 15 (5 ANs) |
| CD13 | -14.240 | .027 | .895 | .002 | .870 | .756 | .722 | .002 | 9 (3 ANs) |
| CD15 | -39.766 | .000 | 1.828 | .000 | .931 | .867 | .861 | .000 | 24 (8 ANs) |
| CD16 | -28.738 | .000 | 1.427 | .000 | .948 | .899 | .888 | .000 | 12 (4 ANs) |
| CD17 | -3.229 | .439 | .367 | .042 | .684 | .468 | .392 | .042 | 9 (3 ANs) |
| CD18 | -34.153 | .000 | 1.564 | .000 | .960 | .921 | .913 | .000 | 12 (4 ANs) |
| CD19 | -34.035 | .000 | 1.563 | .000 | .838 | .702 | .691 | .000 | 30 (10 ANs) |
| CD20 | -42.146 | .000 | 1.838 | .000 | .909 | .826 | .818 | .000 | 24 (8 ANs) |
| CD21 | -35.252 | .000 | 1.749 | .000 | .883 | .780 | .769 | .000 | 21 (7 ANs) |
| CD22 | -9.425 | .096 | .657 | .007 | .726 | .527 | .480 | .007 | 12 (4 ANs) |
| CD25 | -17.332 | .067 | .926 | .014 | .774 | .599 | .541 | .014 | 9 (3 ANs) |

Nevertheless, due to the small sample size (N=3, 2012-2014 August) imposed by the limited time phase of the current AMIS data availability, an alternative was thought about. As seen in section 4.4.2.1, the characteristic of ANs IR data displays that there is very good internal consistency and similarity in terms of the distribution of ANs' monthly

cooling energy use (Sqrt IR) within each CD boundary. Built upon these findings, the Sqrt IR of individual ANs within each CD boundary was used as a dependent variable. The resultant 19 SBR models are displayed in Table 4-12.

### 4.4.3.2. Model accuracy and error statistics (SA2)

To evaluate the SBR model accuracy, error statistics between predicted and observed CD cooling energy use was calculated. The SBR model was taken from ANs' IR data within each CD boundary for August 2012-14 as the training data; the Sqrt of average ANs' IR within each CD boundary for August 2015 (provided by the AMIS) was utilised as the testing data. Five criteria (i.e., Catalina et al., 2013) were worked out using the following equations, where $y_i$ is the predicted and $y_i'$ is the observed: mean absolute error (MAE); mean square error (MSE); root mean square error (RMSE); mean absolute percentage error (MAPE); coefficient of determination ($R^2$).

$$MAE = \frac{\sum_{i=1}^{n} |y_i - y_i'|}{n} \tag{2}$$

$$MSE = \frac{\sum_{i=1}^{n} (y_i - y_i')^2}{n} \tag{3}$$

$$RMSE = \sqrt{\frac{\sum_{i=1}^{n} (y_i - y_i')^2}{n}} \tag{4}$$

$$MAPE = \frac{\sum_{i=1}^{n} \left| \frac{y_i - y_i'}{y_i} \right|}{n} \tag{5}$$

Table 4-13. The error statistics between the predicted and the observed Sqrt of average CD IR for August 2015 in each city district's AWS 1km boundary

| Error statistics | Sqrt CD Avg. IR |
|---|---|
| MAE | .538 |
| MSE | .443 |
| RMSE | .665 |
| MAPE | .062 |
| $R^2$ | .882 |
| | |
| Residuals (%) | |
| Min. residual | -1.294 |
| Max. residual | 1.410 |
| Avg. residual | -.244 |
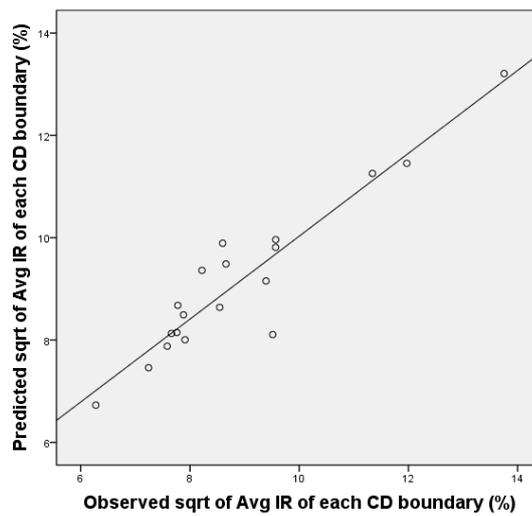


Figure 4-12. Scatter plot between the predicted and the observed Sqrt of average CD IR for August 2015 in each city district's AWS 1km boundary

Table 4-13 shows the output of the error statistics calculation. The average residual was near to 0 (-.244) and the mean absolute percentage error (MAPE) was 6.2 %. Furthermore, the coefficient of determination from the scatter plot between the observed and the predicted was .882 (Figure 4-12), representing over 88% of variance in the observed CD IRs was clarified by the corresponding bivariate regression model. From this, the SBR models are considered rationally acceptable. Also, the other way of using

individual ANs IR within each CD boundary for estimating CD peak cooling energy uses was confirmed methodologically.
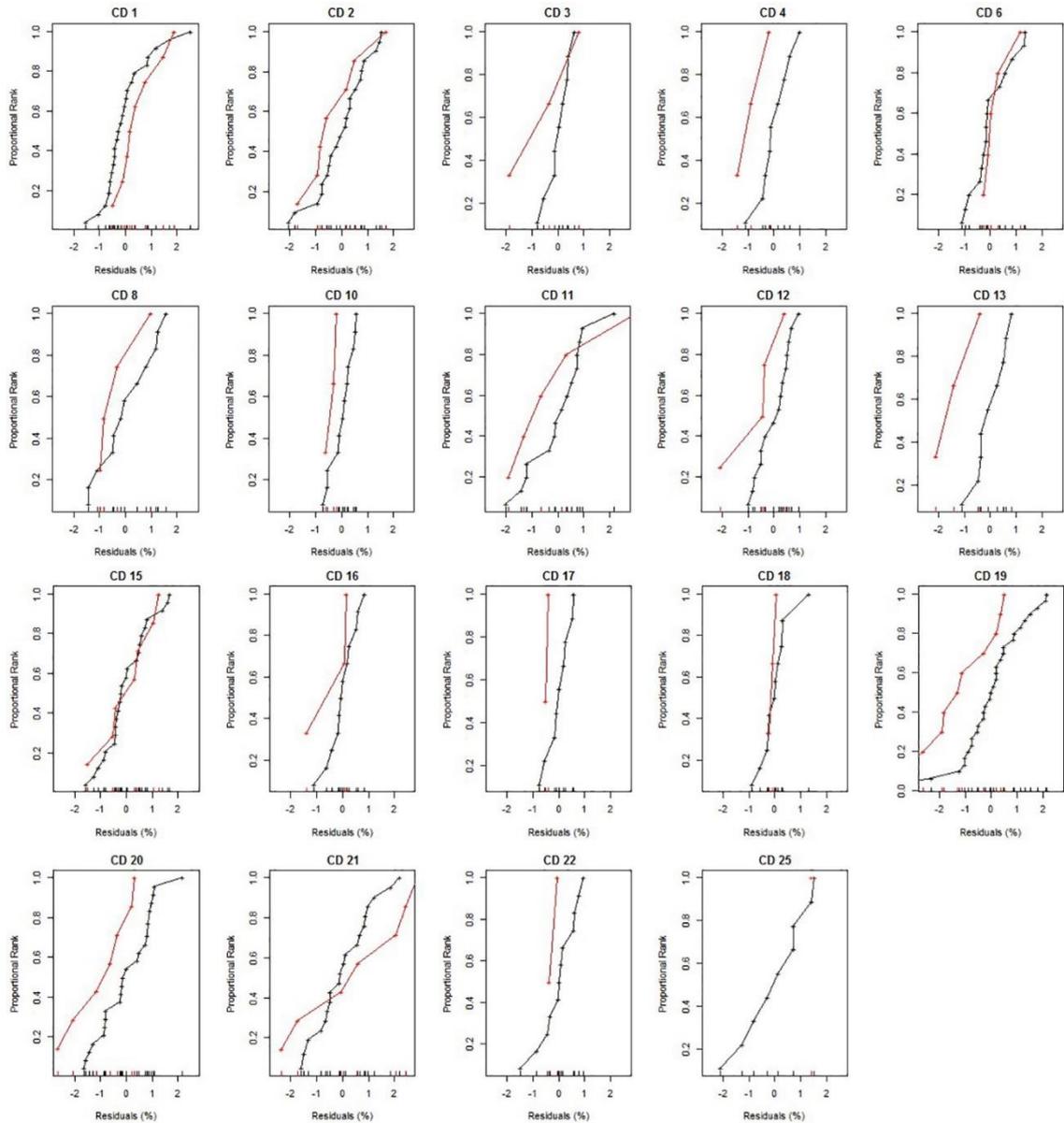


Figure 4-13. Comparative analysis of residuals between observed and estimated Sqrt average IR of each city district's (CD's) AWS 1km boundary for August 2012-14 (in black as the training set) and 2015 (in red as the testing set)

To judge the behaviour (bias) of the two residuals—relatively changed or unchanged, a comparative analysis between 2012-14 (training) and 2015 (testing) was performed on the residuals between predicted and observed AN IR in each CD. Figure 4-13 displays the outputs of the comparative analysis: the training residuals for 2012-14 are in black, and the testing for 2015 are in red.

First of all, the bias between red and black line was looked at. Some CDs, such as CD4, 10, 12, 13, 17, 19, 20, show that all 2015 residuals (red) are to the left of 2012-14 (black), showing that 2015 had lower residuals than 2012-14. This suggests that the presumed energy use (Sqrt IR) for those CDs could be underestimated. CD2, 3, 8 might be close to those CDs because only one 2015 residual in each case was right-biased slightly towards 2012-14. Secondly, a number of CDs had a very similar behaviour between the two residuals, such as CD1, 6, 15, 18, showing similar fit in 2015 to 2012-14 and most of the 2015 residuals were close to 0, meaning the predicted residuals were close to the observed. This shows that the predicted energy uses in these CDs are reasonably sure. Hence, CD16 and CD22 could be similar to these CDs because their 2015 residuals were close to zero even though left-biased.

Conversely, some CDs (CD11, 21, 25) are inconclusive. In CD11, most of 2015 residuals were left-biased but the max residual was primarily right-biased. Given the small sample size, it is hard to draw any conclusion. In CD21, the 2015 residuals were more greatly distributed compared to 2012-14, meaning that less variation shown by the model in 2015 than in 2012-14. CD 25 is a special case where very little can be said due to lack of data for 2015.

### 4.4.3.3. Projection of future peak cooling demands incorporating climate change projections

Thinking about the limitation on accuracy and reliability, the SBR models presented in Table 4-12 can be applied to estimating future summer peak energy demand if future urban climate projections are offered. For the city districts in Seoul, climate change projections made by MK-PRISM (Modified Korean Parameter-elevation Regressions on Independent Slopes Model) is open and two RCP (Representative Concentration Pathways) scenarios were chosen for this study: RCP4.5 and RCP8.5. RCP4.5 is the scenario of $CO_2$ concentration reaching at 540 ppm in 2100, while RCP8.5 at 940 ppm. The hottest August of the year was recognised in both scenarios within 2050s using monthly average temperature between 19th of July and 18th of August (see Figure 5-2 for more detail). Thinking about the same meter-reading day for electricity bill, the temperature projections for 2045 (RCP 8.5) and 2047 (RCP 4.5) were generated.
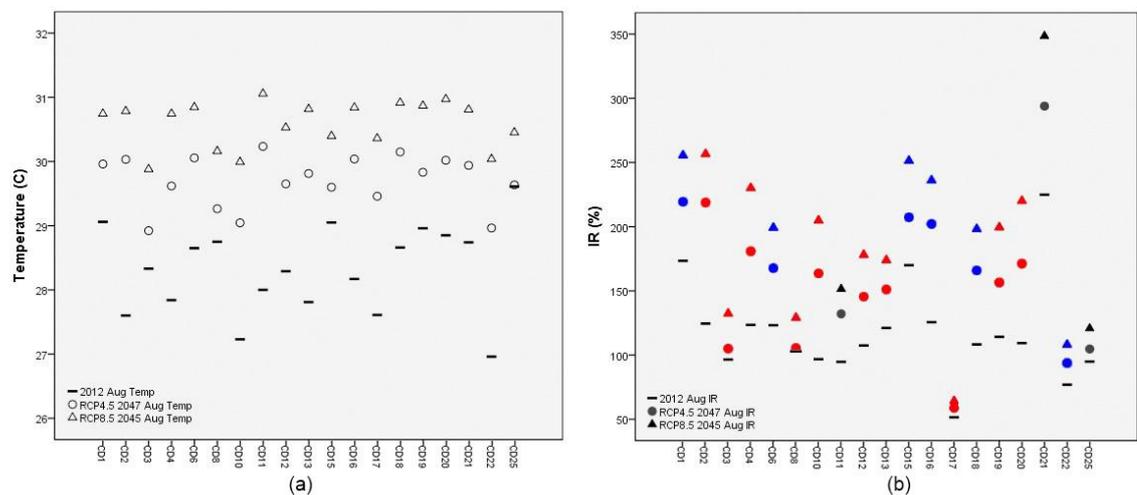


Figure 4-14. Projected August average temperature (a) and predicted future peak (August) cooling demands (b) in each of city districts' AWS 1km boundary using two different climate change RCP scenarios, RCP4.5 (2047) and RCP8.5 (2045). * red for underestimated; blue for reasonably confident; black for non-defined confidence

Figure 4-14 displays the projected August average temperatures and future peak cooling demands predicted by the SBR models. The 2012 Temp-IR profiles (being the hottest year during 2012-14) are included for reference. As discussed in above section 4.4.3.2, the confidence level was shown up using different colours: red for underestimated; blue for reasonably confident: black for non-defined confidence.

As the MK-PRISM climate change dataset was created with a horizontal resolution of 1km x 1km and the CD-AWS data of 2000-2010, the range of temperature changes between 2012 and 2047 RCP4.5 (or 2045 RCP8.5) varies across the city districts. For example, under the RCP4.5, the minimum increase of temperature between 2012 and 2047 occurs in CD25 ($0.03^\circ$C) while the maximum occurs in CD2 ($2.43^\circ$C). Secondly, the projection of cooling energy use (IR) is more dynamic and complicated. For example, the predicted Min and Max IR increase occurs in CD17 (6%, underestimated) and CD2 (96.1%, underestimated) respectively, showing that the predicted cooling energy increase may not always align with projected temperature increase in a linear way (CD 17 is not projected to have the lowest temperature rise between 2012 and 2045/47, as seen in Figure 4-14.

Finally, a comparison between the Min (CD17) and Max (CD21) cooling demands predicted for future years points to a prospective challenge/threat to resident's health and well-being living in CD17 if the neighbourhood environment stays largely unchanged. Though the August average temperature of CD17 and CD21 in 2012 (2047) was $27.61^\circ$C ($29.46^\circ$C) and $28.74^\circ$C ($29.94^\circ$C), and the IR was 51.5% (57.5%) and 224.9% (292.8%), the cooling energy bill of CD21 was predicted to increase by 67.9% due to a rise of $1.2^\circ$C, while CD17 was predicted to increase by just 6% in response to an increase of $1.85^\circ$C. Here it is seen a potentially significant negative impact on the health and well-being of residents living in CD17: potential high indoor temperatures lasting for a protracted period of time without adequate cooling energy uses.

## 4.5. Conclusions

Based on the open data of the city districts in Seoul, South Korea, Chapter 4 offered a relational study on correlating cooling energy use with local weather stations and property price data. The overall macro-level statistical analyses showed that there were temporal (monthly) differences in correlating cooling energy use with urban weather data in terms of strength of correlation coefficients during summer months. A further relational study of sole residential neighbourhoods at the micro-level showed that there were temporal and spatial (city-district) variations. As the August correlation coefficients appeared the most significant across all city districts, up to r=.972, a simple bivariate regression (SBR) model was derived for the residential neighbourhoods within each city district border to predict peak cooling energy use. When taking into account the latest climate change projections for Seoul, the SBR models were used to estimate potential increases of cooling energy use for each city district's residential districts in August 2050s'. The following subsections discussed the details (section 4.5.1-2) and the implications of the proposed future peak cooling energy demands for sustainable resilience as well as citizen's health and wellbeing (section 4.5.3). Finally, the limitations and further developments were discussed to outline a dwelling stock energy modelling framework, specified for the purpose of assessing heat stress vulnerability (section 4.5.4).

### 4.5.1. The temporal (monthly) variations

The connection between cooling energy use and the two factors, urban microclimate data (i.e., monthly average temperature) and property price data, was looked at in the analyses of the aggregated 98 ANs across the 19 CDs' 1km boundaries at the macro-level. The cooling energy use was very strongly linked with both of the two factors for the whole summer period (July to September): urban microclimate (r=.770); property price

(r=.712). Nevertheless, there were significant temporal variations in the strength of correlation coefficients in each month of the summer period. Initially, it was found that there were temporal variations in correlating cooling energy use with urban microclimate data: July (r=.574); August (r=.749); September (r=-.009). Next, the correlation coefficients between cooling energy use and property price also had temporal differences: July (r=.698); August (r=.708); September (r=.101). Thirdly, the joint effect of urban microclimate and property price on cooling energy use varied in each summer month: in July, the impact of property price (Beta, .485) was more instrumental on cooling energy use than urban weather (.331) while the urban weather (.679) was more dominant than the property price (.314) in August. This implies that under the high temperature of August, the effect of weather condition on cooling energy use is more dominant than that of the property price (as reflecting socio-economic backgrounds). However, under lower temperature of July, the socio-economic factor appears more dominant.

### 4.5.2. The temporal and spatial variations

Looking closely at the micro-level, there were unique characteristics of cooling energy use within each of the 19 CD boundaries. It was discovered that the difference in cooling energy use of the 19 CDs was statistically significant ($p$=.000 in all summer months). Furthermore, there was extremely crucial internal consistency and similarity in terms of the distribution of ANs' monthly cooling energy use within each CD boundary. This shows that there are certain aspects that affect a similar range of cooling energy use in each CD boundary, such as homogeneous microclimatic conditions and building physical features or socio-economic factors. Given the characteristics, the relational study between cooling energy use and microclimate data was investigated within each CD's AWS 1km boundary. There were not only temporal (monthly) disparities in relationship

between the two variables, but also spatial (each CD) disparities. This suggests that the residential cooling energy use should be individually studied within each CD AWS boundary to mirror its own characteristics of cooling energy use.

### 4.5.3. Implications of the projected future peak cooling demands

Notwithstanding the temporal and spatial variations, it was commonly found that all CDs had the strongest correlation coefficients for August. The simple bivariate regression (SBR) model for each CD was created to estimate future peak cooling energy requirements. Given Seoul's MK-PRISM climate change projections made at the CD level, the estimates of neighbourhood-specific peak cooling energy demands for future years were created. The variety of temperature changes between 2012 and 2047 RCP4.5 (or 2045 RCP8.5) varied across the 19 CD boundaries. Additionally, following the temperature diversity and the SBR model in each CD boundary, the projection of cooling energy use was more dynamic and complicated, for example CD17 and CD21: while the increased temperature from 2012 to 2047 (RCP4.5) was 1.85$^\circ$C (CD17) and 1.2$^\circ$C (CD21), the increased IR was predicted to only 6% at CD17 but 67.9% at CD21. Furthermore, the absolute amount of IR in 2047 (RCP4.5) was predicted to 57.5% (CD17) but to 292.8% (CD21). This implies that the internal thermal circumstances of the apartment buildings in CD17 may be more inferior to those in CD21, affecting residents' health and well-being if they are unable to increase cooling energy uses due to socio-economic restraints. However, identifying main source of the differentiated residential cooling energy use remains uncertain due to the limited data availability of building characteristics in more detail, such as AC penetration and building facade.

## 4.5.4. Limitations and further developments

First of all, the accuracy of energy model to predict peak cooling energy demands remains unclear due to the small sample size. As the AMIS only started in 2010, going through the system testing period 2010-2013, the study was restricted to the energy bill dataset of 2012-14. Also, as the spatial boundary of AWS 1km radius was set rendering to the urban microclimate scale, the selected number of apartment neighbourhoods within each CD boundary was also limited. Therefore, the temporal and spatial scope set for data collection in this chapter 4 study resulted in small sample size for the statistical analyses. Nevertheless, if the energy use data can be collected constantly into the forthcoming years, the sample size will be significant enough to conduct more relational analyses and identify other key parameters affecting residential cooling energy use. Therefore, prediction of peak cooling energy requirements could perform better through model improvement with an increased sample size.

However, sampling housing stock requires a deep level of consideration in urban climatic variations as this study is developed with the consideration of the relationship between residential cooling energy use and urban microclimate. In a perspective of urban climate zone (UCZ, Oke, 2004), which identifies areas of 'homogeneity' and oppositely distinguishes areas of transition climatically, 1km boundary is an 'acceptable' maximum distance to climatic change in urban area. However, the actual scene is much more complicated in the urban context regionally. For instance, even in the local climate zone (LCZ), which is classified by homogenous built environments or ecosystems (Steward, 2011), the thermal differentiation was observed vertically and horizontally (Stewart and Oke 2012): averaging about 2K in compact high-rise LCZ; and about 1.5K in open high-rise LCZ. Thus, the challenging body of knowledge in sampling housing stock is how to determine neighbourhood scale taking into account climatic homogeneity. A recent urban climate modelling technique has proposed a method to construct urban local

climate with spatial resolution of 200m (Lin et al., 2019). Employing the urban climate modelling method can be considered in sampling housing stock.

Secondly, applying the projected relational analyses framework, further SBR models can be produced at an individual apartment neighbourhood level if urban microclimate data is obtainable for each apartment neighbourhood. In the microclimatic point of view, the range of the urban microclimate could be much smaller than 1km. Although it was thought that the climatic condition within 1km radius of the CD AWS would be similar, in fact there could be variety of climates even 1km boundary such as solar radiation. The lengthy study could include measurements of other climatic variables in affecting cooling energy use, such as humidity, wind pattern and solar radiation. However, including such climatic parameters may be challenging because it should meet certain requirement in terms of data homogeneity: temporal and spatial. The temporal extent of this study was monthly time-based and the spatial was of the neighbourhood scale. Evaluating impacts of wind pattern and solar radiation on residential cooling energy use will involve site-specific spatial data (i.e. around individual apartment complex building) and a narrower time line (i.e. hourly data), considering characteristics of these two parameters. From a microclimatic point of view, the variations of the two factors are far more dynamic spatially and temporally than temperature. Within the neighbourhood range and monthly time-line scope, wind pattern and solar radiation cannot be generalized into monthly value. Also the effect of those climatic variables should be considered incorporating the individual household's building layout and glazing ratio data. To obtain the data required at this spatial-temporal resolution, computation intensive CFD-based urban microclimate simulation might be needed.

Finally, the AMIS energy bill data utilised for extracting IR (%, as the cooling energy use index) was an average monthly energy bill of every apartment neighbourhood not a single residential household's monthly energy bill, reflecting collective energy use for

summer cooling specific to the neighbourhood location. Therefore, there is a limitation to reflect the diversity of households' energy use individually. Furthermore, as concluded in section 4.5.3 above, the implication of energy modelling requires urgent action, looking into dwellings' indoor thermal conditions in relation to residents' health and well-being. However, owing to a complexity of the billing tariff system, the energy bill based modelling method is limited to estimating the actual amount of cooling energy demand (i.e., $kWh/m^2$), which further enables to estimate indoor thermal environment for assessing occupants' health. This implies that for the purpose of dwellers' health related study, using actual energy use data should be considered in the energy modelling process. Moreover, given the characteristics of the similarity and very useful internal consistency in both monthly cooling energy use and building physical configurations within each CD microclimate boundary, the current energy model can be further developed to a stock energy model on the basis of *archetype* potentially.

# Chapter 5. Developing archetypes for building physics

## 5.1. Introduction

In the absence of reliable field measurements of dwellings' indoor thermal conditions in the city context, the possible approach to obtaining a replaceable indicator of indoor thermal measurements can be found in developing archetypes for building physics. As the study in Chapter 4 concluded, the spatial resolution of residential neighbourhoods within a microclimate boundary can capture a set of homogeneous datasets in terms of dwellings' cooling energy use and building physical characteristics, the archetypes can potentially be defined within each boundary. Then, each archetype can be specified with known sources of building and occupancy information as input requirements for EnergyPlus model calibration process to estimate indoor thermal conditions.

EnergyPlus was used for model calibration process in this study. It has been developed by the U.S. Department of Energy's (DOE) Building Technologies Office (BTO) and designed for modelling energy loads for HVAC, lighting, and water use in buildings (EnergyPlus, 2018). As a whole building energy simulation tool, EnergyPlus enables to estimate building thermal interactions between integrated and simultaneous thermal zones, under the given building energy use datasets in relation to the predefined HVAC system and control strategies. The accuracy of EnergyPlus has been largely validated (e.g. Tabares-Velasco et al., 2012; Mateus et al., 2014; Harish and Kumar, 2016).

However, the model calibration process also requires detailed energy use profile and occupancy operation parameters. The question therefore is how can archetypes be developed for estimating present indoor thermal conditions of a city's dwelling stock? To what extent, can the collected data be analysed and developed for the EnergyPlus model calibration? Finally, what do archetypes' present indoor thermal conditions look like? The aim of this chapter is to obtain the HVAC cooling temperature set points as estimated ranges of indoor temperatures, which for the purpose of this thesis reflect a certain level

of dwellers' indoor heat acclimatisation determined under adaptive opportunities (see section 6.2.4 for more details). In turn, these present-day estimates are used in developing neighbourhood specific models for estimating archetypes' peak cooling demands associated with indoor conditions in line with climate projections.

The city of Seoul was identified as a case study to apply the methodological framework described in Chapter 3 to assess potential heat stress vulnerability of Seoul's dwelling stock in a future climate. The data collection of Seoul's apartment neighbourhoods 2014-2050s is presented in section 5.2. Then, the details of data analyses for developing archetypes of Seoul's dwelling stock are described in section 5.3. Finally, the outputs of archetypes' present indoor thermal conditions are presented and discussed in section 5.4. The concluding remarks are provided in section 5.5.


## 5.2. Data collection of Seoul's apartment neighbourhoods 2014-2050s

In general, a number of datasets are considered essential inputs to residential energy modelling including physical characteristics of building envelope, occupancy data, home appliances, historical energy use data, climate conditions and economic data (indicators) (Swan and Ugursal, 2009). For the purpose of heat stress vulnerability assessment, this study focuses on data collection on possible factors affecting residential cooling energy use in the city context of Seoul.

For the Seoul study, the main datasets required as inputs include: (1) urban weather data collected at microclimate boundaries within which one or more residential neighbourhoods reside, (2) residential neighbourhood household energy use data, (3) high-resolution climate projections at city-district level, and (4) building-related information for developing archetypes representative of a city's dwelling stock. After a

preliminary survey of the availability of residential energy use data, 18 city-district microclimate boundaries were identified for data collection and analysis.

### 5.2.1. Urban microclimate data

Climate is one of the most influential parameters in building thermal and energy performance modelling. Here temperature (dry-bulb) was chosen to represent the key characteristics of urban microclimate as measured by the city-district AWS sites in Seoul. The detailed background information of the 18 CD AWS sites identified for data collection is shown in Table 5-1.

Table 5-1. The location and height information of Seoul's 18 City District (CD) Automatic Weather Stations (AWS) and size information of the apartment stock within 1km radius of each CD-AWS (Source: KMA; AMIS, 2018b). *The street level was estimated from the sea level height with 3m for each floor

| City-district Neighbour-hood | CD AWS | | | | Dwelling stock | | | |
|---|---|---|---|---|---|---|---|---|
| | Lat. | Long | Sea lv. (m) | Street lv. (m) | No. Apt. Neighbour-hoods | Avg. Top floor lv. (storey) | No. Apt. Building | No. Apt. House-hold |
| CD1 | 37.5134 | 127.0470 | 59.6 | 50.6 | 7 | 20 | 42 | 3054 |
| CD2 | 37.5555 | 127.1450 | 56.9 | 47.9 | 6 | 17 | 53 | 4405 |
| CD3 | 37.6397 | 127.0257 | 55.7 | 34.7 | 3 | 17 | 15 | 1517 |
| CD4 | 37.5499 | 126.8425 | 79.1 | 64.1 | 2 | 18 | 43 | 2355 |
| CD6 | 37.5336 | 127.0853 | 38.0 | 38.0 | 3 | 18 | 12 | 1071 |
| CD8 | 37.4655 | 126.9001 | 41.5 | 29.5 | 4 | 21 | 30 | 2156 |
| CD10 | 37.6661 | 127.0295 | 55.5 | 43.5 | 1 | 15 | 7 | 690 |
| CD11 | 37.5846 | 127.0604 | 49.4 | 34.4 | 4 | 20 | 40 | 2587 |
| CD12 | 37.4937 | 126.9181 | 33.8 | 33.8 | 4 | 21 | 15 | 1665 |
| CD13 | 37.5655 | 126.9027 | 25.0 | 13.0 | 3 | 16 | 18 | 1192 |
| CD15 | 37.4889 | 127.0156 | 35.5 | 26.5 | 7 | 18 | 58 | 5491 |
| CD16 | 37.5472 | 127.0388 | 33.7 | 18.7 | 3 | 18 | 17 | 1429 |
| CD18 | 37.5115 | 127.0967 | 53.6 | 29.6 | 3 | 19 | 75 | 7310 |
| CD19 | 37.5296 | 126.8782 | 9.7 | 6.7 | 8 | 18 | 115 | 7176 |
| CD20 | 37.5271 | 126.9070 | 24.4 | 12.4 | 7 | 21 | 49 | 3722 |
| CD21 | 37.5204 | 126.9761 | 32.6 | 20.6 | 7 | 21 | 52 | 4681 |
| CD22 | 37.6077 | 126.9338 | 65.0 | 56.0 | 1 | 15 | 15 | 662 |
| CD25 | 37.5855 | 127.0868 | 40.2 | 28.2 | 1 | 15 | 3 | 178 |

Moreover, the CD-AWS climatic data shows the diversity of urban microclimate in Seoul. Figure 5-1 shows the recorded August (the hottest summer month of the year) monthly average temperature of the 18 CD-AWS sites during 2014-17. The actual duration for the August monthly temperature record was set between the 19th of July and the 18th of August, as the meter-reading day for electricity use in Seoul is on the18th of each month.
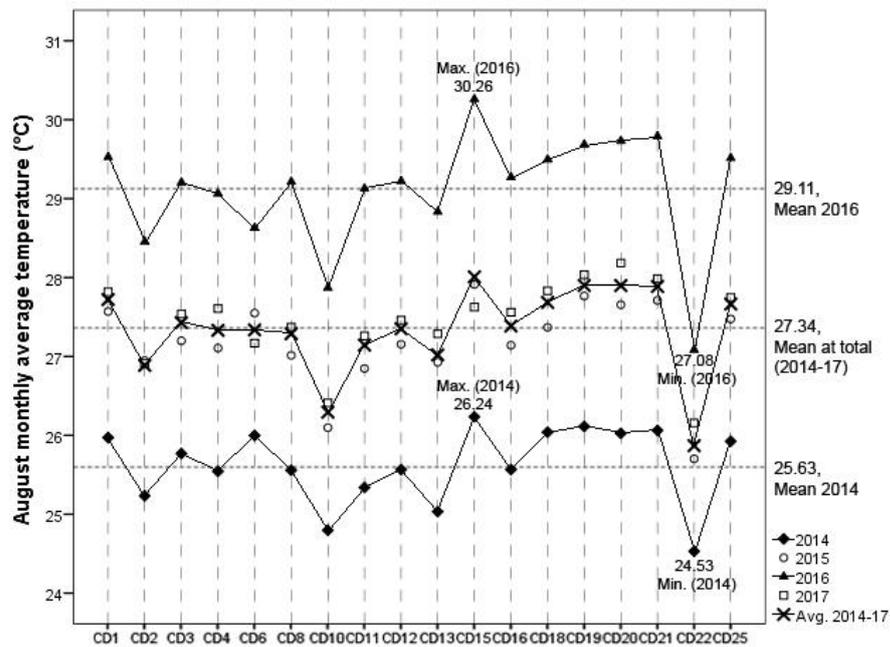


Figure 5-1. External August monthly average temperatures of 18 CD-AWS in Seoul, August 2014-17

The fluctuation of the August temperature distributions during 2014-17 is observed: August 2016 was the hottest (Max, 30.28°C; Min, 27.08°C) while August 2014 was the mildest (Max, 26.24°C; Min, 24.53°C). August 2015 and 2017 were close to the average of August 2014-17. According to the climatic analysis report published by KMA (2016), August 2016 was the warmest summer month on record since 1908, while August 2014 was one of the mildest summer months in Seoul. The variance of the hottest year (2016)

was much larger than the mildest year (2014): standard deviation of 2016 and 2014 was .745 and .484 respectively. This indicates the extent of urban heat island effect increased by hot weather conditions in Seoul.

### 5.2.2. Energy use data of housing stock

Electricity usage data (kWh/m$^2$), which is different from Chapter 4 (electricity bill data, KRW/m$^2$) was used in this study as it is attributed to cooling energy use, such as air-conditioning and electric fans. August was chosen as the month for the proposed heat stress risk assessment when peak cooling demand is most likely to occur.

The AMIS started reporting electricity use data (kWh/m$^2$) in 2014, hence 2014-17 was set as the study period. Given the time frame and the CD-AWS microclimate boundaries, the availability of electricity usage data on AMIS was checked, and finally, 18 (out of 25) CD microclimate boundaries were identified (Table 5-1). Within these boundaries, the electricity usage data collected from 74 apartment neighbourhoods (659 apartment buildings, 51,351 households) were used in the analysis.

### 5.2.3. MK-PRISM climate change projections

As described in section 4.2.4, Seoul's Climate change datasets projected by MK-PRISM are collected at city district level. The RCP4.5 and RCP8.5 scenarios were chosen in this study. Also, the projected daily mean temperature data for August was used to generate future peak monthly average temperature on the basis of the same metre reading day for electricity use data. Figure 5-2 shows the projected monthly temperature distribution of the 18 CDs during 2030-2050. Since the warmest August months are predicted to

occur in 2047 (RCP4.5) and in 2045 (RCP8.5), both years were chosen as the assessment points for heat stress vulnerability analysis in Chapter 6.
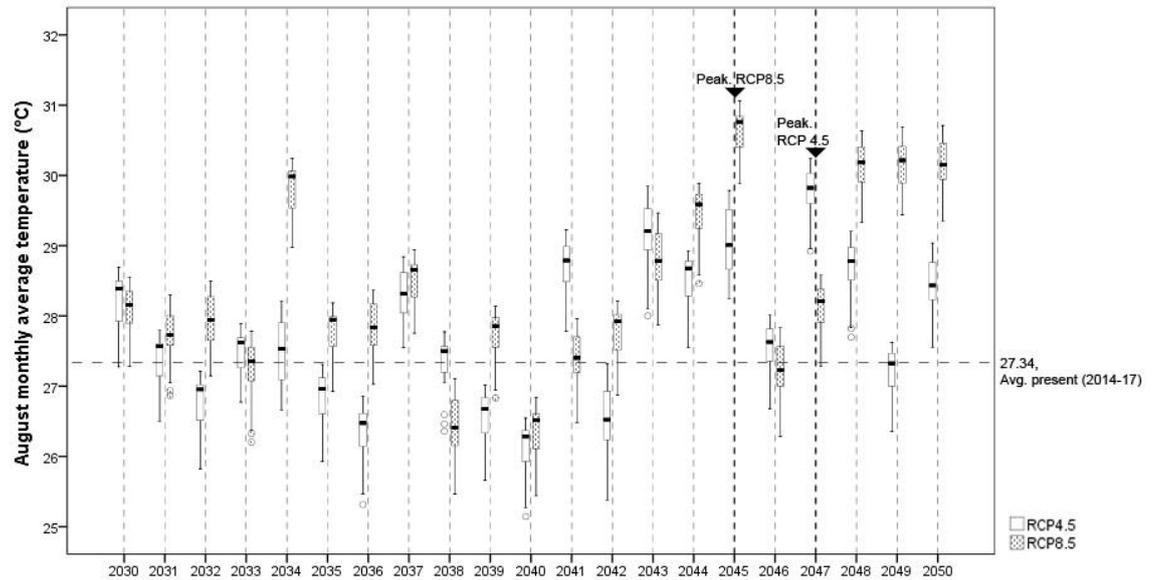


Figure 5-2. Projected August (peak) monthly average temperature ranges of 18 CD boundaries in 2030-2050 under RCP4.5 and RCP8.5 scenarios (Source: CIP). * Each bar represents the temperature range of the18 CDs selected for the study

## 5.2.4. Other factors

Firstly, the data of built year and the number of apartment household by floor area in each neighbourhood were collected to obtain building physical characteristics such as building envelope and floor plan. These two datasets were used as the main sources for determining thermal characteristics and geometric configuration in developing apartment archetypes representative of Seoul's current housing stock (see section 5.3.1 for more detail).
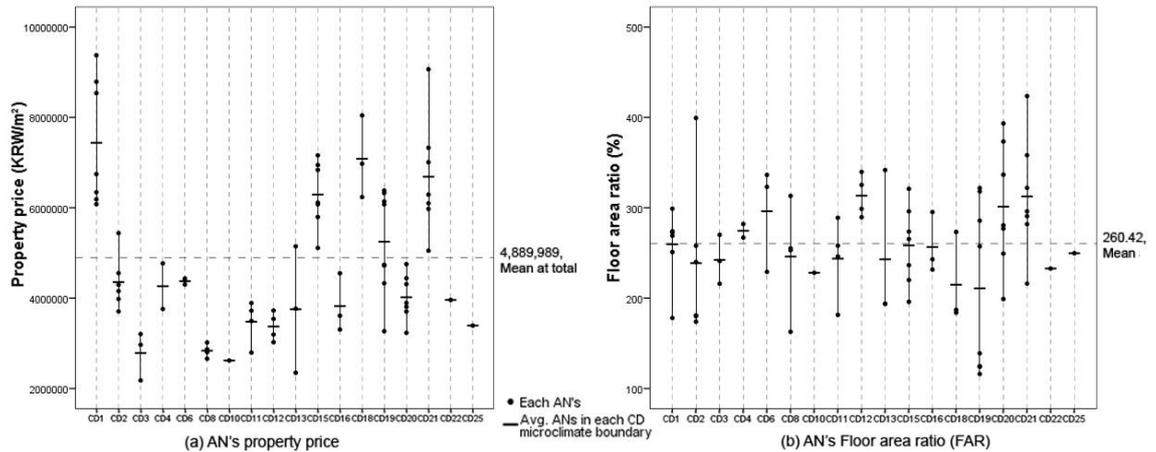
Figure 5-3. (a) Distribution of apartment neighbourhood property prices based on publicly noticed value, (b) Distribution of floor area ratio (FAR) across the 18 CDs

Secondly, the property price data (KRW/m$^2$) were collected from Korea Appraisal Board (KAB, 2015b). Thirdly, floor area ratio (FAR) was calculated based on the total floor area and site area provided by AMIS. It was used as a morphological (built) density indicator in the modelling process. Figure 5-3 shows the property price and FAR across the 18 CDs (all within each CD's AWS boundary).

## 5.3. Developing archetypes for building physics

Following the modelling framework presented in chapter 3, the intensive data analysis was carried for developing archetypes for the purpose of estimating archetypes' present HVAC cooling temperature set point as an indicator of indoor thermal conditions in five tasks as presented below: (1) archetype development (section 5.3.1), (2) analysis of archetypes' peak cooling energy use (section 5.3.2), (3) analysis of archetypes' household non-weather dependent electricity use profile (section 5.3.3), (4) adjustment of archetypes' on-site EnergyPlus weather files (section 5.3.4), and (5) configuration of archetypes' household operation parameters and occupancy scheduling (section 5.3.5).

### 5.3.1. Developing archetypes

To model indoor thermal condition of a city's housing stock in the present climate, this study first develops a collection of housing archetypes as an approximate representation of the stock population. Each archetype can then be modelled in EnergyPlus in its urban microclimate context with available building information and measured energy usage data. Parekh (2005) outlined three basic criteria for archetype energy modelling of housing stock: geometric configurations, thermal characteristics and operating parameters. Here, thermal characteristics, geometric configurations and city-district microclimate boundaries were the main factors considered in developing the archetypes. As a common occupancy scheduling profile was configured and applied in the modelling process, household operation parameters was not considered in developing the archetypes (see section 5.3.5 for more detail).

Firstly, the building insulation criteria (U-values, Table 4-9) according to the year of building regulation applied were gathered into groupings of thermal characteristics. As shown in Table 4-9, Seoul's apartment buildings were built through seven periods (epochs) of building regulations (R1-R7, from September 1979 to June 2010). Each building regulation period adopted a set of building component U-values (Kim et al., 2013b). These building regulation epochs were used in developing the archetypes as apartment neighbourhoods tend to be built with a similar material assembly and structural system under the building regulation applied. Taking R4 (July 1987) as an example, Table 5-2 shows the details of the construction material assembly profile drawn from two randomly selected apartment neighbourhoods, which is the most dominant insulation criteria in Seoul's housing stock. The construction material assembly profile (Table 5-2) developed from the two ANs (built under R4) was equally applied into other building regulation epochs through adjusting the insulation thickness (polyurethane) to

fit U-value of the criteria. Data for construction material assembly profiling are available at city district councils.

Table 5-2. R4 construction material assembly profiles (↓, outside to inside) as an example.

| | Materials | Thick-ness (mm) | Heat Conductivity W/(m*K) | Density Kg/m$^3$ | Specific Heat Capacity J/(kg*K) | Resistance m$^2$K/W | Vapour Resistivity GN*s/(kg*m) | U-value W/m$^2$*K |
|---|---|---|---|---|---|---|---|---|
| Roof | Concrete deck | 100 | 2.000 | 2400 | 1000 | 0.050 | - | 0.401 |
| | Membrane | 10 | 1.000 | 1100 | 1000 | 0.010 | - | |
| | Polyurethane board | 50 | 0.025 | 30 | 1400 | 1.600 | 550 | |
| | Cast concrete | 100 | 1.400 | 1900 | 1000 | 0.136 | 500 | |
| | Cavity | 100 | - | - | - | 0.160 | - | |
| | Gypsum plasterboard | 10 | 0.160 | 950 | 840 | 0.059 | 45 | |
| Floor/ceiling | Flooring sheet | 10 | 0.130 | 500 | 1600 | 0.077 | - | 0.531 |
| | Cement mortar | 40 | 1.400 | 2100 | 840 | 0.029 | 500 | |
| | Polyurethane board | 30 | 0.025 | 30 | 1400 | 1.600 | 550 | |
| | Cast concrete | 150 | 1.400 | 1900 | 1000 | 0.136 | 500 | |
| | Cavity | 210 | - | - | - | 0.160 | - | |
| | Gypsum plasterboard | 10 | 0.160 | 950 | 840 | 0.059 | 45 | |
| External Wall | Water-resistant paint | 10 | 0.500 | 1300 | 1000 | 0.019 | 50 | 0.456 |
| | Cast concrete | 200 | 1.400 | 1900 | 1000 | 0.136 | 500 | |
| | Polyurethane board | 45 | 0.025 | 30 | 1400 | 1.600 | 550 | |
| | Gypsum plasterboard | 10 | 0.160 | 950 | 840 | 0.059 | 45 | |
| Ground/ Exposed floor | Water-resistant sheet | 10 | 0.500 | 1300 | 1000 | 0.019 | 50 | 0.538 |
| | Cast concrete | 150 | 1.400 | 1900 | 1000 | 0.136 | 500 | |
| | Polyurethane board | 35 | 0.025 | 30 | 1400 | 1.600 | 550 | |
| | Cement mortar | 60 | 1.400 | 2100 | 840 | 0.029 | 500 | |
| | Flooring sheet | 10 | 0.130 | 500 | 1600 | 0.077 | - | |
| Internal Partition | Wallpaper | 10 | 0.072 | 480 | 1400 | 0.139 | 125 | 1.500 |
| | Cast concrete | 180 | 1.400 | 1900 | 1000 | 0.136 | 500 | |
| | Wallpaper | 10 | 0.072 | 480 | 1400 | 0.139 | 125 | |
| Window | Single glazing | 10 | 1.060 | - | - | 0.009 | - | 3.092 |

Secondly, in developing the archetypes for EnergyPlus modelling, the number of households counted by floor areas of apartment buildings was used to generate geometric configurations. In AMIS, the range of apartment floor areas (m$^2$) were classified into four sizes based on the lettable area: A1 ≤ 60; 60 < A2 ≤ 85; 85 < A3 ≤ 135; A4 > 135. The detailed floor plan for each area size was sourced from the typical apartment floor plan according to the guideline for evaluating design and performance of green houses established by MoLIT (2009) in Korea.

(a) A2: 84m$^2$          (b) A3: 125m$^2$
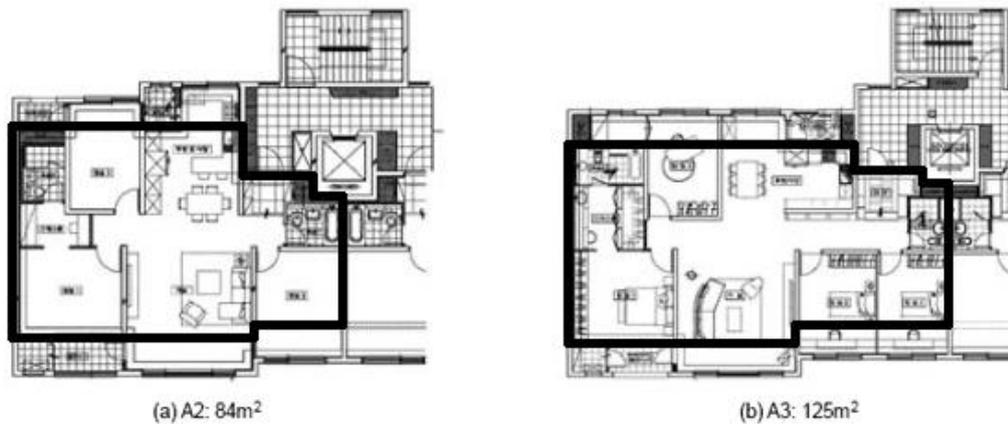
Figure 5-4. Applied floor plans from typical apartment flats based on lettable area (solid line): A2 (84m$^2$) and A3 (125m$^2$) (Source: MoLIT, 2009; Tae et al., 2011)

The MoLIT guideline classifies five apartment floor plans set by the number of bedrooms on the floor area: 36m$^2$ (one bedroom); 46m$^2$ (two); 59m$^2$ (three); 84m$^2$ (three); 125m$^2$ (four). Thus, the MoLIT floor plans were associated to each area classification of AMIS: A1 (59m$^2$), A2 (84m$^2$), and A3 (125m$^2$). Those three floor areas can be considered as the most dominant ones in Seoul. According to the KOSIS (2018a), the percentage of households of 49.5-66m$^2$ (A1, 59m$^2$) is 12% and of 66-99m$^2$ (A2, 84m$^2$) is 30% and of 99-132 (A3, 125m$^2$) is 33%, meaning that about 75% Seoul's apartment households' floor area belongs to these three types of floor area. Figure 5-3 shows the floor plan of A2 (84m$^2$) and A3 (125m$^2$) which are the two floor area sizes and plans sourced for archetype development.

Finally, based on combined thermal and geometric characteristics (i.e., the building regulation epochs and typical floor plans), the archetypes were developed by considering the highest proportion of households in each of the 18 city-district AWS boundaries (Table 5-1). The result is the six archetypes: R1/A2, R3/A2, R3/A3, R4/A2, R4/A3, and

R5/A2. Table 5-3 shows the distribution of the archetypes across the 18 city districts sampled for the study. The other seven city districts of Seoul were not included in this study due to lack of data availability consistent with the other districts. The current outcome of $R_i/A_j$ descriptors suggests that R6, A1, and A4 do not appear in the present formation of archetypes representative of Seoul's housing stock up to 2017.

Table 5-3. Archetype analysis based on the number of apartment households within each microclimate boundary according to the year of building insulation criteria applied (R1-R7, Table 4-9) and the floor area size (A1-A4). * The survey shows R6, A1 and A4 do not appear in archetype formation

| City-district Neighbour-hood | Building Regulation Epochs ($R_i$) | | | | | | | Floor Area m$^2$ ($A_j$) | | | | Arche-type |
|---|---|---|---|---|---|---|---|---|---|---|---|---|
| | Sep 1979 (R1) | Dec 1980 (R2) | Dec 1984 (R3) | Jul 1987 (R4) | Jan 2001 (R5) | Nov 2008 (R6) | Jun 2010 (R7) | ≤ 60 (A1) | < 60 ≤ 85 (A2) | < 85 ≤ 135 (A3) | >135 (A4) | |
| CD1 | - | 478 | - | 502 | 1914 | - | 160 | 427 | 1389 | 993 | 245 | R5 / A2 |
| CD2 | - | 768 | 1844 | 448 | 203 | - | 1142 | 560 | 2857 | 733 | 255 | R3 / A2 |
| CD3 | - | - | 824 | 693 | - | - | - | 439 | 907 | 152 | 19 | R3 / A2 |
| CD4 | - | - | - | - | 2355 | - | - | 542 | 1192 | 621 | - | R5 / A2 |
| CD6 | - | 444 | - | 627 | - | - | - | 142 | 485 | 289 | 155 | R4 / A2 |
| CD8 | 639 | - | - | 786 | 741 | - | - | 728 | 1187 | 251 | - | R4 / A2 |
| CD10 | - | - | - | 690 | - | - | - | 270 | 420 | - | - | R4 / A2 |
| CD11 | - | - | - | 1423 | 445 | - | 719 | 668 | 1300 | 619 | - | R4 / A2 |
| CD12 | - | - | - | 1508 | 157 | - | - | 230 | 1302 | 101 | 32 | R4 / A2 |
| CD13 | - | - | - | - | 1192 | - | - | 237 | 779 | 172 | 4 | R5 / A2 |
| CD15 | 615 | - | 2390 | 1357 | 1129 | - | - | 20 | 2554 | 2130 | 787 | R3 / A2 |
| CD16 | - | - | - | 1054 | 375 | - | - | 494 | 732 | 203 | - | R4 / A2 |
| CD18 | 4632 | - | - | - | 2678 | - | - | 1496 | 3210 | 1900 | 704 | R1 / A2 |
| CD19 | - | - | 6232 | 217 | 727 | - | - | 1216 | 2104 | 3206 | 650 | R3 / A3 |
| CD20 | - | 410 | - | 1848 | 1464 | - | - | 920 | 1577 | 1147 | 78 | R4 / A2 |
| CD21 | 192 | - | - | 3833 | 656 | - | - | 1360 | 1030 | 1477 | 814 | R4 / A3 |
| CD22 | - | - | - | - | 662 | - | - | 206 | 343 | 113 | - | R5 / A2 |
| CD25 | - | - | - | - | 178 | - | - | - | 178 | - | - | R5 / A2 |
| Total | 6078 | 2100 | 11290 | 14986 | 14876 | - | 2021 | 9955 | 23546 | 14107 | 3743 | |

Other input data required of building energy modelling such as apartment building type, height, orientation and glazing ratio, which are not available or applicable at individual household (or apartment neighbourhood) level, were inferred from relevant statistical data. According to the Korean Statistical Information Service (KOSIS, 2018b), about 67% (989,176) of the total number of apartments (1,483,460) are of *Tower* type and the rest

are of *Slab* type in Seoul. Also, 27% (400,634) are 15-storey tall apartment building. Therefore, tower type and 15-storey high were identified as the representative apartment building type. The height of individual apartment unit was fixed to 3m tall. Moreover, the glazing to wall ratio and orientation of apartment building was referred to in a recent study (Kim et al., 2010, Table 4-10) and the current MoLIT energy-saving building design guideline (MoLIT, 2018) respectively. This is due to the fact that the cost of collecting such thorough building information is prohibitive given the large sample size. As the MoLIT design guideline recommends south facing building orientation for apartment housing developments, it was assumed that the orientation of existing apartment stock could be south facing mostly. In the case of south facing orientation of tower type building, the number of walls exposed to external climates are typically three sides but the opening areas are two sides oriented to the south and the north (see also section 2.3.2 and Figure 2-1). Thus, the glazing ratio with 61.48% for South and 56.49% for North; South faced orientation. Those four geometric configurations (*Tower* type, 15-storey tall, the glazing ratio above and south faced orientation) were equally applied to all archetypes.

## 5.3.2. Estimating archetypes' peak cooling energy use

The AMIS dataset provides monthly electricity use data at apartment neighbourhood level, containing not only heating/cooling energy use but also energy use for other home appliances. It is therefore necessary to deduce the monthly electricity use data into two types: non-weather-dependent (NWD) use for operating home appliances and weather-dependent (WD) use for cooling or heating. This study assumes that NWD energy use is the minimum monthly electricity use for the study period 2014-17, and peak (August) cooling energy use can be estimated as the net of August total energy use minus the NWD use identified. Here, the estimated NWD energy use drawn from the 2014-17

dataset was adopted as a constant value applied to the subsequent energy modelling of the six archetypes.

To confirm the assumption above, the relationship between cooling degree days (CDD), heating degree days (HDD) was analysed, and monthly electricity use 2014-16. CDD and HDD were calculated by 17.1°C as the base temperature for Seoul (Lee et al., 2014). As shown in Figure 5-5 (a), the heating, cooling and mixed period can be clearly identified by CDD and HDD: Nov-Apr (heating); Jun-Sep (cooling); May and Oct (mixed). The mixed period had a relatively small amount of CD/HD days, implying a high probability of NWD energy use occurring in both months (May and October). The actual energy use profile in Figure 5-5 (b) supports this conclusion: the minimum electricity use occurred in both May and October of each year.

The assumption in estimating NWD energy use was further considered statistically through Pearson correlation analysis. If the minimum electricity use can be attributed to NWD use and the minimum use occurred in May and Oct, it can be expected that the correlation coefficients between CDD and monthly electricity use for May and October would be weak or negative in explaining the relationship. A relational study was carried out for each season separately for cooling and the mixed period. However, as the main heating source in South Korea is gas and gas energy use for heating specifically was not available on the AMIS or elsewhere, the analysis for the heating period (Nov-Apr) is due to be carried out in a future study. Also, for the normality in variables, the cooling period's variables (CDD and electricity data) were transformed using a square root (sqrt) and logarithm (log) respectively. Table 5-4 shows the outputs: The relationship between CDD and electricity use in the cooling period (Jun-Sep) was very strong and positive. However, in the mixed period (May and October), there was a very strong but negative correlation coefficient between CDD and electricity use, suggesting that the electricity use in this period cannot be explained by external weather conditions.
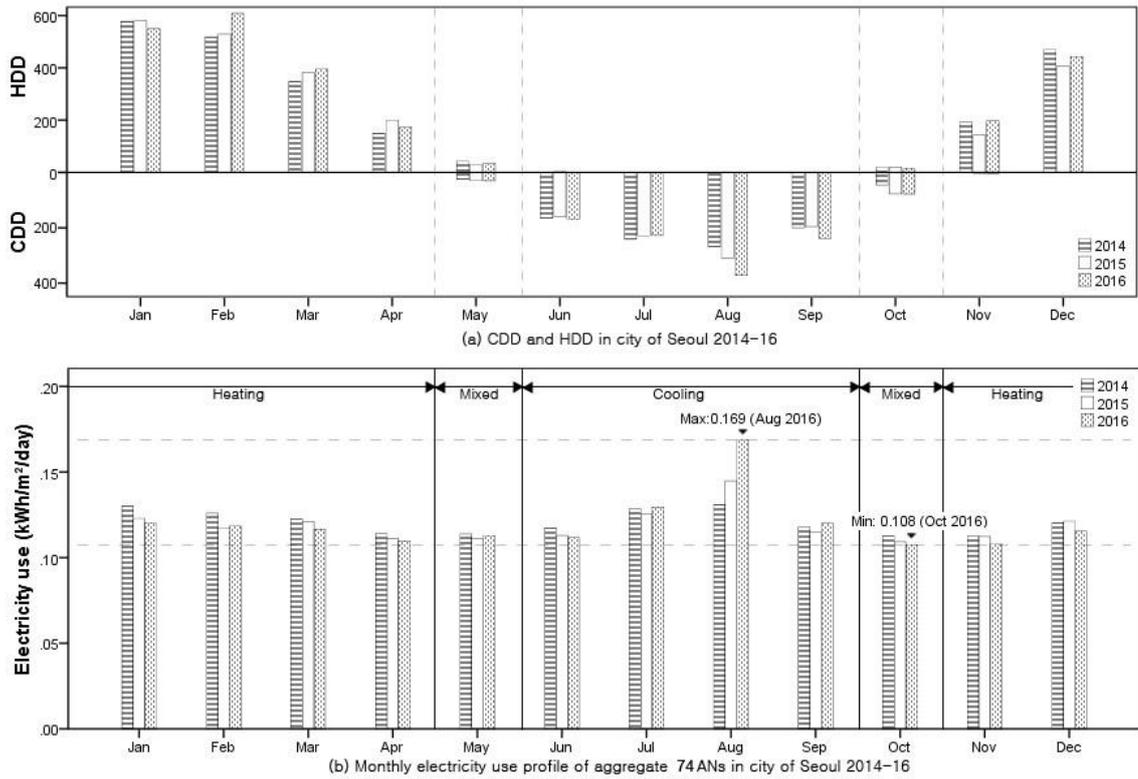
Figure 5-5. (a) HDD and CDD based on daily temperature dataset from the Seoul city weather station; (b) monthly electricity use profile from aggregated 74 apartment neighbourhoods in Seoul, 2014-16

Table 5-4. Correlation between monthly electricity use and HDD and CDD for heating, cooling and mixed periods. **. $p<0.01$ and *. $p<0.05$

|  | Cooling period (Jun-Sep) | Mixed period (May and Oct) |
|---|---|---|
|  | CDD (sqrt) and Electricity (log) | CDD and Electricity |
| Pearson-C | .951** | -.887* |
| Sig. | .000 | .018 |
| r squared | .905 | .787 |
| N | 12 (4mon*3yr) | 6 (2mon*3yr) |

Despite the relational study between CDD and HDD and monthly electricity use data of 2014-16, the assumption can still lead to over or under estimate of NWD energy use due to the current limit of data availability. However, it can be argued that there will be minimized inclusion of weather-dependent energy use in certain months, such as May

and October in Seoul. The expectation is that non-weather-dependent electricity use estimated according to the minimum use days would be close to the actual NWD use if the temporal span of data coverage is sufficiently large enough. Table 5-5 shows the NWD and peak cooling energy use estimated for each neighbourhood archetype. These estimates were later used in the EnergyPlus model calibration process to output cooling temperature set points as estimates of archetypes' indoor thermal conditions in present years.

Table 5-5. Archetypes' NWD and peak cooling energy use data for peak cooling energy model calibration

| Neighbourhood Archetype | | NWD electricity use (kWh/m$^2$) | Peak cooling energy use (kWh/m$^2$) | | | |
|---|---|---|---|---|---|---|
| City District | Type | | 2014 | 2015 | 2016 | 2017 |
| CD1 | R5A2 | 3.010 | 1.210 | 1.624 | 2.342 | 1.922 |
| CD2 | R3A2 | 3.354 | 1.218 | 1.486 | 1.993 | 1.484 |
| CD3 | R3A2 | 3.127 | .857 | 1.242 | 1.954 | 1.311 |
| CD4 | R5A2 | 3.345 | .775 | 1.099 | 1.939 | 1.535 |
| CD6 | R4A2 | 2.691 | 1.044 | 1.195 | 2.025 | 1.201 |
| CD8 | R4A2 | 2.992 | .792 | 1.373 | 1.580 | 1.566 |
| CD10 | R4A2 | 3.365 | .605 | 1.098 | 2.060 | 1.243 |
| CD11 | R4A2 | 3.632 | 1.144 | 1.407 | 1.739 | 1.734 |
| CD12 | R4A2 | 3.276 | 1.134 | 1.760 | 2.610 | 1.971 |
| CD13 | R5A2 | 3.373 | 1.196 | 1.211 | 1.843 | 1.683 |
| CD15 | R3A2 | 2.702 | .965 | 1.487 | 2.268 | 1.531 |
| CD16 | R4A2 | 3.067 | .875 | 1.219 | 2.511 | 1.461 |
| CD18 | R1A2 | 3.346 | 1.041 | 1.560 | 2.181 | 1.360 |
| CD19 | R3A3 | 2.852 | .890 | 1.307 | 2.350 | 1.190 |
| CD20 | R4A2 | 2.836 | .684 | 1.069 | 2.001 | 1.090 |
| CD21 | R4A3 | 2.685 | 1.069 | 2.046 | 2.862 | 1.887 |
| CD22 | R5A2 | 3.301 | .667 | 1.994 | 2.661 | 2.902 |
| CD25 | R5A2 | 3.085 | .740 | 1.409 | 1.968 | 1.792 |

### 5.3.3. Estimating archetypes' household NWD electricity use by component equipment

Obtaining a detailed account of energy use of individual household equipment from total NWD electricity use is important in building thermal modelling as each piece of equipment has a different heat property in affecting internal sensible heat gains. In this study, the household NWD equipment energy use profile was required to extract internal

loads for calibrating internal heat gains in EnergyPlus modelling. This is due to the fact that a detailed household equipment energy use profile is unavailable for Seoul's housing stock, a certain proportion (%) of total NWD electricity use was estimated by referring to the household equipment energy use profile survey from both the UK (Palmer and Cooper, 2014) and Korea (Seo and Hone, 2014). This cross-nation referencing was to combine the limited Korean survey covering only a small sample size (30 apartment households) in a different city (Daegu) for a short time period (2 weeks) with the UK survey, which is of a national and annual scale. This may be justified by a good degree of similarity between South Korea and the UK in geographical circumstances (middle latitude, heating dominant) and socio-economic developments. However, without spatial and temporal-specific field measurements, it remains uncertain.

Table 5-6. Modified % of Seoul's household equipment electricity use profile of total NWD electricity use based on the UK survey data (Palmer and Cooper, 2014)

| Areas | Characteristics | % of total electricity use (UK) | Applied % of total electricity use in NWD month (Seoul) |
|---|---|---|---|
| Lighting | | 15 or more | 18 |
| Appliances | Cold appliances (Fridges and freezers) | 16 | 20 |
| | Wet appliances (Washing machines and dishwashers) | 14 | 16 |
| | Consumer electronics | 14 | 17 |
| | Information and communication technology (IT) | 6 | 9 |
| Cooking | Microwave, cattle and fan-assisted oven | 14 | 20 |
| Total | | 79 or more | 100 |

The actually applied % of total NWD electricity use for Seoul was adjusted by considering Seoul's social cultural circumstances with reference to the UK household equipment energy use profile (Table 5-6). For instance, one of the unique characteristics of Korean food is the fermentation process for long term food preservation and this technique requires spending relatively more effort in the cooking process (Kim et al., 2016).

Therefore, the percentage for cold appliances and cooking had more weight than others. Approximate 2-3% of weight was equally applied to the rest of household equipment for Seoul as the UK proportion is annual based. The proportion in Table 5-6 was equally applied into each archetype's model calibration to extract internal loads as the basis for estimating internal heat gains. Considering the similarity of the operating schedule of the equipment to avoid complexity of input in modelling process, the cold and wet appliances were grouped into machinery and consumer electronics while IT was combined into Miscellaneous. Table 5-7 shows the details of archetypes' NWD household equipment energy use profile which would be used as a calibration data to extract internal loads in NWD energy model.

Table 5-7. Detailed amount of NWD household equipment in each neighbourhood archetype as a calibration data in NWD energy model

| Neighbour-hood (arche-type) | NWD elec use (kWh/m$^2$) | Floor area (m$^2$) | Total NWD elec use (kWh) | Lighting (18%, kWh) | Machinery (36%, kWh) | Miscellaneous (26%, kWh) | Cooking (20%, kWh) |
|---|---|---|---|---|---|---|---|
| CD1(R5/A2) | 3.010 | A2 (84) | 252.84 | 45.51 | 91.02 | 65.74 | 50.57 |
| CD2(R3/A2) | 3.354 | A2 (84) | 281.73 | 50.71 | 101.42 | 73.25 | 56.35 |
| CD3(R3/A2) | 3.127 | A2 (84) | 262.64 | 47.28 | 94.55 | 68.29 | 52.53 |
| CD4(R5/A2) | 3.345 | A2 (84) | 281.02 | 50.58 | 101.17 | 73.07 | 56.20 |
| CD6(R4/A2) | 2.691 | A2 (84) | 226.05 | 40.69 | 81.38 | 58.77 | 45.21 |
| CD8(R4/A2) | 2.992 | A2 (84) | 251.29 | 45.23 | 90.46 | 65.34 | 50.26 |
| CD10(R4/A2) | 3.365 | A2 (84) | 282.69 | 50.88 | 101.77 | 73.50 | 56.54 |
| CD11(R4/A2) | 3.632 | A2 (84) | 305.07 | 54.91 | 109.82 | 79.32 | 61.01 |
| CD12(R4/A2) | 3.276 | A2 (84) | 275.20 | 49.54 | 99.07 | 71.55 | 55.04 |
| CD13(R5/A2) | 3.373 | A2 (84) | 283.33 | 51.00 | 102.00 | 73.67 | 56.67 |
| CD15(R3/A2) | 2.702 | A2 (84) | 226.93 | 40.85 | 81.69 | 59.00 | 45.39 |
| CD16(R4/A2) | 3.067 | A2 (84) | 257.66 | 46.38 | 92.76 | 66.99 | 51.53 |
| CD18(R1/A2) | 3.346 | A2 (84) | 281.05 | 50.59 | 101.18 | 73.07 | 56.21 |
| CD19(R3/A3) | 2.852 | A3 (125) | 356.48 | 64.17 | 128.33 | 92.69 | 71.30 |
| CD20(R4/A2) | 2.836 | A2 (84) | 238.23 | 42.88 | 85.76 | 61.94 | 47.65 |
| CD21(R4/A3) | 2.685 | A3 (125) | 335.68 | 60.42 | 120.84 | 87.28 | 67.14 |
| CD22(R5/A2) | 3.301 | A2 (84) | 277.26 | 49.91 | 99.81 | 72.09 | 55.45 |
| CD25(R5/A2) | 3.085 | A2 (84) | 259.11 | 46.64 | 93.28 | 67.37 | 51.82 |

## 5.3.4. Generating archetypes' on-site EnergyPlus weather files

In building energy simulation, Chan (2011) highlighted the importance of the modification of a typical meteorological year (TMY) site-specifically as weather input to reflect local

urban climatic diversity (e.g. UHI). Among the open TMY weather files available on energyplus.net, the TMY weather file (epw) of Incheon, which is the closest to Seoul, was selected as the default weather file to be modified with on-site weather inputs. In generating the final EnergyPlus weather files for archetype modelling, this study incorporated urban microclimate conditions local to each archetype's city district context by combining the weather datasets collected by the City District Automatic Weather Station (CDAWS) sites and Seoul central city weather station site. The CDAWS datasets are available only for hourly dry-bulb temperature, wind direction and wind speed.

The data for dry-bulb temperature and wind pattern collected from each CDAWS site was applied into the Incheon TMY file. For the remaining weather variables, such as relative humidity, dew point temperature, air pressure, solar radiation and cloud cover, the historical weather data collected from Seoul central city weather station was used. Furthermore, the time frame (day) in all modelling process was set to the electricity meter reading day (18$^{th}$ of month) and therefore, the weather input for peak cooling (August) model was set for the period between 19$^{th}$ of July and 18$^{th}$ of August 2014-17. Finally, 72 (18 archetype neighbourhoods $*$ 4 years) on-site TMY weather files were generated for estimating each archetype's present-day indoor thermal conditions through iterative EnergyPlus model calibration.

### 5.3.5. Archetypes' household operation parameters in zoning inputs

The operation parameters in building energy modelling include detailed occupancy scheduling profiles of household equipment and the placement in zones. As user behaviour has been shown to be one of the key determinants in residential energy use (Yu et al., 2011; Yun & Steemers, 2011), accurate values to the operation parameters are required for model accuracy and reliability. To establish an estimated occupancy

scheduling profile in the energy modelling for each neighbourhood archetype, this study first analysed hourly residential electricity use profile (KOSIS, 2016) and then, identified relevant energy standard and guidelines for partially inferring the scheduling profile.
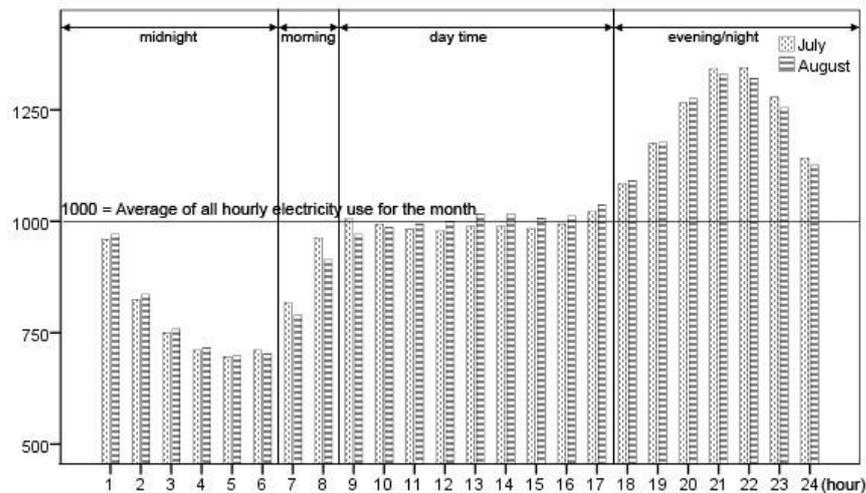


Figure 5-6. Index of relative coefficient of hourly residential electricity use profile for July and August 2015. (Source: KOSIS, 2016)

Figure 5-6 shows the index of relative coefficient of hourly residential electricity use profile for July and August 2015 (the hottest months in Korea) at national level. The index was calculated by $D_n/A \cdot 1000$ $(n=1,2,...,24)$, where $A$ is the average of all hourly electricity uses for the month, and $D_n$ is average of specific hourly electricity use for the month. In this case, 1000 is used as the base reference line to differentiate high or low energy use by hour, and there are four temporal segments identified by the transition points of electricity use. Firstly, during the midnight segment, most of the energy use activities may be stopped excluding operational use of essential home appliances. Secondly, the morning segment from 7 am, certain activity started and increased until 9 am. Thirdly, between 9 am and 17 pm (day time), there was consistent electricity use near to the

average, implying mixed activities occurred but there may be no or minimal cooling. Finally, the dramatic change and diversity occurred in the evening/night segment, implying mixed activities including cooling activity.

Table 5-8. Assumptions of placement of household equipment and occupancy scheduling profile in zoning inputs. * (*a*: master bedroom, *b*: bedrooms, *c*: bathroom, *d*: kitchen, *e*: living room, *f:* balcony)

| | Placement | | | | | | Occupancy scheduling profile |
|---|---|---|---|---|---|---|---|
| | *a* | *b* | *c* | *d* | *e* | *f* | |
| Lighting | o | o | o | o | o | - |  |
| Machinery | - | - | - | o | - | - |  |
| Miscellaneous | o | o | o | - | o | - | |
| Cooking | - | - | - | o | - | - |  |
| People (residents) | o | o | o | o | o | - |  |
| Cooling | o | - | - | - | o | - |  |

| Opening profile | Type | Openable area (%) | Opening threshold (ºC) | Degree of opening |
|---|---|---|---|---|
| External window | Sliding | 50 | 26 | On continuously |
| Internal window | Sliding | 50 | - | Off continuously |
| Door | Side hung | 100 | - | Off continuously |

Based on the analysis of hourly residential electricity use profile, this study selected a standard and guideline of occupancy profile database of the IES VE package (IES, 2017) that is the closest to the profile analysis shown in Table 5-8. For instance, the majority of electricity use occurred between 18:00 and 24:00. Thus, most of the household activities were scheduled during those times. Moreover, taking into account the seasonal peak summer condition, the lighting schedule was set up at evening. Ideally, in case of application of certain standard profile into energy modelling, the occupancy profile should

be calibrated for the model specifically through the iterative model calibration process (Raftery et al., 2011b) as the occupancy profile plays a certain role in energy use, especially weather dependent heating and cooling energy use (Yang and Becerik-Gerber, 2014). However, this study was carried out on the basis of aggregated housing stock energy use data, and an archetype may not be a real physical entity corresponding to a household's occupancy scheduling profile. To validate such operation and behaviour scheduling for archetypes in their urban context requires a more extensive investigation. Here, it is assumed that the reference occupancy profile of household equipment can be equally applied to all archetypes in the city context of Seoul.

However, as HVAC operation plays a key role in influencing energy use and indoor thermal conditions (Yang and Becerik-Gerber, 2014), the cooling profile requires a more detailed consideration. As described in Literature review (section 2.3.2), this study infers that the AC was mostly installed in two of the household's major spaces: the master bedroom and the open space between the living room and the kitchen. Furthermore, the AC operation scheduling profile takes into account the residents' household occupancy profile and hourly electricity use profile: AC is on during the morning and evening/night time period. Thirdly, the window and door opening schedule was assumed under the extreme condition of potential heat stress. Finally, the AC system capacity profile was assumed based on the IES VE system database for residential HVAC system: nominal energy efficiency ratio (EER, kW/kW) is 3.125, seasonal EER (2.500), and system seasonal EER (2.000).

## 5.4. Estimated archetypes' present indoor thermal conditions

Given the dataset analysed in section 5.2 and the model calibration process shown in Figure 3-2, modelling of the city's housing archetypes' peak (August) cooling energy was

carried out in each city-district neighbourhood. This is to estimate the peak HVAC cooling temperature set points as an indicator of the archetypes' present (2014-17) indoor thermal conditions. As each floor of an archetype apartment was built with the same thermal characteristics (insulation criteria and material assembly profile) and geometric configurations (floor plan, building type, height, glazing ratio and orientation), the energy modelling process was conducted using one apartment household unit located in the middle of an archetype building (e.g., the 8th floor in a 15-story apartment), meaning that the air flow and thermal heat transition of floor and ceiling areas were fully tightened to external climates.
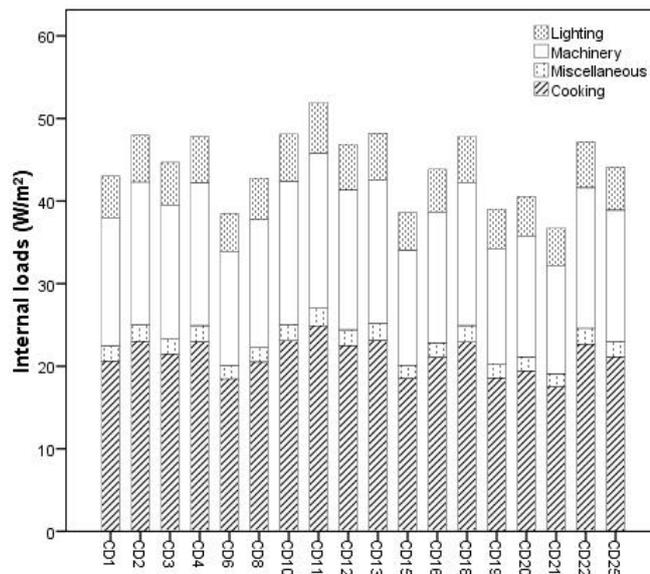


Figure 5-7. Profiles of calibrated internal loads (maximum power consumption) for non-weather dependent (NWD) household electricity use among the neighbourhood archetypes in Seoul

Firstly, archetypes' internal loads (maximum power consumption) of household non-weather dependent (NWD) equipment (lighting, machinery, cooking and miscellaneous)

were estimated through the iterative calibration process of the initial archetype NWD energy model. As shown in Figure 5-7, there are spatial (neighbourhood archetypes) variations in the estimations of each NWD equipment component energy use due to the differentiated NWD calibration inputs (Table 5-7). This highlights the need to consider the diversity of internal heat gains among the archetypes of the city's residential neighbourhoods in addition to the variations observed in the surrounding external climate conditions.

Table 5-9. Estimated internal heat gains of household NWD equipment based on the determining heat gain ratio (25%) to the calibrated internal loads (max power consumption). * People (4W/m$^2$) and Lighting (3W/m$^2$) are equally applied to all neighbourhood archetypes

| Neighbourhood | Internal sensible heat gain (W/m$^2$) | | |
|---|---|---|---|
| (Archetype) | Machinery | Miscellaneous | Cooking |
| CD1(R5/A2) | 3.883 | .445 | 5.160 |
| CD2(R3/A2) | 4.327 | .495 | 5.750 |
| CD3(R3/A2) | 4.034 | .462 | 5.360 |
| CD4(R5/A2) | 4.316 | .494 | 5.735 |
| CD6(R4/A2) | 3.472 | .398 | 4.613 |
| CD8(R4/A2) | 3.859 | .442 | 5.128 |
| CD10(R4/A2) | 4.342 | .497 | 5.769 |
| CD11(R4/A2) | 4.685 | .537 | 6.226 |
| CD12(R4/A2) | 4.227 | .484 | 5.616 |
| CD13(R5/A2) | 4.351 | .498 | 5.782 |
| CD15(R3/A2) | 3.485 | .399 | 4.631 |
| CD16(R4/A2) | 3.957 | .453 | 5.258 |
| CD18(R1/A2) | 4.316 | .494 | 5.736 |
| CD19(R3/A3) | 3.491 | .423 | 4.642 |
| CD20(R4/A2) | 3.659 | .419 | 4.862 |
| CD21(R4/A3) | 3.287 | .399 | 4.371 |
| CD22(R5/A2) | 4.258 | .488 | 5.658 |
| CD25(R5/A2) | 3.979 | .456 | 5.288 |

Secondly, the internal heat gains of household NWD equipment were estimated by the determining heat gain ratio to the calibrated internal loads, and 25% (Hosni et al., 1999) was used as the determinant ratio in this estimation except lighting. For the lighting, 3W/m$^2$, which is the standard lighting gain for office stair (ASHRAE, 2004), was equally applied to all archetypes, taking into account the range of the calibrated archetypes'

internal loads for lighting (between 4.512 and 6.122W/m$^2$). The lighting gain used in this study is relatively low, compared to other benchmark allowances: i.e. general office (8-12W/m$^2$); hospital wards (9W/m$^2$) (CIBSE, 2015, pp6-3). In determining internal heat gain for lighting, the details of lighting components are required, such as total electrical input power, heat entering the space, and details of radiant, convective and conductive components (CIBSE, 2015, pp.6-3). However, due to the complexity and limited availability of data in the determination of lighting gains, the lighting gain was benchmarked to the closest allowance within the range of calibrated internal loads (Figure 5-7) as internal heat gain cannot be higher than the calibrated internal loads. In addition, for the people, low density office with light work was benchmarked from CIBSE (2015, pp6-2): 4W/m$^2$.
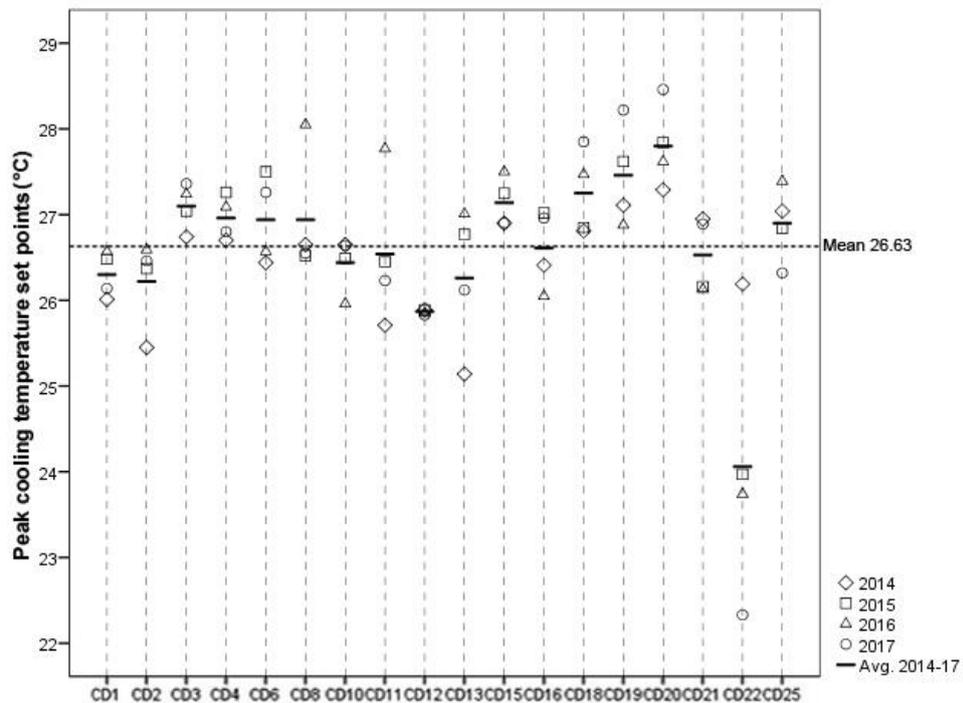


Figure 5-8. Estimated peak cooling temperature set points as an indicator of the indoor thermal conditions of the archetypes in Seoul's 18 city-district neighbourhoods, based on the data collected for the August months of 2014-17

Finally, the initial archetype NWD energy model was updated to a peak cooling energy model through updating the zoning inputs, including calibration data of total peak electricity use (NWD + peak cooling use in Table 5-5), operating parameters of occupancy cooling scheduling (Table 5-8), and HVAC and estimated internal heat gains (Table 5-9). Figure 5-8 shows the modelling outputs of the archetypes' peak cooling temperature set points estimated for Seoul, August 2014-2017.

Table 5-10. Descriptive variance analysis of the estimated peak cooling temperature set points, August 2014-2017, Seoul

| Neighbourhood (archetype) | Min | Max | Mean | Std. Deviation, $S$ | Variance, $S^2$ |
|---|---|---|---|---|---|
| CD1(R5/A2) | 26.01 | 26.57 | 26.30 | .268 | .072 |
| CD2(R3/A2) | 25.45 | 26.59 | 26.22 | .520 | .270 |
| CD3(R3/A2) | 26.74 | 27.36 | 27.10 | .271 | .073 |
| CD4(R5/A2) | 26.70 | 27.26 | 26.96 | .258 | .067 |
| CD6(R4/A2) | 26.44 | 27.50 | 26.94 | .517 | .268 |
| CD8(R4/A2) | 26.52 | 28.05 | 26.94 | .740 | .548 |
| CD10(R4/A2) | 25.96 | 26.65 | 26.44 | .325 | .106 |
| CD11(R4/A2) | 25.71 | 27.77 | 26.54 | .877 | .769 |
| CD12(R4/A2) | 25.83 | 25.89 | 25.87 | .030 | .001 |
| CD13(R5/A2) | 25.14 | 27.01 | 26.26 | .836 | .699 |
| CD15(R3/A2) | 26.90 | 27.50 | 27.14 | .293 | .086 |
| CD16(R4/A2) | 26.05 | 27.02 | 26.61 | .463 | .215 |
| CD18(R1/A2) | 26.81 | 27.85 | 27.25 | .504 | .254 |
| CD19(R3/A3) | 26.88 | 28.22 | 27.46 | .595 | .354 |
| CD20(R4/A2) | 27.29 | 28.46 | 27.80 | .493 | .243 |
| CD21(R4/A3) | 26.13 | 26.95 | 26.53 | .448 | .201 |
| CD22(R5/A2) | 22.33 | 26.19 | 24.06 | 1.596 | 2.547 |
| CD25(R5/A2) | 26.32 | 27.39 | 26.90 | .447 | .200 |

Overall, across the 18 neighbourhood archetypes during the data collection period, there were spatial and temporal variations in the estimates of peak cooling temperature set points (Figure 5-8). However, looking at each archetype individually, the ranges of peak cooling temperature set points appear somewhat consistent during the four years modelled even though these city districts were experiencing wide variations in microclimate conditions (Figure 5-1). In comparison, archetype CD12 ($S$=0.03, $S^2$=0.001) and CD22 ($S$=1.596, $S^2$=2.547) are two extreme cases (Table 5-10). Also, there appears a trend that most of the highest set points occurred in 2016, the year of the largest cooling

degree day (CDD) count, while the lowest set points occurred in 2014 with the lowest CDD count (see Figure 5-5 - August). This suggests that there may be a certain process of indoor heat acclimatisation, which contains dwellers' adaptive opportunities associated with each archetype in neighbourhood context.

## 5.5. Conclusions

To apply the methodological framework for assessing potential heat stress vulnerability of a city's dwelling stock in the future climate, the city of Seoul was chosen as case study. Then, the main datasets required in stock energy modelling as inputs were collected within each city districts' microclimate boundary setting: urban microclimate data; energy use data of housing stock; Seoul's climate change projection data; property price data (as a socio-economic indicator); building physical information (i.e., building thermal characteristics and geometric configuration). Finally, data analysis was carried out for developing archetypes as a preliminary preparation for building physics, which is the EnergPlus energy modelling for estimating present indoor thermal conditions.

Firstly, housing archetypes were developed within urban microclimate context as approximate representation of the stock population based on building physical criteria, i.e., thermal characteristics ($R_i$) and geometric configuration ($A_j$). Six archetypes were identified by the combination ($R_i/A_j$ descriptors) across the 18 city districts sampled for the study. Other geometric configurations, such as building type, height, glazing ratio to wall and orientation were equally applied to all archetypes: *Tower* type, 15-storey tall, the glazing ratio (61.48% for South and 56.49% for North) and south faced orientation.

Secondly, two types of electricity use were deduced from the collected monthly (August) data through the assumption that the NWD energy use is the minimum monthly electricity use during the study period, and peak (August) cooling energy use can be estimated as the net of August electricity use minus the NWD use identified. The assumption was testified by the relational analysis between cooling/heating degree days (CDDs/HDDs) and monthly electricity use. In the analysis, it was found that the heating (Nov-Apr), cooling (Jun-Sep) and mixed (May and Oct) periods were clearly identified by CDDs and HDDs in Seoul. However, the amount of CDDs and HDDs in mixed period was relatively

very small, implying that a high probability of NWD energy use occurs in May and Oct. This implication was confirmed by actual energy use profile. Moreover, the assumption was further confirmed by Pearson correlation analysis statistically, that is the monthly electricity use in May and Oct was not explained by CDDs for both months. The estimated NWD and peak cooling energy use were used as the calibration inputs to estimate archetypes' present indoor thermal conditions in the EnergyPlus model calibration.

Thirdly, the EnergyPlus modelling for estimating archetypes' present indoor thermal conditions requires a detailed household NWD equipment energy use profile as each component equipment has a different heat property in affecting internal heat gains. The UK household electricity use profile was referred and adjusted to estimate the actually applied proportion (%) of total NWD electricity use for Seoul, taking into account local socio-cultural circumstances. The detailed NWD equipment energy use profile then would be used as calibration data to extract internal loads in NWD energy model.

Fourthly, 72 (18 archetype neighbourhoods * 4 years) on-site EnergyPlus typical meteorological year (TMY) weather files were generated to estimate each archetype's present indoor thermal conditions. As data availability of city district automatic weather station is limited to hourly dry-bulb temperature, wind direction and wind speed, the remaining weather variables used the historical weather data collected from Seoul's central city weather station.

Fifthly, archetypes' household operation parameters in zoning inputs were established, including detailed occupancy scheduling profiles of household equipment and the placement. To achieve this, hourly residential electricity use profile during hottest summer months (July and August) was analysed, and then the relevant standard and guidelines were identified.

Finally, given the developed archetypes and the dataset analysed, modelling of archetypes' peak cooling energy was carried out to estimate the peak HVAC cooling temperature set points as an indicator of the archetypes' present (2014-17) indoor thermal conditions. The estimates showed that there were spatial (each city district's neighbourhood) and temporal (each year) variations. This is owing to differentiated responses (dwellers' cooling energy use behaviours) to the external climates (August average temperature) observed in the metred peak cooling energy uses. However, there appeared a trend that most of the highest set points occurred in 2016, the year of the largest cooling degree day (CDD) count, while the lowest set points occurred in 2014 with the lowest CDD count. This implies that there may be certain process of indoor heat acclimatisation, which contains dwellers' adaptive opportunities associated with each archetype in a neighbourhood context.

# Chapter 6. Assessing potential heat stress vulnerability of Seoul's dwelling stock

## 6.1. Introduction

This chapter presents Seoul's neighbourhood dwelling stock modelling and the heat stress vulnerability (HSV) assessment. Given the collected and estimated archetypes' present and future datasets from chapter 5, the stock energy modelling is carried out following the two perspectives of HSV assessments. Section 6.2 presents modelling indoor thermal conditions for Cooling *Temperature* Set Points based HSV assessment (HSV-A$_T$, HSV-B$_T$). Section 6.3 presents modelling peak cooling demands for Cooling *Energy* Demand based HSV assessment (HSV-A$_E$, HSV-B$_E$). Section 6.4 summarises key findings and concludes remarks.

## 6.2. Cooling *Temperature* Set Points based HSV assessment (HSV-A$_T$, HSV-B$_T$)

This section presents the Seoul neighbourhood dwelling stock modelling and heat stress vulnerability assessment in four sets of results in accordance with the key steps shown in Figure 3-1. Based on the data collected (2014-2017) and estimated present HVAC peak cooling temperature set points, the key determinants of archetypes' present indoor thermal conditions were identified (section 6.2.1). A multiple regression model for predicting archetypes' future indoor thermal conditions during the peak cooling month (August in Seoul) is presented in section 6.2.2. As an input required of building energy modelling of the housing archetypes in the future climate (2050s), the modelling outcome of the future peak cooling energy use per neighbourhood archetype is given in section 6.2.3, presupposing no housing stock renovation/replacement has taken place. Finally, section 6.2.4 reports on the estimated future HVAC cooling temperature set points for the purpose of Seoul's HSV assessment.

**6.2.1. Identified key determinants of peak indoor thermal conditions**

As described in section 3.4, a multiple regression analysis was carried out at the macro level (i.e. aggregate of the 18 neighbourhood archetypes) to identify likely key determinants of indoor thermal conditions as represented by the cooling temperature set points during the peak cooling period. Six independent variables were used in this study taking into account factors which can potentially be determinants affecting indoor thermal conditions and Seoul's open data availability at the same time.

In detail, August (peak) average temperature ($^{\circ}$C) in each city-district neighbourhood (Figure 5-1) was used as the external climate conditions. The energy use datasets (kWh/m$^2$) were divided into two types: (a) NWD household equipment energy use, and (b) cooling energy use (Table 5-5), as each plays a different role in indoor thermal conditions. The former can produce a certain amount of sensible internal heat gains while the latter is opposite. The collected property price (KRW/m$^2$) and floor area ratio (%) datasets of each apartment neighbourhood (Figure 5-3) were abstracted into the average value within each archetype neighbourhood (microclimate boundary) to reflect representative archetype property. Finally, U-value (W/m$^2$*K) of the external wall (Table 4-9) which was matched to the applied archetype's building regulation (Table 5-3) was used as the building envelop of physical characteristics. Therefore, the total number of the sample was 72, 4 years (present 2014-17) * 18 neighbourhood archetypes. Notably, all the inputs for this multiple regression analysis were collected (or estimated) at micro level and then, they were aggregated at macro level, as the bottom-up modelling approach was adapted in this study.

Table 6-1. Coefficients of multiple regression analysis to identify key determinants in present indoor thermal conditions

| | Dependent | Independent | $B$ | Std. error | Beta | Sig. |
|---|---|---|---|---|---|---|
| $R^2 = .984$, $R^2$ (adj.)=.982 $p = .000$ N=72 (18 * 4 yrs) | August (peak) cooling temperature set points (°C) | (Constant) | 5.331 | .584 | | .000 |
| | | August average temperature (°C) | .881 | .017 | 1.265 | .000 |
| | | August cooling energy use (kWh/m²) | -2.262 | .042 | -1.282 | .000 |
| | | Property Price (KRW/m²) | .000 | .000 | .041 | .039 |
| | | Floor Area Ratio (%) | .001 | .001 | .025 | .177 |
| | | NWD energy use (kWh/m²) | -.026 | .072 | -.008 | .717 |
| | | Building envelop (W/m²*K) | .740 | .142 | .095 | .000 |

Table 6-1 shows the output of the multiple regression analysis. Overall, $R^2$ was .984 (.982, adjusted $R^2$) and $p$ was .000, representing that 98.4% of the variance in the present indoor thermal condition (dependent) was explained by the model and this model was statistically significant respectively. In evaluating each of the independent variables, the highest standardised coefficients (Beta) occurred in August average temperature (1.265) and cooling energy use (-1.282), meaning that those two variables made the strongest contribution on indoor thermal conditions within the statistically significant level (Sig.=.000). Finally, August's average temperature and cooling energy use were identified as key determinants in the indoor thermal conditions. In fact, the key determinants would be different in each of the neighbourhoods as this study is looking at Seoul's residential building stock. However, this can only be testified within a large enough sample size of each of the archetype neighbourhoods. Those two identified parameters were used in the modelling process to predict archetypes' future indoor thermal conditions in following subsection.

## 6.2.2. Modelling indoor thermal conditions under peak cooling energy use

Given the external August average temperature and the August cooling energy use as the two key determinants identified, the archetypes' indoor thermal conditions under

peak cooling in future years can be estimated from multiple regression modelling with the input of Seoul's latest climate change projection. Considering the current data sample scope and size, a decision was made to perform the multiple regression analysis at a macro-level, that is, aggregate of all city-district archetypes.
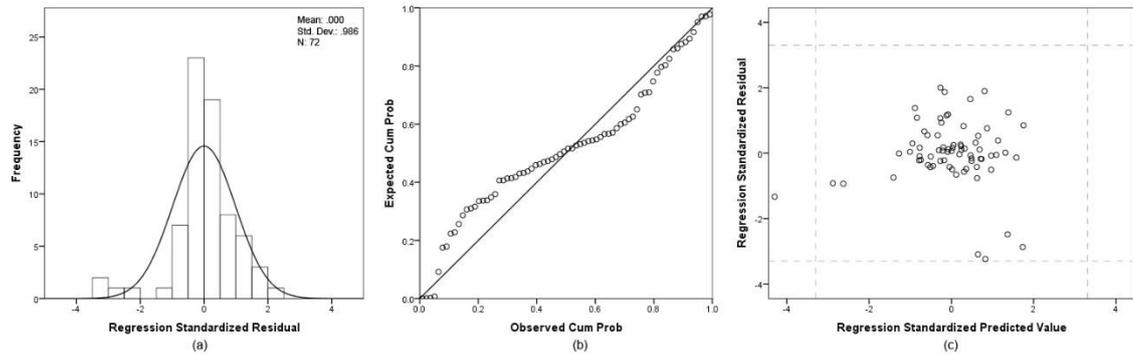


Figure 6-1. A preliminary analysis for the multiple regression model: (a) Normality histogram, (b) normal probability plot (P-P) and (c) scatterplot of regression standardised residuals. * Dependent variable: estimated neighbourhood archetypes' present HVAC cooling temperature set points. ** Dot lines of (c) are at ±3.3

A preliminary analysis was carried out to check outliners, normality, homoscedasticity and independence of residuals through inspecting the normal probability plot (P-P) of the regression standardised residual and the scatterplot (Figure 6-1). From the preliminary analysis, a CD22's 2017 data was detected as outlier: its' standardised residual was less than -3.3 (see Figure 6-1. c) and also, the Mohalanobis distance was 19.25 which was above 13.82, critical value for 2 independent variables model (Tabachnick and Fidell, 2007). However, the regression modelling was carried out without deleting CD22 as only one was found. The resultant multi-regression model is presented in Figure 6-2 (scatter plot) and Table 6-2 (model details).
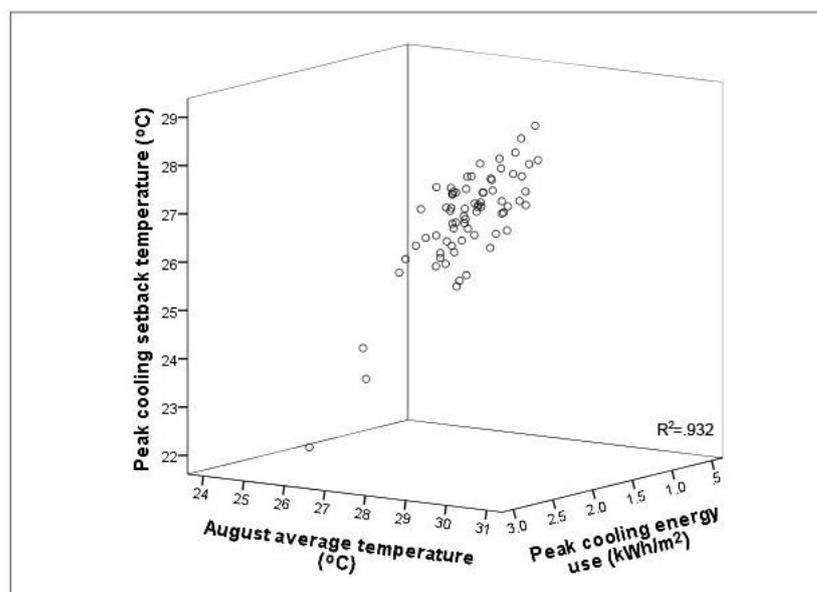
Figure 6-2. Scatter plot of estimated peak cooling temperature set points based on the two key determinants identified (August average external temperature and Peak cooling energy use)

Table 6-2. Coefficients of a multi-regression model for estimating the indoor thermal conditions of Seoul's 18 neighbourhood archetypes based on the 2014-17 datasets

|  | Dependent | Independent | *B* | Std. error | Beta | Sig. |
|---|---|---|---|---|---|---|
| $R^2$ = .932, *p* = .000 | Peak cooling temperature set point (°C) | (Constant) | 6.478 | .755 |  | .000 |
|  |  | August average temperature (°C) | .854 | .030 | 1.226 | .000 |
| N=72 (18 * 4 yrs) |  | Cooling energy use (kWh/m²) | -2.122 | .075 | -1.230 | .000 |

*K*-fold cross validation was applied to evaluate the model accuracy. Four folds were generated as there were four years' datasets (2014-17). For instance, *k*=1 fold used 2014, 2015, 2016 datasets as the training set and 2017 as the testing set. Moreover, five criteria were used in error statistics: mean absolute error (MAE); mean square error (MSE); root mean square error (RMSE); mean absolute percentage error (MAPE);

coefficient of determination ($R^2$). The predicted data represents the output resulted from each *k*-fold multiple regression model while the observed represents the outcome estimated by EnergyPlus peak cooling energy model (Figure 5-8).

Table 6-3. Coefficients of modelling archetypes' peak indoor thermal conditions of each *k*-fold to evaluate model accuracy and the error statistics between the predicted and the observed of each *k*-fold. * *y*: cooling temperature set points (°C), $x_1$: August average temperature (°C), $x_2$: peak cooling energy use (kWh/m²).

| *k*-fold model $y(x_1, x_2)=a+bx_1+cx_2$ | *a* | *b* | *c* | $R^2$ | Sig. |
|---|---|---|---|---|---|
| *k*=1 (2014, 15, 16) | 7.273 | .820 | -2.040 | .916 | .000 |
| *k*=2 (2014, 15, 17) | 5.789 | .880 | -2.109 | .932 | .000 |
| *k*=3 (2014, 16, 17) | 6.275 | .865 | -2.174 | .934 | .000 |
| *k*=4 (2015, 16, 17) | 5.919 | .874 | -2.117 | .944 | .000 |

| Error statistics | MAE (°C) | MSE (°C) | RMSE (°C) | MAPE (%) | $R^2$ |
|---|---|---|---|---|---|
| *k*=1 (testing 2017) | .196 | .067 | .259 | .738 | .986 |
| *k*=2 (testing 2016) | .161 | .034 | .183 | .605 | .977 |
| *k*=3 (testing 2015) | .112 | .022 | .147 | .423 | .969 |
| *k*=4 (testing 2014) | .143 | .039 | .198 | .536 | .935 |
| At total | .153 | .040 | .197 | .576 | .958 |

Table 6-3 shows the model details and the outputs of the error statistics of each *k*-fold. Overall, the coefficient of determination from the scatter plot between the observed and the predicted was .958 (Figure 6-3), representing about 96% of variance in the observed peak cooling setback temperature could be explained by the corresponding fourfold multiple regression models. Moreover, all four *k*-fold's errors were near to zero, representing that there are no over fitting training datasets to the testing sets in all four cases. From this cross validation, the multiple regression model is considered acceptable to be used in predicting the archetypes' cooling temperature set points in forthcoming years for heat stress vulnerability assessment (section 6.2.4).
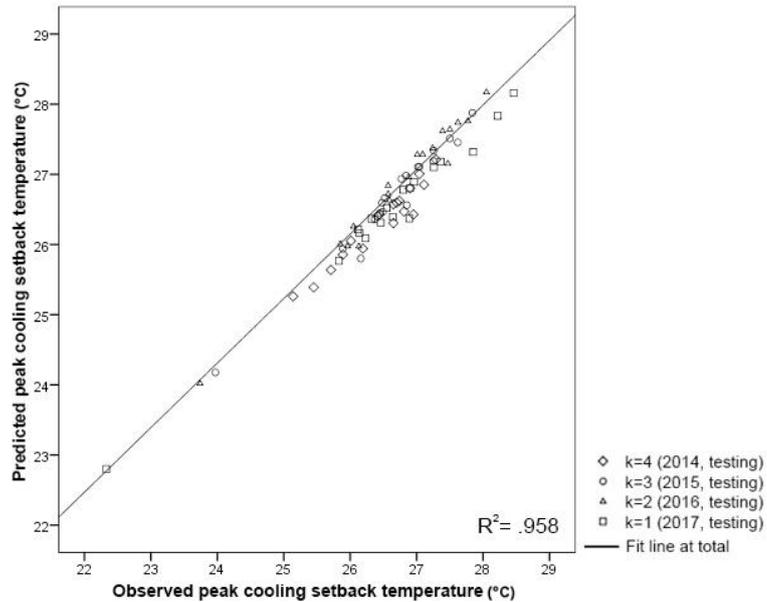
Figure 6-3. Coefficient of determination ($R^2$) between the predicted and observed peak cooling set point temperature at total (aggregate of all four *k*-folds).

### 6.2.3. Modelling archetype-specific peak cooling energy use

According to the multi-regression analysis reported in section 6.2.2, to predict the housing archetypes' indoor thermal conditions during August in forthcoming years, the model will need two inputs: (1) estimates of the archetypes' peak cooling energy uses in future years, and (2) climate change projections for Seoul at the city-district level. According to the data collection (section 5.2.3), the most recent climate change projections for Seoul have been published by the Korean Meteorological Administration (KMA; available at CIP). This subsection presents the estimates of the archetypes' peak cooling energy uses in accordance with the KMA climate projections for Seoul in 2050s.

Table 6-4 shows archetypes' correlation coefficients between the two variables at the city-district (micro) level. Despite of the relatively small sample (N=4, 2014-17), the correlation coefficients (Pears-C) of all neighbourhood archetypes were very strong and positive. The Pears-C of the aggregate of all 18 archetypes (Macro) was relatively weak

(.706), implying that it is preferable to explain the relationship between the two variables at the micro level.

Table 6-4. Correlation coefficients between peak cooling energy use and August average temperature in each neighbourhood archetype. *. Macro: aggregate of all 18 neighbourhood archetypes (N=72, 18 * 4yrs) **. $p$ <0.01 and *. $p$ <0.05

| Neighbourhood (archetype) | Pears-C | Sig. | Neighbourhood (archetype) | Pears-C | Sig. | Neighbourhood (archetype) | Pears-C | Sig. |
|---|---|---|---|---|---|---|---|---|
| CD1(R5/A2) | .982* | .018 | CD10(R4/A2) | .993** | .007 | CD18(R1/A2) | .948 | .052 |
| CD2(R3/A2) | .968* | .032 | CD11(R4/A2) | .873 | .127 | CD19(R3/A3) | .930 | .070 |
| CD3(R3/A2) | .993** | .007 | CD12(R4/A2) | .998** | .002 | CD20(R4/A2) | .950* | .050 |
| CD4(R5/A2) | .974* | .026 | CD13(R5/A2) | .843 | .157 | CD21(R4/A3) | .986* | .014 |
| CD6(R4/A2) | .879 | .121 | CD15(R3/A2) | .993** | .007 | CD22(R5/A2) | .892 | .108 |
| CD8(R4/A2) | .852 | .148 | CD16(R4/A2) | .964* | .036 | CD25(R5/A2) | .928 | .072 |
| Macro | .706** | .000 | | | | | | |
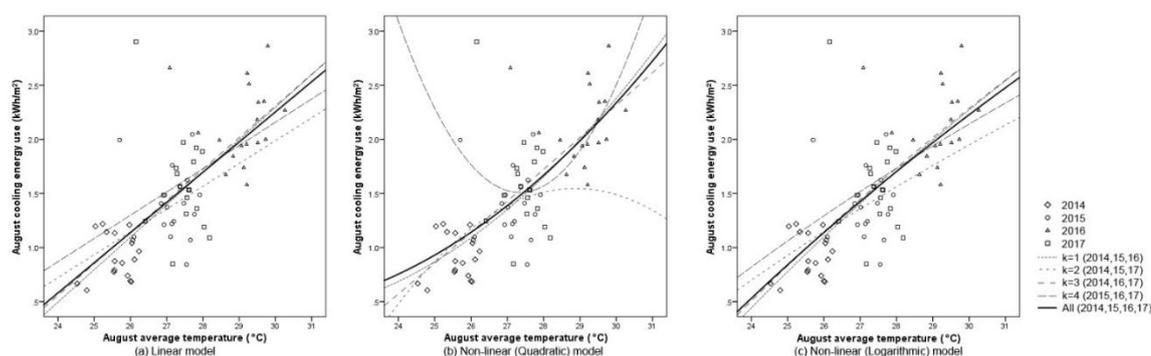


Figure 6-4. Scatter plots between peak cooling energy use and August average temperature at Macro level (aggregate of all 18 neighbourhood archetypes), and the three types of bivariate regression models in each $k$-fold. *The model fit in All (2014-17) is for predicting peak cooling energy use of each neighbourhood archetype in future years

This implication can be further confirmed by the macro bivariate regression modelling for estimating archetypes' future cooling energy use and to evaluate the model accuracy. Three types of bivariate model were tested at macro level (aggregate of all 18

neighbourhood archetypes): (a) linear, (b) quadratic and (c) logarithmic. Seen in Figure 6-4 overall, the relationship between peak cooling energy use and the external temperature were largely distributed out of those three types of linear fits. This represents that the peak cooling energy use cannot be explained by the external temperature in all three types of bivariate model at macro level. Fourfold cross validation was carried out to evaluate the model accuracy. Table 6-5 shows the output of the error statistics and Figure 6-5 shows coefficients of determination ($R^2$) between the predicted and observed peak cooling energy use at total (aggregate of all four k-folds). As the accuracy outcomes do not meet the criteria of acceptance level, the modelling for archetypes' peak cooling energy use needs to be performed at the micro level (i.e., at each neighbourhood archetype independently).

Table 6-5. Error statistics between the predicted and the observed peak cooling energy use at each *k*-fold (with MAPE, %) and at total (aggregate of all four *k*-folds)

|  |  | Linear | Quadratic | Logarithmic |
|---|---|---|---|---|
| Each k-fold's MAPE (%) | *k*=1, 2017 test | 18.6 | 18.5 | 18.7 |
|  | *k*=2, 2016 test | 16.9 | 27.9 | 17.6 |
|  | *k*=3, 2015 test | 18.4 | 18.3 | 18.7 |
|  | *k*=4, 2014 test | 36.9 | 120.6 | 35.9 |
|  |  |  |  |  |
| Avg. MAE (kWh/m$^2$) |  | .317 | .558 | .319 |
| Avg. MSE (kWh/m$^2$) |  | .187 | .516 | .190 |
| Avg. RMSE (kWh/m$^2$) |  | .425 | .663 | .427 |
| Avg. MAPE (%) |  | 22.7 | 46.3 | 22.7 |
| $R^2$ |  | .377 | .290 | .367 |
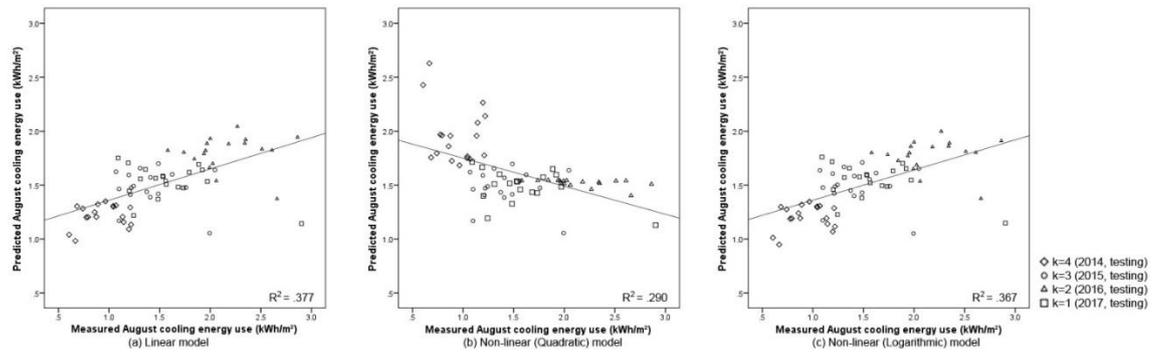
Figure 6-5. Coefficient of determination ($R^2$) between the predicted and observed peak cooling energy use at total (aggregate of all four *k*-folds).

Finally, the modelling peak cooling energy use was carried out at micro level (neighbourhood archetype independently). Figure 6-6 presents the resultant bivariate regression model derived from 2014-17 for each neighbourhood archetype that gives estimates of peak cooling energy use (kWh/m$^2$) given the archetype's external August temperatures ($^o$C). To evaluate the model accuracy, the leave-one-out cross validation (LOOCV) was used. Due to the small sample size (N=4), only linear regression was applied in the modelling.

The modelling shows that most of the neighbourhoods' present peak cooling energy use are well fitted to the external temperature on the linear model. However, some neighbourhoods, such as CD6 ($R^2$=.773), CD8 ($R^2$=.726), CD11 ($R^2$=.762) and CD13 ($R^2$=.711), show relatively weak overall relationships. This suggests that other model types, such as non-linear models, may achieve a better fit for some neighbourhoods in consideration of the form of the scattered.
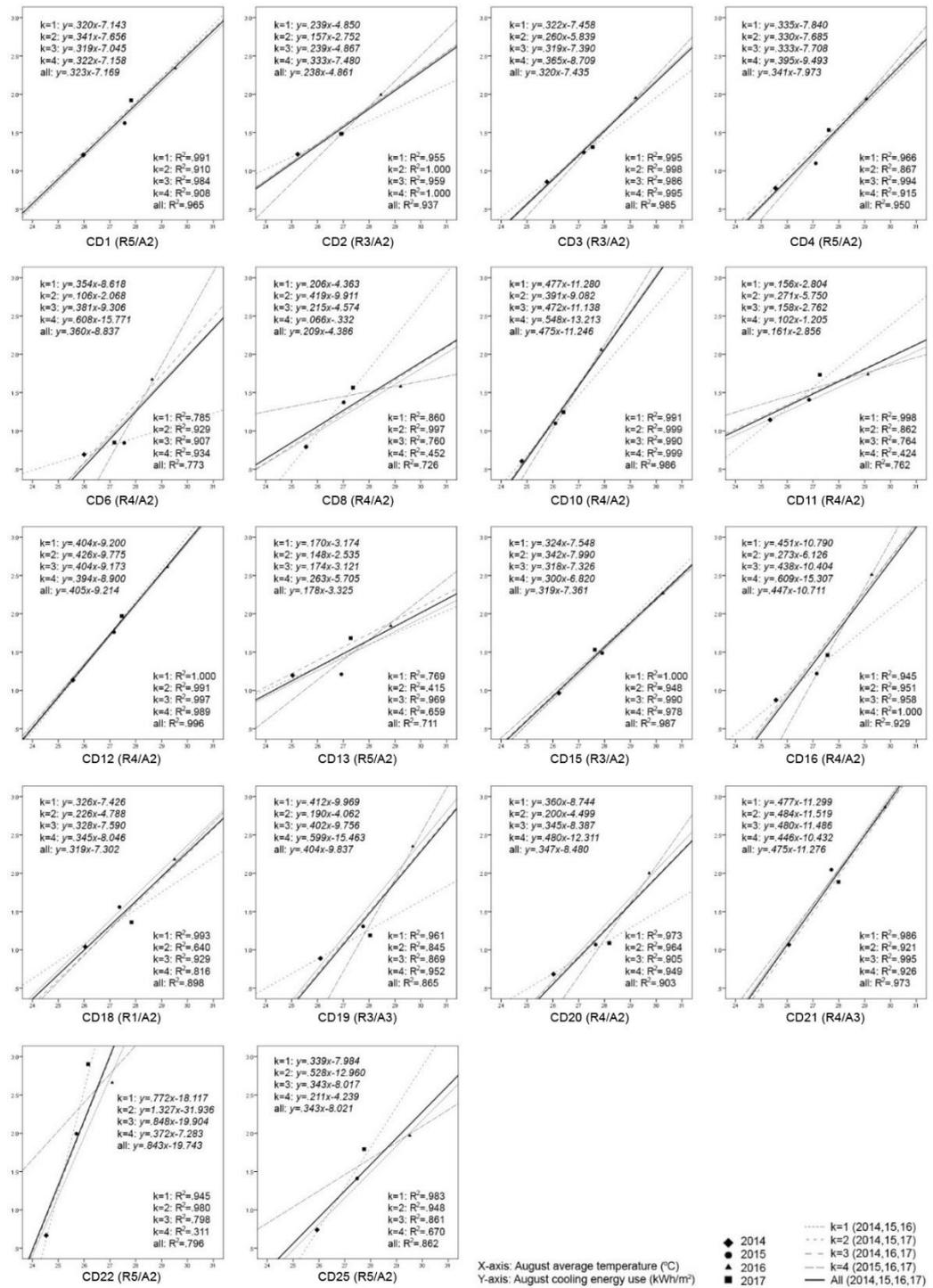
Figure 6-6. Scatter plots between present measured peak (August) cooling energy use (kWh/m²) and August external temperature (ºC) in each archetype of neighbourhood (micro level), and the detailed coefficients of bivariate regression models in each *k*-fold. *The model fit in All (2014-17) is for predicting peak cooling energy use of each neighbourhood archetype in future years

As LOOCV was applied here to evaluate model accuracy within a small sample size (N=4), and only three data points were taken into account in generating the model fit, the coefficient of determination ($R^2$) of the relationship between the two variables is rather sensitive to certain small and irregular changes. For examples, CD8 ($k4$, $R^2$=.452), CD11 ($k4$, $R^2$=.424), CD13 ($k2$, $R^2$=.415), CD18 ($k2$, $R^2$=.640), CD22 ($k4$, $R^2$=.311) and CD25 ($k4$, $R^2$=.670), compared to other folds, these neighbourhoods show a particularly low $R^2$ in only one fold. Interestingly, common to the $k$-formation of those folds ($k2$ and $k4$) was the combination between 2 typical summer years (2015 and 2017) and one abnormal summer years (2014, the mildest or 2016, the warmest). This suggests that there could be another key determinant involved if such irregular patterns occur. However, this can only be confirmed by further investigation of larger data sample sizes.

Table 6-6 shows the LOOCV error statistics output of each neighbourhood archetype. To show the differentiated errors in each testing year, percentage error (PE, %) was used. MAPE (mean absolute percentage error) represents average of each year's PE. Overall, half of neighbourhood archetypes (9/18) are considered reasonably acceptable including CD1, 2, 3, 4, 10, 12, 15, 18, 21.  However, the rest of the archetypes had relatively weak reliability in terms of model accuracy.

In detail, firstly, CD22 had the largest error as this archetype was already identified as an outlier. Secondly, those low model accuracy archetypes had a tendency that only one or two testing years' model had weak reliability (high PE) within the four testing years. This can result from a small sample in relation to the irregular pattern of an archetype's cooling energy use in certain years. Figure 6-7 shows the coefficient of determination ($R^2$) of aggregate of all 18 archetypes. As all datasets for this aggregation came from each archetype specific bivariate regression model, the accuracy of the macro modelling test result (Table 6-5 and Figure 6-5) was much improved in the micro modelling approach.

Table 6-6. Error statistics of the LOOCV between the predicted and the observed peak

cooling energy use in each neighbourhood (archetype)

| Neighbourhood (archetype) | k-fold's percentage error (%) | | | | MAPE | $R^2$ |
|---|---|---|---|---|---|---|
| | k=1, 2017 test | k=2, 2016 test | k=3, 2015 test | k=4, 2014 test | | |
| CD1 (R5/A2) | 0.1 | 8.3 | 2.7 | 8.1 | 4.8 | .936 |
| CD2 (R3/A2) | 24.4 | 6.6 | 13.5 | 6.1 | 12.6 | .643 |
| CD3 (R3/A2) | 18.9 | 2.8 | 10.3 | 6.7 | 9.7 | .901 |
| CD4 (R5/A2) | 24.6 | 19.8 | 2.1 | 9.1 | 13.9 | .888 |
| CD6 (R4/A2) | 96.5 | 1.3 | 51.7 | 17.6 | 41.8 | .152 |
| CD8 (R4/A2) | 70.9 | 10.1 | 46.7 | 18.8 | 36.6 | .144 |
| CD10 (R4/A2) | 38.3 | 7.4 | 12.5 | 6.9 | 16.3 | .903 |
| CD11 (R4/A2) | 20.7 | 5.0 | 23.3 | 16.1 | 16.3 | .366 |
| CD12 (R4/A2) | 3.7 | 2.2 | 2.9 | 4.0 | 3.2 | .988 |
| CD13 (R5/A2) | 26.2 | 28.2 | 6.6 | 12.2 | 18.3 | .435 |
| CD15 (R3/A2) | 9.1 | 4.0 | 3.8 | 8.0 | 6.2 | .966 |
| CD16 (R4/A2) | 70.9 | 20.9 | 25.4 | 12.3 | 32.4 | .585 |
| CD18 (R1/A2) | 9.3 | 11.0 | 14.5 | 21.9 | 14.1 | .702 |
| CD19 (R3/A3) | 78.9 | 7.5 | 32.7 | 33.6 | 38.2 | .368 |
| CD20 (R4/A2) | 72.6 | 7.2 | 28.3 | 27.3 | 33.9 | .522 |
| CD21 (R4/A3) | 10.5 | 10.8 | 1.2 | 8.9 | 7.8 | .946 |
| CD22 (R5/A2) | 178.0 | 5.3 | 50.6 | 28.7 | 65.6 | .225 |
| CD25 (R5/A2) | 66.6 | 0.3 | 32.9 | 21.4 | 30.3 | .480 |
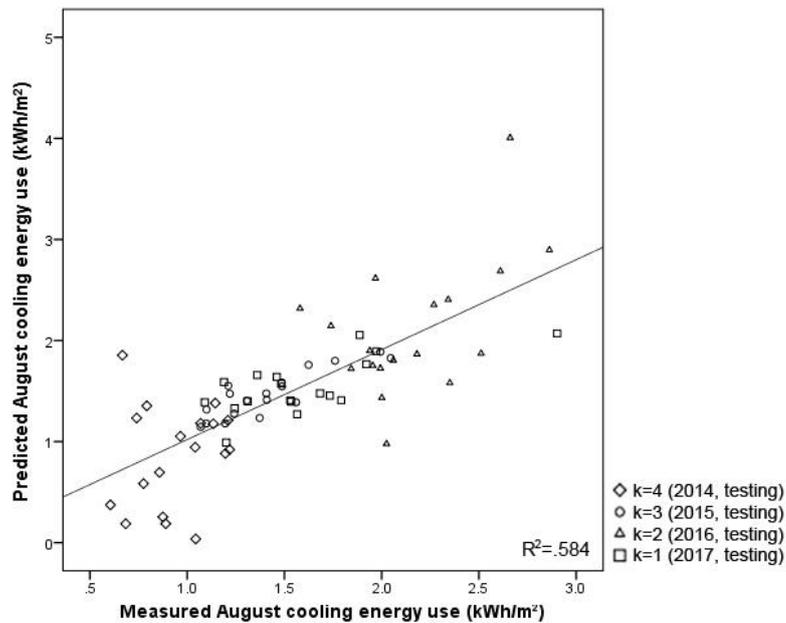


Figure 6-7. Coefficient of determination ($R^2$) between the predicted and measured peak

cooling energy use at total (aggregate of all archetypes of 18 neighbourhoods).

Finally, based on the regression model, future peak cooling energy use was estimated

(Figure 6-8. b). As the bivariate cooling energy model was built on the correlation

coefficients with external temperatures (CD-AWS), a comparison between present and future external temperatures is shown in Figure 6-8 (a). Overall, the estimated future peak cooling energy use will increase as the projected temperatures rise in 2050s. However, some districts (e.g., CD6, CD19, and CD20) are different: Common to these districts, the projected temperatures (RCP4.5) are higher than 2016 (the hottest year during the study period 2014-17), but the estimated cooling energy uses are lower than the ones metred in 2016. However, under the RCP8.5 climate change scenario, dramatic increases of peak cooling energy use in 2045 (projected the hottest year in 2050s under RCP8.5) are predicted for all archetypes in their city districts. Here, the predicted peak cooling energy uses and the KMA climate projections were then used as inputs to estimate each archetype's indoor thermal conditions in 2050s.
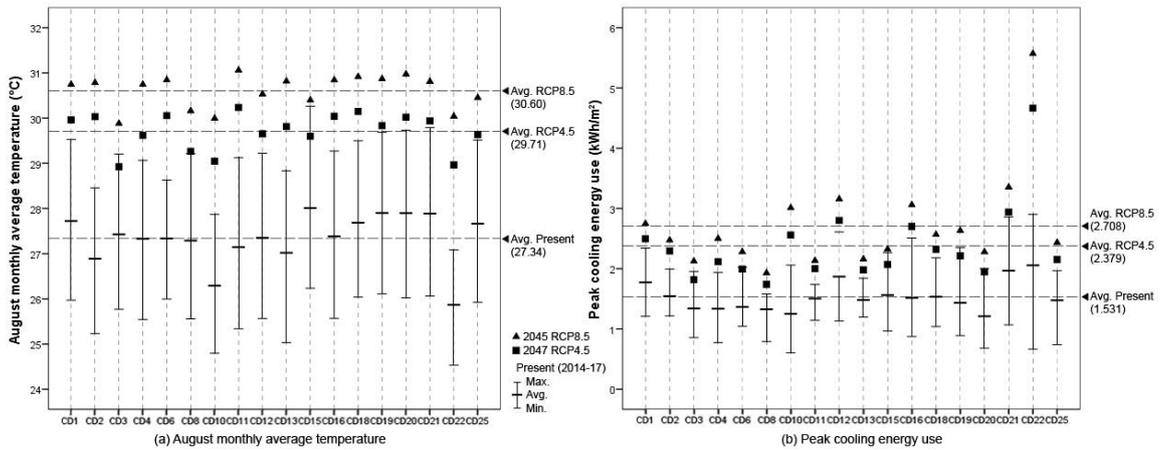


Figure 6-8. (a) 2014-17 and 2045 RCP8.5 and 2047 RCP4.5 August monthly average temperatures, (b) neighbourhood archetypes 2014-17 and 2045 RCP8.5 and 2047 RCP4.5 peak cooling energy uses estimated by each neighbourhood archetype bivariate regression model

Table 6-7 shows descriptive variation of peak (August) temperature and cooling energy use in future years based on the present (2014-17) mean and maximum values. In RCP4.5 (2047), the average of all archetype neighbourhoods' temperature variations by present mean value (by Max.) was 2.37°C (.60°C) within the range of 1.49°C (-.66°C) and 3.15°C (1.88°C). The future peak cooling energy use was predicted an average increase of 54.5% (8.7%) within the range of 31.2% (-8.7%) and 126% (60.7%). Looking at neighbourhood (archetype) individually, even though CD2(R3/A2) and CD22(R5/A2), their future August temperature variations were similar (close to Max.) but the estimated cooling energy uses varied significantly: 48.5% (15.1%) in CD2(R3/A2); 126.9% (60.7%) in CD22(R5/A2). Only two neighbourhoods, CD3(R3/A2) and CD15(R3/A2), are projected lower August temperatures (-.28°C and -.66°C by Max); and for five neighbourhoods, CD3(R3/A2), CD6(R4/A2), CD15(R3/A2), CD19(R3/A3), CD20(R4/A2), the cooling energy uses were estimated decreases of -6.9%, -1.5%, -8.7%, -5.8%, -2.6% respectively.

On the other hand, in RCP8.5 2045, all CDs were predicted to both have an average temperature increase (3.2°C by mean; 1.49°C by Max.) and average cooling energy use increase (75.8%; 23.4%). The range of temperature variation was between 2.39°C by mean (.14°C by Max.) and 4.17°C (2.95°C), and of cooling energy use was between 41.8% (2.5%) and 170.9% (91.9%) respectively. Clearly, the variation of estimated peak cooling energy uses in 2045 RCP8.5 (high-emission scenario) is much higher than in 2047 RCP4.5 (lower-emission scenario).

Table 6-7. Descriptive variation of August monthly average temperature ($^{\circ}$C) and peak cooling energy use (kWh/m$^2$) in future years (RCP4.5 2047 and RCP8.5 2045) based on their present (2014-17) Mean and Maximum values. * (): variation by present Max

| Neighbour-hood (Archetype) | August monthly average temperature ($^{\circ}$C) | | | | Peak (August) cooling energy use (kWh/m$^2$) | | | | | |
|---|---|---|---|---|---|---|---|---|---|---|
| | Present (2014-17) | | RCP4.5 (2047) | RCP8.5 (2045) | Present (2014-17) | | RCP4.5 (2047) | | RCP8.5 (2045) | |
| | Mean | Max. | Variation by mean, $^{\circ}$C | Variation by mean, $^{\circ}$C | Mean | Max. | Estim-ation | variation by mean, % | Estim-ation | variation by mean, % |
| CD1(R5/A2) | 27.72 | 29.53 | 2.24 (1.43) | 3.02 (1.22) | 1.774 | 2.342 | 2.497 | 40.7 (6.6) | 2.750 | 55.0 (17.4) |
| CD2(R3/A2) | 26.89 | 28.45 | 3.15 (1.58) | 3.90 (2.33) | 1.545 | 1.993 | 2.295 | 48.5 (15.1) | 2.474 | 60.1 (24.1) |
| CD3(R3/A2) | 27.43 | 29.20 | 1.49 (-.28) | 2.45 (.68) | 1.341 | 1.954 | 1.819 | 35.7 (-6.9) | 2.126 | 58.5 (8.8) |
| CD4(R5/A2) | 27.33 | 29.06 | 2.29 (.55) | 3.41 (1.68) | 1.337 | 1.939 | 2.117 | 58.3 (9.2) | 2.500 | 87.0 (29.0) |
| CD6(R4/A2) | 27.34 | 28.63 | 2.72 (1.43) | 3.51 (2.22) | 1.366 | 2.025 | 1.994 | 46.0 (-1.5) | 2.279 | 66.8 (12.6) |
| CD8(R4/A2) | 27.29 | 29.21 | 1.98 (.05) | 2.87 (.95) | 1.328 | 1.580 | 1.741 | 31.2 (10.2) | 1.929 | 45.3 (22.1) |
| CD10(R4/A2) | 26.29 | 27.87 | 2.75 (1.18) | 3.70 (2.12) | 1.252 | 2.060 | 2.560 | 104.5 (24.3) | 3.011 | 140.5 (46.2) |
| CD11(R4/A2) | 27.14 | 29.13 | 3.09 (1.11) | 3.92 (1.93) | 1.506 | 1.739 | 2.003 | 33.0 (15.2) | 2.135 | 41.8 (22.8) |
| CD12(R4/A2) | 27.35 | 29.22 | 2.30 (.43) | 3.18 (1.31) | 1.869 | 2.610 | 2.802 | 49.9 (7.3) | 3.158 | 68.9 (21.0) |
| CD13(R5/A2) | 27.02 | 28.83 | 2.79 (.98) | 3.80 (1.98) | 1.483 | 1.843 | 1.981 | 33.5 (7.5) | 2.159 | 45.5 (17.1) |
| CD15(R3/A2) | 28.01 | 30.26 | 1.59 (-.66) | 2.39 (.14) | 1.563 | 2.268 | 2.070 | 32.4 (-8.7) | 2.324 | 48.7 (2.5) |
| CD16(R4/A2) | 27.38 | 29.27 | 2.65 (.77) | 3.46 (1.57) | 1.517 | 2.511 | 2.702 | 78.1 (7.6) | 3.060 | 101.8 (21.9) |
| CD18(R1/A2) | 27.68 | 29.50 | 2.46 (.65) | 3.23 (1.42) | 1.536 | 2.181 | 2.322 | 51.2 (6.5) | 2.567 | 67.2 (17.7) |
| CD19(R3/A3) | 27.90 | 29.69 | 1.93 (.15) | 2.97 (1.18) | 1.434 | 2.350 | 2.215 | 54.5 (-5.8) | 2.634 | 83.6 (12.0) |
| CD20(R4/A2) | 27.90 | 29.73 | 2.12 (.29) | 3.07 (1.24) | 1.211 | 2.001 | 1.948 | 60.9 (-2.6) | 2.279 | 88.2 (13.9) |
| CD21(R4/A3) | 27.89 | 29.79 | 2.05 (.15) | 2.92 (1.02) | 1.966 | 2.862 | 2.941 | 49.5 (2.7) | 3.354 | 70.6 (17.2) |
| CD22(R5/A2) | 25.87 | 27.08 | 3.10 (1.88) | 4.17 (2.95) | 2.056 | 2.902 | 4.665 | 126.9 (60.7) | 5.570 | 170.9 (91.9) |
| CD25(R5/A2) | 27.66 | 29.51 | 1.97 (.12) | 2.79 (.94) | 1.477 | 1.968 | 2.154 | 45.8 (9.5) | 2.434 | 64.8 (23.7) |
| Avg. | 27.34 | 29.11 | 2.37 (.60) | 3.26 (1.49) | 1.531 | 2.174 | 2.379 | 54.5 (8.7) | 2.708 | 75.8 (23.4) |
| Min. | 25.87 | 27.08 | 1.49 (-.66) | 2.39 (.14) | 1.211 | 1.580 | 1.741 | 31.2 (-8.7) | 1.929 | 41.8 (2.5) |
| Max. | 28.01 | 30.26 | 3.15 (1.88) | 4.17 (2.95) | 2.056 | 2.902 | 4.665 | 126.9 (60.7) | 5.570 | 170.9 (91.9) |

### 6.2.4. HSV-A$_T$ and HSV-B$_T$: Heat stress vulnerability in terms of future indoor thermal conditions

Given the outputs from the multiple regression modelling presented above, the potential heat stress vulnerability (HSV) of Seoul's dwelling stock under climate projections is assessed in terms of the perspective of dwellers' health and well-being under the "no change of peak cooling energy use behaviour" scenario. The peak cooling temperature set points of the 18 neighbourhood archetypes can be estimated by the multiple regression model ($y = 6.478 + .854x_1 - 2.122x_2$, where $x_1$ is August average temperature ($^{\circ}$C) and $x_2$ is cooling energy use (kWh/m$^2$). Figure 6-9 shows the result of estimated peak cooling temperature set points for present (2014-17) and future years (2047 RCP4.5 & 2045 RCP8.5).
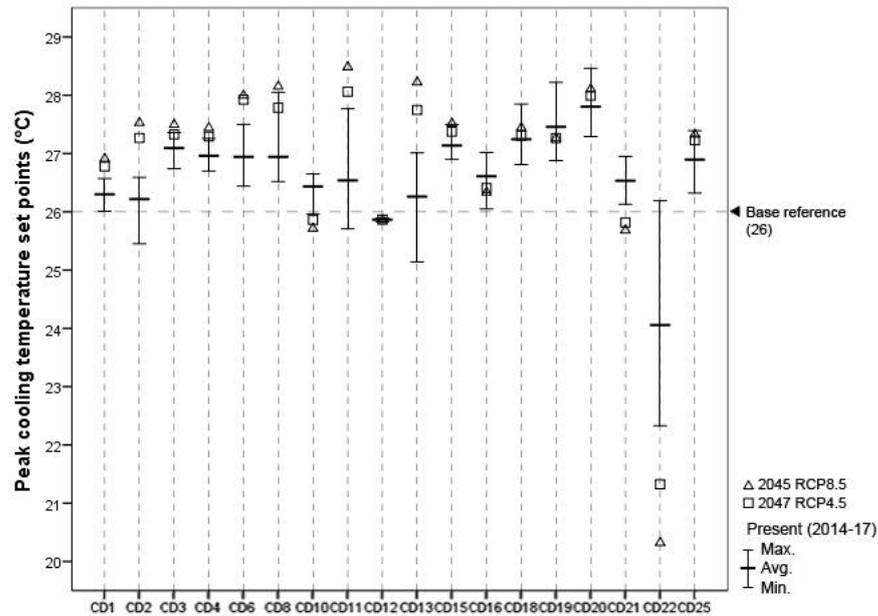
Figure 6-9. Estimated neighbourhood archetypes' peak (August) cooling temperature set points for present (2014-17) and future years (RCP4.5 2047 and RCP8.5 2045) in Seoul

Here the cooling temperature set points are considered as an indicator of indoor thermal conditions with which this study further concludes an assessment of potential heat stress vulnerability of the housing stock in future climate. However, the household's indoor thermal condition itself does not represent any details of occupants' thermal comfort or discomfort as it only represents HVAC cooling set point temperature deduced from the history of each neighbourhood's peak cooling energy uses which has been already paid by dwellers. The key part where we pay attention to is the history which is determined by neighbourhood-specific cooling energy use behaviour responding to the external climate under the occupants' own circumstances. Therefore, the cooling temperature set point can be considered as an indicator of the maximized level of indoor heat acclimatisation (IHA). Therefore, this study assumes that if the predicted future years' cooling temperature set point is higher than the present Max., there can be increased HSV in a view of historical IHA.

Table 6-8 shows the differences of neighbourhood archetypes' future indoor thermal conditions from the two points of reference HSV-A$_T$ and HSV-B$_T$. Overall, the average difference in HSV-A$_T$ under RCP4.5 climate change scenario (or RCP8.5) was .81°C (.88°C) within the range from -4.68°C (-5.68°C) to 2.06°C (2.48°C), while in HSV-B$_T$, it was much reduced to -.42°C (-.36°C) within the range from -4.87°C (-5.87°C) to .74°C (1.22°C). In comparison between HSV-A$_T$ and HSV-B$_T$, there are significant difference changes commonly found under both climate change scenarios: all differences in HSV-B$_T$ are more reduced than in HSV-A$_T$. This shows that the estimated future indoor thermal condition will be far higher than the 26°C threshold as recommended by the local HVAC design guide; yet it is actually closer to each neighbourhood's present highest IHA level (Max. IHA) - the neighbourhood-specific demographic heat-related indoor set-point temperature.

Moreover, it was observed in HSV-A$_T$ that only four (out of 18) neighbourhoods were found to have lower set points than 26°C. On the other hand, in HSV-B$_T$, many neighbourhoods (12 out of 18 in RCP4.5; 9 out of 18 in RCP8.5) were found to have lower set point temperatures than the historical Max. IHA. This suggests that the rest of the neighbourhoods will likely be exposed to certain heat stress in the future. This indoor thermal condition based HSV assessment assumes that future cooling energy demand will be met by suppliers and affordable by dwellers to maintain below those indoor thermal thresholds (26°C in HSV-A$_T$ and neighbourhood-specific historical Max. IHA in HSV-B$_T$) in future climate.

Table 6-8. Descriptive variation (difference) of neighbourhood-archetype's August (peak) cooling temperature set point (°C) in future years (RCP4.5 2047 and RCP8.5 2045) from 26°C fixed point (HSV-$A_T$) and from each neighbourhood-archetype's present (2014-17) Max. (HSV-$B_T$)

| Neighbour-hood (Archetype) | Present Max. indoor Temp (°C) | RCP4.5 (2047) | | | | RCP8.5 (2045) | | | |
|---|---|---|---|---|---|---|---|---|---|
| | | Est. Indoor Temp. (°C) | Change of cooling load to present Max (%) | Difference (°C) | | Est. Indoor Temp. (°C) | Change of cooling load to present Max (%) | Difference (°C) | |
| | | | | HSV-$A_T$ | HSV-$B_T$ | | | HSV-$A_T$ | HSV-$B_T$ |
| CD1(R5/A2) | 26.57 | 26.78 | 6.6 | .78 | .21 | 26.91 | 17.4 | .91 | .34 |
| CD2(R3/A2) | 26.59 | 27.27 | 15.1 | 1.27 | .68 | 27.53 | 24.1 | 1.53 | .94 |
| CD3(R3/A2) | 27.36 | 27.33 | -6.9 | 1.33 | -.03 | 27.50 | 8.8 | 1.50 | .14 |
| CD4(R5/A2) | 27.26 | 27.29 | 9.2 | 1.29 | .03 | 27.44 | 29.0 | 1.44 | .18 |
| CD6(R4/A2) | 27.50 | 27.92 | -1.5 | 1.92 | .42 | 28.00 | 12.6 | 2.00 | .50 |
| CD8(R4/A2) | 28.05 | 27.79 | 10.2 | 1.79 | -.26 | 28.15 | 22.1 | 2.15 | .10 |
| CD10(R4/A2) | 26.65 | 25.86 | 24.3 | -.14 | -.79 | 25.71 | 46.2 | -.29 | -.94 |
| CD11(R4/A2) | 27.77 | 28.06 | 15.2 | 2.06 | .29 | 28.48 | 22.8 | 2.48 | .71 |
| CD12(R4/A2) | 25.89 | 25.87 | 7.3 | -.13 | -.02 | 25.86 | 21.0 | -.14 | -.03 |
| CD13(R5/A2) | 27.01 | 27.75 | 7.5 | 1.75 | .74 | 28.23 | 17.1 | 2.23 | 1.22 |
| CD15(R3/A2) | 27.50 | 27.38 | -8.7 | 1.38 | -.12 | 27.52 | 2.5 | 1.52 | .02 |
| CD16(R4/A2) | 27.02 | 26.41 | 7.6 | .41 | -.61 | 26.33 | 21.9 | .33 | -.69 |
| CD18(R1/A2) | 27.85 | 27.31 | 6.5 | 1.31 | -.54 | 27.44 | 17.7 | 1.44 | -.41 |
| CD19(R3/A3) | 28.22 | 27.27 | -5.8 | 1.27 | -.95 | 27.26 | 12.0 | 1.26 | -.96 |
| CD20(R4/A2) | 28.46 | 27.99 | -2.6 | 1.99 | -.47 | 28.10 | 13.9 | 2.10 | -.36 |
| CD21(R4/A3) | 26.95 | 25.82 | 2.7 | -.18 | -1.13 | 25.68 | 17.2 | -.32 | -1.27 |
| CD22(R5/A2) | 26.19 | 21.32 | 60.7 | -4.68 | -4.87 | 20.32 | 91.9 | -5.68 | -5.87 |
| CD25(R5/A2) | 27.39 | 27.23 | 9.5 | 1.23 | -.16 | 27.33 | 23.7 | 1.33 | -.06 |
| Avg. | 27.24 | 26.81 | 8.7 | .81 | -.42 | 26.88 | 23.4 | .88 | -0.36 |
| Min. | 25.89 | 21.32 | -8.7 | -4.68 | -4.87 | 20.32 | 2.5 | -5.68 | -5.87 |
| Max. | 28.46 | 28.06 | 60.7 | 2.06 | .74 | 28.48 | 91.9 | 2.48 | 1.22 |

It was considered at the same time the percentage change of future peak cooling loads against present Max cooling energy use along with the indoor thermal differences. The future peak cooling loads of many neighbourhoods (13 out of 18 under RCP4.5) and in all neighbourhoods (RCP8.5) were predicted to increase. This highlights a potential trend in that even though the peak cooling demands may be met there are many neighbourhoods whose future indoor thermal levels are elevated to the extent of causing potential heat stress. For some of the neighbourhoods such as CD11 and CD13, not only their future peak cooling loads are higher than present Max cooling usages but also, the future cooling temperature set points are predicted to be above their historical Max. IHA. Here raises the question if there is a point of no return in Max. IHA for an urban population

living in a particular neighbourhood beyond which large-scale outbreak of heat-related illness occurs.

## 6.3. Cooling *Energy* Demand based HSV assessment (HSV-A$_E$, HSV-B$_E$)

This section presents another Seoul neighbourhood dwelling stock modelling and the heat stress vulnerability assessment in three sets of results in accordance with the key steps shown in Figure 4-1. Based on the data collected (2014-2017) and estimated present HVAC peak cooling temperature set points, the key determinants of archetypes' present peak cooling energy use were identified (section 6.3.1). A multiple regression model for predicting archetypes' future peak cooling demands (PCDs) during the peak cooling month (August in Seoul) is presented and evaluated in section 6.3.2. Finally, section 6.3.3 reports on the estimated future PCDs for the purpose of Seoul's HSV assessment in terms of implications for cooling energy supply and demand over the timeframe of climate projection under the "no stock change" scenario.

### 6.3.1. Identified key determinants of peak cooling energy use

As carried out in section 6.2.1, a multiple regression analysis was carried out at the macro level (i.e. aggregate of the 18 neighbourhood archetypes) to identify likely key determinants of present peak cooling energy use. The only difference from section 6.2.1 analysis was the dependent variable which was swapped from the estimated cooling temperature set points to peak cooling energy use. Therefore, six independent variables were used in this section taking into account factors which can potentially be determinants affecting peak cooling energy use and Seoul's open data availability at the same time: (1) August (peak) average temperature ($^{\circ}$C) in each city-district

neighbourhood (Figure 5-1); (2) NWD household equipment energy use (Table 5-5); (3) estimated present peak cooling temperature set points (Figure 5-8); (4) the collected property price (KRW/m$^2$) and (5) floor area ratio (%) datasets of each apartment neighbourhood (Figure 5-3); (6) U-value (W/m$^2$*K) of the external wall (Table 4-9). Also, total number of sample was 72, 4 years (present 2014-17) * 18 neighbourhood archetypes.

Table 6-9. Coefficients of multiple regression analysis to identify key determinants in present peak cooling energy use

|  | Dependent | Independent | *B* | Std. error | Beta | Sig. |
|---|---|---|---|---|---|---|
| R$^2$ = .990, R$^2$ (adj.)=.989 *p* = .000 | August (peak) cooling energy use (kWh/m$^2$) | (Constant) | 2.119 | .282 |  | .000 |
|  |  | August average temperature (ºC) | .387 | .005 | .981 | .000 |
| N=72 (18 * 4 yrs) |  | August cooling temperature set points (ºC) | -.432 | .008 | -.763 | .000 |
|  |  | Property Price (KRW/m$^2$) | .000 | .000 | .035 | .023 |
|  |  | Floor Area Ratio (%) | .000 | .000 | .021 | .144 |
|  |  | NWD energy use (kWh/m$^2$) | .001 | .032 | .000 | .978 |
|  |  | Building envelop (W/m$^2$*K) | .311 | .063 | .071 | .000 |

Table 6-9 shows the output of the multiple regression analysis. Overall, R$^2$ was .990 (.989, adjusted R$^2$) and *p* was .000, representing that 99% of the variance in the present peak cooling energy use (dependent) was explained by the model and this model was statistically significant respectively. In evaluating each of the independent variables, the highest standardised coefficients (Beta) occurred in August the average temperature (.981) and peak cooling temperature set points (-.763), meaning that those two variables made the strongest contribution to peak cooling energy use within the statistically significant level (Sig.=.000). Finally, August average temperature and peak cooling temperature set points were identified as key determinants in peak cooling energy use. Those two identified parameters were used in modelling process to predict archetypes' future peak cooling demands (PCDs) in following subsection.

## 6.3.2. Modelling peak cooling demands

Given the external August average temperature and the August cooling temperature set points as the two key determinants identified, the archetypes' PCDs in future years can be estimated from multiple regression modelling with input of Seoul's latest climate change projection. Considering the current data sample scope and size, a decision was made to perform the multiple regression analysis at a macro-level, that is, an aggregate of all city-district archetypes.

A preliminary analysis was carried out to check outliners, normality, homoscedasticity and independence of residuals through inspecting the normal probability plot (P-P) of the regression standardised residual and the scatterplot (Figure 6-10). From the preliminary analysis, a CD22's 2017 data was detected as outlier: its' Mohalanobis distance was 21.06 which was above 13.82, critical value for 2 independent variables model (Tabachnick and Fidell, 2007). However, the regression modelling was carried out without deleting CD22 as only one was found. The resultant multi-regression model is presented in Figure 6-11 (scatter plot) and Table 6-10 (model details).
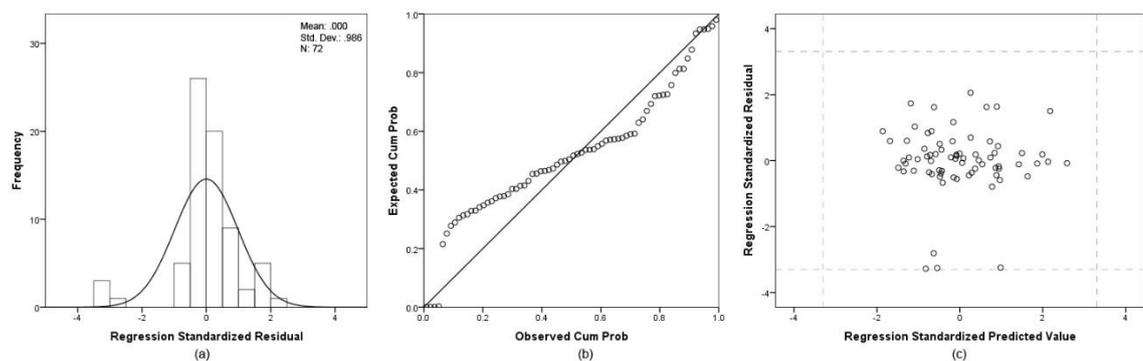


Figure 6-10. A preliminary analysis for the multiple regression model: (a) Normality histogram, (b) normal probability plot (P-P) and (c) scatterplot of regression standardised residuals. * Dependent variable: estimated neighbourhood archetypes' present peak cooling energy use. ** Dot lines of (c) are at ±3.3
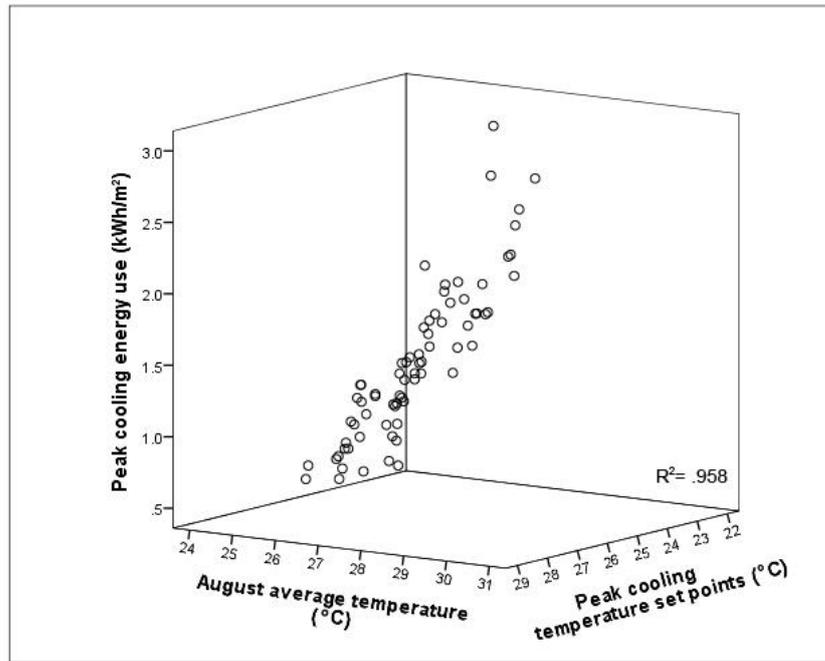
Figure 6-11. Scatter plot of peak cooling energy use based on the two key determinants identified (August average external temperature and Peak cooling temperature set points)

Table 6-10. Coefficients of a multi-regression model for estimating peak cooling demands (PCDs) of Seoul's 18 neighbourhood archetypes based on the 2014-17 datasets

| | Dependent | Independent | *B* | Std. error | Beta | Sig. |
|---|---|---|---|---|---|---|
| $R^2$ = .958, *p* = .000  N=72 (18 * 4 yrs) | Peak cooling energy use (kWh/m$^2$) | (Constant) | 2.324 | .403 | | .000 |
| | | August average temperature (°C) | .393 | .011 | .973 | .000 |
| | | Peak cooling temperature set points (°C) | -.424 | .015 | -.749 | .000 |

*K*-fold cross validation was also applied to evaluate the model accuracy. Four folds were generated as there were four year datasets (2014-17). For instance, *k*=1 fold used 2014, 2015, 2016 datasets as the training set and 2017 as the testing set. Moreover, five criteria were used in the error statistics: mean absolute error (MAE); mean square error (MSE); root mean square error (RMSE); mean absolute percentage error (MAPE); coefficient of determination ($R^2$). The predicted data represents the output resulted from each *k*-fold

multiple regression model while the observed represents the outcome estimated by NWD energy use assumption (Table 5-5).

Table 6-11. Coefficients of modelling archetypes' peak cooling demands of each $k$-fold to evaluate model accuracy and the error statistics between the predicted and the observed of each $k$-fold. * $y$: peak cooling energy use (kWh/m$^2$), $x_1$: August average temperature (°C), $x_2$: cooling temperature set points (°C).

| $k$-fold model $y(x_1, x_2)=a+bx_1+cx_2$ | $a$ | $b$ | $c$ | $R^2$ | Sig. |
|---|---|---|---|---|---|
| $k$=1 (2014, 15, 16) | 2.544 | .392 | -.441 | .962 | .000 |
| $k$=2 (2014, 15, 17) | 2.142 | .400 | -.434 | .933 | .000 |
| $k$=3 (2014, 16, 17) | 2.175 | .390 | -.425 | .966 | .000 |
| $k$=4 (2015, 16, 17) | 2.309 | .399 | -.440 | .946 | .000 |

| Error statistics | MAE (kWh/m$^2$) | MSE (kWh/m$^2$) | RMSE (kWh/m$^2$) | MAPE (%) | $R^2$ |
|---|---|---|---|---|---|
| $k$=1 (testing 2017) | .069 | .009 | .095 | 4.67 | .975 |
| $k$=2 (testing 2016) | .055 | .005 | .073 | 2.63 | .958 |
| $k$=3 (testing 2015) | .051 | .005 | .068 | 3.62 | .950 |
| $k$=4 (testing 2014) | .050 | .006 | .074 | 5.68 | .908 |
| At total | .057 | .006 | .078 | 4.15 | .981 |

Table 6-11 shows the model details and the outputs of the error statistics of each $k$-fold. Overall, the coefficient of determination from the scatter plot between the observed and the predicted was .981 (Figure 6-12), representing about 98% of variance in the observed peak cooling energy use could be explained by the corresponding fourfold multiple regression models. Moreover, all four $k$-fold's errors were near to zero, representing that there are no over fitting training datasets to the testing sets in all four cases. From this cross validation, the multiple regression model is considered acceptable to be used in predicting the archetypes' peak cooling demands in future years for heat stress vulnerability assessment.
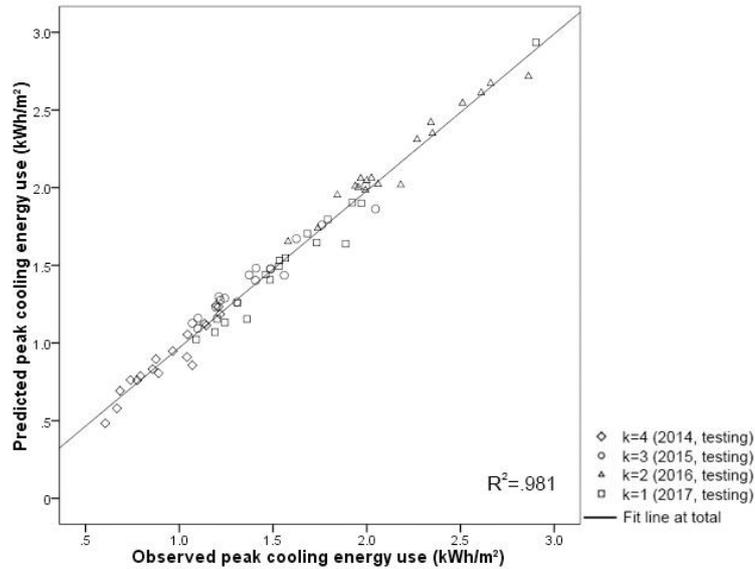
Figure 6-12. Coefficient of determination ($R^2$) between the predicted and observed peak cooling energy use at total (aggregate of all four $k$-folds).

### 6.3.3. HSV-A$_E$ and HSV-B$_E$: Heat stress vulnerability in terms of future peak cooling demands

Given the outputs from the multiple regression modelling presented above, another set of assessments were carried out in terms of peak cooling energy loads estimated to maintain the two types of indoor thermal thresholds. Similarly, the assessments of are two sub-types: HSV-A$_E$ in terms of peak cooling loads estimated by 26°C as a fixed cooling temperature set point for all neighbourhoods. HSV-B$_E$ in terms of peak cooling loads estimated by each neighbourhood's present Max. cooling set point temperature as derived from the Max. IHA of each neighbourhood. The peak cooling demands can be estimated by the multiple regression model in Table 6-10: $y = 2.324 + .393x_1 - .424x_2$, where $y$ is peak cooling demands (PCDs, kWh/m$^2$), $x_1$ is August average temperature (°C), and $x_2$ is cooling temperature set points (°C). Finally, this part of the HSV assessment is quantified by the variation (difference) of future peak cooling loads against certain base reference points.

This study considers that the historical maximum cooling energy use is a quantity resultant from dwellers' living experiences in spending energy from a socio-economic viewpoint. Here, it is assumed that the estimated future cooling energy demands going above the historical maximum cooling energy use (as a cooling energy supply threshold) could ultimately lead to increased heat stress vulnerability (i.e., cooling demands simply cannot be met even if affordable). Therefore, each neighbourhood's historical Max cooling energy use is used here as the base reference point to measure the variation (difference) in assessing both HSV-A$_E$ (according to the load meeting the 26°C threshold), and HSV-B$_E$ (according to the load meeting the Max. IHA threshold).

Table 6-12. Estimated neighbourhood archetypes' August (peak) cooling demands in future years to maintain a fixed cooling set point (26°C) to all 18 neighbourhoods for HSV-A$_E$ and to maintain each neighbourhood's present Max cooling set point to each neighbourhood individually for HSV-B$_E$, and descriptive variation (difference, %) from each neighbourhood's present Max. cooling energy use

| Neighbour-hood (Archetype) | Present Max. cooling (kWh/m$^2$) | RCP4.5 (2047, kWh/m$^2$) | | | | RCP8.5 (2045, kWh/m$^2$) | | | |
| | | HSV-A$_E$ | | HSV-B$_E$ | | HSV-A$_E$ | | HSV-B$_E$ | |
| | | Est. load | Difference (%) | Est. load | Difference (%) | Est. load | Difference (%) | Est. load | Difference (%) |
|---|---|---|---|---|---|---|---|---|---|
| CD1(R5/A2) | 2.342 | 2.814 | 20.2 | 2.567 | 9.6 | 3.122 | 33.3 | 2.875 | 22.8 |
| CD2(R3/A2) | 1.993 | 2.842 | 42.6 | 2.586 | 29.7 | 3.137 | 57.4 | 2.881 | 44.6 |
| CD3(R3/A2) | 1.954 | 2.406 | 23.1 | 1.816 | -7.1 | 2.782 | 42.4 | 2.193 | 12.2 |
| CD4(R5/A2) | 1.939 | 2.680 | 38.2 | 2.133 | 10.0 | 3.122 | 61.0 | 2.575 | 32.8 |
| CD6(R4/A2) | 2.025 | 2.851 | 40.8 | 2.200 | 8.7 | 3.161 | 56.1 | 2.511 | 24.0 |
| CD8(R4/A2) | 1.580 | 2.540 | 60.8 | 1.651 | 4.5 | 2.893 | 83.1 | 2.004 | 26.8 |
| CD10(R4/A2) | 2.060 | 2.454 | 19.1 | 2.172 | 5.5 | 2.827 | 37.2 | 2.545 | 23.5 |
| CD11(R4/A2) | 1.739 | 2.922 | 68.0 | 2.154 | 23.9 | 3.245 | 86.6 | 2.477 | 42.4 |
| CD12(R4/A2) | 2.610 | 2.692 | 3.1 | 2.740 | 5.0 | 3.037 | 16.3 | 3.085 | 18.2 |
| CD13(R5/A2) | 1.843 | 2.756 | 49.5 | 2.318 | 25.8 | 3.150 | 70.9 | 2.712 | 47.1 |
| CD15(R3/A2) | 2.268 | 2.672 | 17.8 | 2.022 | -10.9 | 2.985 | 31.6 | 2.335 | 2.9 |
| CD16(R4/A2) | 2.511 | 2.845 | 13.3 | 2.402 | -4.3 | 3.160 | 25.8 | 2.718 | 8.2 |
| CD18(R1/A2) | 2.181 | 2.888 | 32.4 | 2.085 | -4.4 | 3.189 | 46.2 | 2.387 | 9.4 |
| CD19(R3/A3) | 2.350 | 2.763 | 17.6 | 1.801 | -23.4 | 3.170 | 34.9 | 2.207 | -6.1 |
| CD20(R4/A2) | 2.001 | 2.837 | 41.8 | 1.770 | -11.5 | 3.211 | 60.5 | 2.144 | 7.2 |
| CD21(R4/A3) | 2.862 | 2.805 | -2.0 | 2.393 | -16.4 | 3.147 | 10.0 | 2.735 | -4.4 |
| CD22(R5/A2) | 2.902 | 2.423 | -16.5 | 2.340 | -19.4 | 2.845 | -2.0 | 2.762 | -4.8 |
| CD25(R5/A2) | 1.968 | 2.686 | 36.5 | 2.083 | 5.9 | 3.007 | 52.8 | 2.404 | 22.2 |
| Avg. | 2.174 | 2.715 | 28.1 | 2.180 | 1.7 | 3.066 | 44.7 | 2.530 | 18.3 |
| Min. | 1.580 | 2.406 | -16.5 | 1.651 | -23.4 | 2.782 | -2.0 | 2.004 | -6.1 |
| Max. | 2.902 | 2.922 | 68.0 | 2.740 | 29.7 | 3.245 | 86.6 | 3.085 | 47.1 |

Table 6-12 shows the estimations of future peak cooling demands (kWh/m$^2$) to maintain two types of HVAC cooling temperature set points and the variation (difference, %) for HSV-A$_E$ and HSV-B$_E$. Overall, the average difference (%) in HSV-A$_E$ under RCP4.5 climate change scenario (or RCP8.5) was 28.1% (44.7%) within the range from -16.5% (-2.0%) to 68.0% (86.6%). Moreover, there are only two neighbourhoods, CD21(R4/A3) and CD22(R5/A2), which have lower cooling energy demands than their historical Max cooling energy uses under RCP4.5; while only CD22(R5/A2) has a lower demand under RCP8.5. This suggests that Seoul's 16 (out of 18) neighbourhoods have increased vulnerability in terms of peak cooling loads to maintain 26$^o$C of indoor cooling set point in future years.

On the other hand, in HSV-B$_E$, the average difference (%) under RCP4.5 (or RCP8.5) was 1.7% (18.3%) within the range from -23.4% (-6.1%) to 29.7% (47.1%). Compared to HSV-A$_E$, the average difference in HSV-B$_E$ was much reduced. Moreover, there appeared more neighbourhoods (8 out of 18), which have less future cooling energy demands than the historical Max. use under RCP4.5. However, the number of such neighbourhoods is reduced to only three under RCP8.5. Pessimistically speaking, this suggests that 10 out of 18 under RCP4.5 and 15 out of 18 neighbourhoods under RCP8.5 have increased vulnerability in future climate.

To bring HSV-A$_E$ and HSV-B$_E$ together, this study introduced 'proportion' in sorting differences and produced a relative ranking of each HSV assessment under each climate change scenario. Here the difference value was converted to a value of proportion, ranging from 0.0 (Min. of difference) to 1.0 (Max. of difference), representing each neighbourhood (archetype) in relation to the whole city stock. Therefore, higher proportion values indicate higher levels of heat stress vulnerability and vice versa (Figure 6-13).
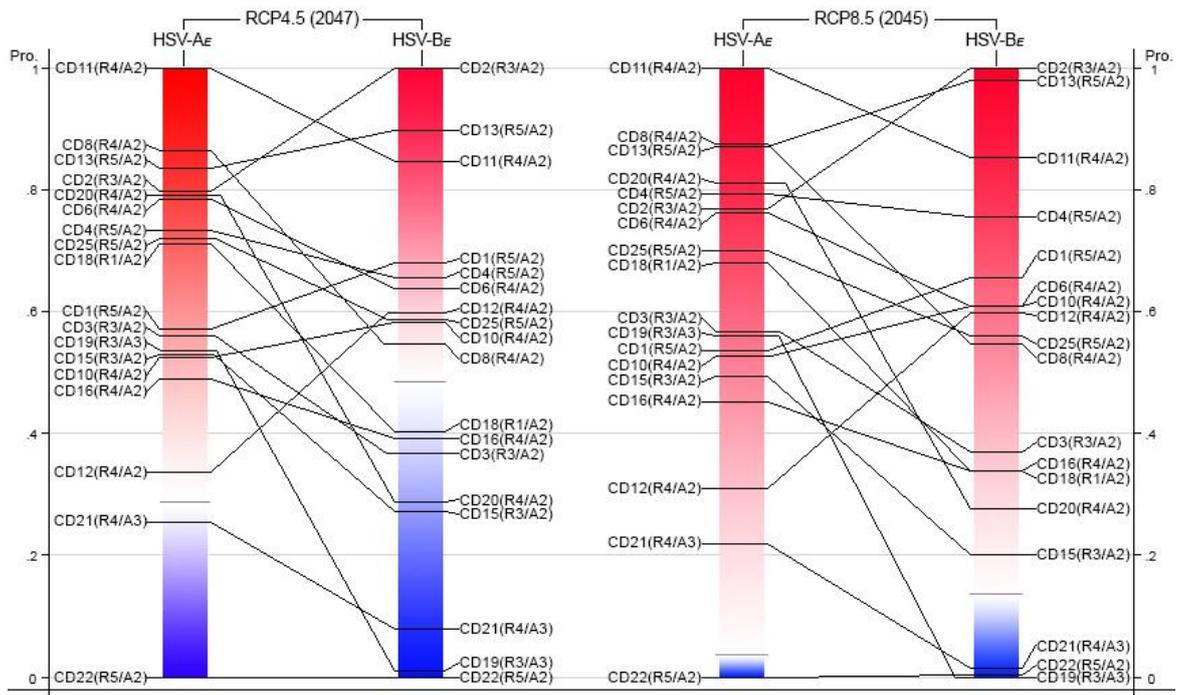
Figure 6-13. Relative ranking of potential heat stress vulnerability among the six archetypes in Seoul's 18 city district (CD) neighbourhoods in HSV-A$_E$ (26°C fixed cooling set point temperature based) and HSV-B$_E$ (neighbourhood-specific indoor heat acclimatisation based). *↓ higher to lower vulnerability ** The transition points (in white) between red and blue are set by the zero difference

From the ranking result, it was observed that the repeated instances where the same archetypes appear in neighbourhoods of different ranking positions. Special attention should be paid to the substantial differences between HSV-A$_E$ and HSV-B$_E$, in terms of the relative vulnerability ranking and the level of HSV (proportion). CD19(R3/A3) and CD20(R4/A2) are good examples: The ranking changes are due to the large differences in cooling temperature set points between 26°C, set by the fixed point as design criteria in HSV-A$_E$, and 28.22°C (or 28.46°C), set by CD19 (or CD20) neighbourhood-specific Max. IHA in HSV-B$_E$.

## 6.4 Conclusions

This chapter presented Seoul's neighbourhood dwelling stock modelling and the heat stress vulnerability (HSV) assessment in two approaches: HSV-A is based on a fixed threshold temperature (26°C as the local statutory standard adopted in Seoul), and HSV-B is based on the historical metred energy uses reflecting households' indoor heat acclimatisation histories. Furthermore, under HSV-A and HSV-B, this study employed two sub-methods: Cooling *Temperature* Set Points based (HSV-A$_T$, HSV-B$_T$), and Cooling *Energy* Demand based (HSV-A$_E$, HSV-B$_E$). The former perspective points to implications for dwellers' health and wellbeing under the "no change of peak cooling energy use behaviour" scenario. The latter peak cooling demand perspective points to implications for cooling energy supply and demand over the timeframe of climate change projections under the "no stock change" scenario. Those HSV assessments were summarised as the differences between the estimations and base reference points, following that neighbourhood archetypes further away from the reference points present higher HSV.

Firstly, for Cooling *Temperature* Set Points based assessments (HSV-A$_T$, HSV-B$_T$), the stock modelling for indoor thermal conditions was carried out. Two key determinants of peak indoor thermal conditions were identified by a multiple regression analysis at the macro level (aggregate of the 18 neighbourhood archetypes): August (peak) average temperature and the cooling energy use. Then, given the two identified determinants, a multiple regression model was generated to estimate archetypes' indoor thermal conditions under peak cooling in future years and the model accuracy was evaluated by *K*-fold cross validation.

To predict the archetypes' peak indoor thermal conditions in future years, estimates of the archetypes' peak cooling energy uses in were modelled at the micro level, in

accordance with the climate change projections for Seoul at the city district level. The model accuracy was checked by leave one out cross validation statistically. Overall, it was found that under the RCP4.5 climate change scenario, the future peak cooling energy use was predicted to have an average increase of 8.7% by each archetype's historical Max. cooling energy use within the range of -8.7% and 60.7%. On the other hand, under the RCP8.5, the average increase by Max. was predicted to be 23.4% within the range of 2.5% and up to 91.9%.

Given the outputs of the indoor thermal condition model, the Cooling *Temperature* Set Points based assessments were carried out. The outcomes showed that 14 (out of 18) neighbourhoods were predicted to be likely exposed to certain heat stress in future years in HSV-A$_T$, while 6 (out of 18 in RCP4.5) and 9 (out of 18 in RCP8.5) in HSV-B$_T$, under the assumption that future cooling energy demand will be met by suppliers and affordable by dwellers. Furthermore, particular attention should be paid to some neighbourhoods (i.e., CD11 and CD13), where not only their future peak cooling loads are higher than present Max cooling usages but also, the future cooling temperature set points are predicted to be above their historical Max. IHA.: hence, the high probability of dwellers' potential heat-related illnesses.

Secondly, for Cooling *Energy* Demand based assessments (HSV-A$_E$, HSV-B$_E$), the stock modelling for indoor thermal conditions was carried out. Two key determinants of peak cooling energy use were identified by a multiple regression analysis at the macro level (aggregate of the 18 neighbourhood archetypes): August (peak) average temperature and indoor cooling temperature set points. Then, given the two identified determinants, a multiple regression model was generated to estimate archetypes' peak cooling demands in future years and the model accuracy was evaluated by *K*-fold cross validation.

Finally, in Cooling *Energy* Demand based assessments, Seoul's 16 (out of 18) neighbourhoods have increased vulnerability in terms of peak cooling loads to maintain 26°C of indoor cooling set point in future years in HSV-A$_E$, while 10 out of 18 under RCP4.5 and 15 out of 18 neighbourhoods under RCP8.5 have increased vulnerability in future climate in HSV-B$_E$. Furthermore, a relative ranking of heat stress vulnerability of a city' dwelling stock was proposed based on the estimated peak cooling demands according to a statutory cooling temperature set point for all neighbourhoods (HSV-A$_E$) and to each neighbourhood archetype's present Max cooling set point temperature as the vulnerability threshold (HSV-B$_E$). There are three neighbourhoods, CD2(R3/A2), CD11(R4/A2), and CD13(R5/A2), are ranked at the top three positions persistently, which are the most vulnerable segments if their estimated peak cooling demand cannot be met in the 2050s.



(a) CD22        (b) CD2
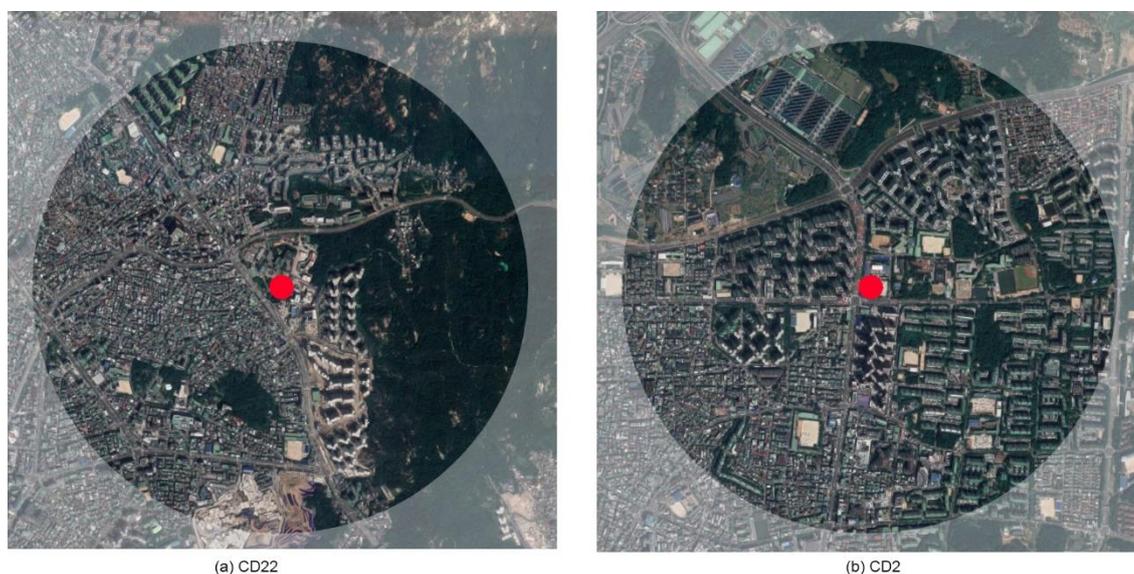
Figure 6-14. Unban context of CD22, the lowest HSV neighbourhood (a) and CD2, the highest HSV (b) *. Red dot: location of the weather station **. 1km radius circular boundary

Furthermore, two neighbourhoods were ranked at the top (CD2) and the bottom positions (CD22) persistently between the HSV-A$_E$ and HSV-B$_E$ paired relative rankings. It was important to think about what the main source of the opposite HSV results was caused by. Due to that fact this study is carried out within a limited availability of data in relation to on-site building characteristics, there is a limit to identify this. However, as the urban microclimate was identified as the key determinant in modelling, the urban context in two extreme cases was compared.  As seen in Figure 6-14, a clear difference was found in terms of green coverage ratio (GCR) within the microclimate boundary. This suggests that outdoor mitigation strategies could be developed for the neighbourhoods identified with increasing GCR, leading to a reduction in peak cooling demands.

Table 6-13. Estimated neighbourhood archetypes' August (peak) cooling demands in future years for HSV-A$_E$ and HSV-B$_E$ according to the ±1°C of the current climate change projections (RCP4.5 2047 as an example), and descriptive variation (difference, %) from each neighbourhood's present Max. cooling energy use

| Neighbour-hood (Archetype) | Present Max. cooling (kWh/m²) | -1°C scenario | | | | +1°C scenario | | | |
|---|---|---|---|---|---|---|---|---|---|
| | | HSV-A$_E$ | | HSV-B$_E$ | | HSV-A$_E$ | | HSV-B$_E$ | |
| | | Est. load | Difference (%) | Est. load | Difference (%) | Est. load | Difference (%) | Est. load | Difference (%) |
| CD1(R5/A2) | 2.342 | 2.421 | 3.4 | 2.174 | -7.2 | 3.207 | 36.9 | 2.960 | 26.4 |
| CD2(R3/A2) | 1.993 | 2.449 | 22.9 | 2.193 | 10.0 | 3.235 | 62.3 | 2.979 | 49.4 |
| CD3(R3/A2) | 1.954 | 2.013 | 3.0 | 1.424 | -27.2 | 2.799 | 43.2 | 2.209 | 13.0 |
| CD4(R5/A2) | 1.939 | 2.287 | 18.0 | 1.741 | -10.2 | 3.073 | 58.5 | 2.526 | 30.3 |
| CD6(R4/A2) | 2.025 | 2.458 | 21.4 | 1.808 | -10.7 | 3.244 | 60.2 | 2.593 | 28.1 |
| CD8(R4/A2) | 1.580 | 2.148 | 35.9 | 1.259 | -20.3 | 2.933 | 85.6 | 2.044 | 29.4 |
| CD10(R4/A2) | 2.060 | 2.062 | .1 | 1.780 | -13.6 | 2.847 | 38.2 | 2.565 | 24.5 |
| CD11(R4/A2) | 1.739 | 2.529 | 45.4 | 1.761 | 1.3 | 3.315 | 90.6 | 2.547 | 46.4 |
| CD12(R4/A2) | 2.610 | 2.300 | -11.9 | 2.347 | -10.1 | 3.085 | 18.2 | 3.133 | 20.0 |
| CD13(R5/A2) | 1.843 | 2.363 | 28.2 | 1.925 | 4.4 | 3.149 | 70.8 | 2.711 | 47.1 |
| CD15(R3/A2) | 2.268 | 2.279 | .5 | 1.629 | -28.2 | 3.065 | 35.1 | 2.414 | 6.4 |
| CD16(R4/A2) | 2.511 | 2.452 | -2.4 | 2.009 | -20.0 | 3.237 | 28.9 | 2.795 | 11.3 |
| CD18(R1/A2) | 2.181 | 2.495 | 14.4 | 1.692 | -22.4 | 3.280 | 50.4 | 2.478 | 13.6 |
| CD19(R3/A3) | 2.350 | 2.371 | .9 | 1.408 | -40.1 | 3.156 | 34.3 | 2.193 | -6.7 |
| CD20(R4/A2) | 2.001 | 2.444 | 22.2 | 1.377 | -31.2 | 3.230 | 61.4 | 2.163 | 8.1 |
| CD21(R4/A3) | 2.862 | 2.413 | -15.7 | 2.000 | -30.1 | 3.198 | 11.7 | 2.786 | -2.7 |
| CD22(R5/A2) | 2.902 | 2.030 | -30.1 | 1.947 | -32.9 | 2.815 | -3.0 | 2.733 | -5.8 |
| CD25(R5/A2) | 1.968 | 2.293 | 16.6 | 1.691 | -14.1 | 3.079 | 56.5 | 2.476 | 25.8 |
| Avg. | 2.174 | 2.323 | 9.6 | 1.787 | -16.8 | 3.108 | 46.7 | 2.572 | 20.3 |
| Min. | 1.580 | 2.013 | -30.1 | 1.259 | -40.1 | 2.799 | -3.0 | 2.044 | -6.7 |
| Max. | 2.902 | 2.529 | 45.4 | 2.347 | 10.0 | 3.315 | 90.6 | 3.133 | 49.4 |

What if a certain outdoor mitigation strategy is applied into the Seoul context and therefore, 1$^{\circ}$C reduction of air temperature is achieved in future years? On the other hand, what if the future temperature is 1$^{\circ}$C higher than current climate change projections due to the effect of an urban heat island? Table 6-13 shows the changed peak cooling demands of archetype neighbourhoods according to the two scenarios (±1$^{\circ}$C) under RCP4.5 (2047) as an example. Compare to Table 6-12, the effect of outdoor mitigation strategy is obvious in terms of peak cooling demands in future years.

# Chapter 7. Conclusions

A bottom-up approach to modelling peak cooling demand and assessing potential heat stress vulnerability of a city's housing stock in a future climate was presented. It is proposed that housing archetypes can be developed to represent a city's housing stock in terms of three key descriptors: (1) building epoch (in terms of legislation years of residential building codes governing thermal performance standards), (2) building geometry (typical floor plans and sizes), and (3) urban microclimate boundary defined as an urban area of 1 km radius from an urban automatic weather station.

Historical energy use data metred in aggregates of neighbourhood units are analysed to obtain an estimate of peak cooling energy use for each archetype. In this study, building energy modelling of archetypes always takes into account available local weather station data as the microclimate contexts of the archetypes. This model calibration process gives an estimate of the range of (peak) cooling temperature set points for each archetype in its urban microclimate boundary. The same archetype may appear in multiple locations and exhibit different ranges of peak cooling temperature set points. However, the defined archetypes always lie with the neighbourhood of microclimate boundary. The estimated cooling temperature set points are then taken as simulated measurements of indoor thermal conditions for assessing potential heat stress vulnerability of each dwelling archetype in context.

Presupposing no housing stock replacement or renovation over the timeframe of climate projections, this study makes use of a city's climate change projection data to estimate peak cooling energy demand and heat stress vulnerability in the future climate. This is intended as a scenario of "business as usual" to inform a city's dwelling stock management policies and strategies towards a sustainable future. Predicted heat stress vulnerability attributed to dwelling stock archetypes in context could rise or fall depending on whether peak cooling energy demand may or may not be met in the future climate.

Successful dwelling stock management therefore needs to know where and how peak cooling energy demand can be reduced to lower heat stress vulnerability for city dwellers.

## 7.1. Key findings

### 7.1.1. Characteristics of urban dwelling's cooling energy use

To understand the characteristics of urban dwelling's cooling energy use, the relationship between residential cooling energy use and the two factors, urban microclimate data (i.e., monthly average temperature) and property price data, was explored in the two different spatial resolutions: (1) Macro level, aggregated all apartment neighbourhoods in city of Seoul; (2) Micro level, apartment neighbourhoods individually within city-district (CD) urban microclimate boundary setting.

In Macro level analysis, there were temporal (monthly) variations in correlating cooling energy use with both urban microclimate data and property price data during the summer months (July – September). However, the combined effect of urban microclimate and property price on cooling energy use varied in each summer month: in the mild temperature of July, the impact of property price was more influential on cooling energy use than urban weather while the urban weather was more dominant than property price in the high temperature of August.

In the Micro level analysis, there were unique characteristics of cooling energy use within each of the microclimate boundary neighbourhoods. It was found that there was very good internal consistency and similarity in terms of the distribution of apartment neighbourhoods' monthly cooling energy use within each boundary. This implies that there are certain aspects which affect a similar range of cooling energy use in each CD boundary, such as homogeneous microclimatic conditions and building physical

characteristics or socio-economic factors. Given the characteristics, the relational study between cooling energy use and microclimate data was explored within each CD's AWS 1km boundary. There were not only temporal (monthly) variations in relationship between the two variables, but also spatial (each CD) variations. This suggests that the residential cooling energy use should be individually studied within each CD microclimate boundary to reflect its own characteristics of cooling energy use.

Despite the temporal and spatial variations, it was commonly found that all CDs had the strongest correlation coefficients for August, the hottest summer month. The simple bivariate regression (SBR) model for each CD was generated to estimate future peak cooling energy demands. The estimates showed dramatic differences in each CD neighbourhood in terms of the predicted peak cooling demands responding to external temperature of climate change projections. This implies that there can be substantial differences in individual households' indoor thermal conditions. Therefore, there can be varying levels of indoor heat exposure experienced by the residents, affecting residents' health and well-being if they are unable to increase cooling energy use due to socio-economic constraints.

### 7.1.2. Housing archetype development for building physics

The implication of the study into historical cooling energy use required the urgent action of looking into dwelling's indoor thermal conditions in relation to residents' health and wellbeing in future years. To assess potential heat stress vulnerability of a city's dwelling stock, the knowledge of a possible range of indoor air temperatures under such condition is essential. However, to obtain such knowledge through field survey campaigns for a city's entire dwelling stock would be cost-prohibitive if not impossible. In the absence of reliable city-wide measurements of indoor thermal conditions, the possible approach to

obtaining a replaceable indicator of indoor thermal measurements was found in developing archetypes for building physics.

The results derived from the characteristics of urban dwelling's cooling energy use showed that the spatial resolution of residential neighbourhoods within a microclimate boundary can capture a set of homogeneous datasets in terms of dwellings' cooling energy use and building physical characteristics. Given the findings, housing archetypes were developed within an urban microclimate context as approximate representation of the stock population based on building physical criteria, i.e., thermal characteristics ($R_i$) and geometric configuration ($A_i$). Six archetypes were identified by the combination ($R_i/A_j$ descriptors) across the 18 city districts sampled for the study of Seoul. However, the six housing archetypes defined by building physical characteristics, always lie with the neighbourhood of 18 city-districts' microclimate boundary (as a key factor in segmentation process, $CD_i$): hence, 18 housing archetypes, $CD_i(R_i/A_j)$. As a virtual archetype development, the details of each $CD_i$ archetype are associated with (1) the construction assembly profile (Table 5-2) according to the built year of building epoch (Table 4-9, $R_i$) and (2) the predefined typical apartment floor plans (Figure 5-4) in relation to floor area size ($A_i$).

Furthermore, as the EnergyPlus model calibration process for estimating archetypes' present indoor thermal conditions required a detailed energy use profile, such as energy use only for cooling and detailed household non-weather-dependent (NWD) equipment energy use profile. However, the energy use data was limited into monthly (August) total energy (electricity) use data. Thus, this study intensively analysed the datasets to extract the exact details. Firstly, two types of electricity use were deduced from the collected monthly (August) data through the assumption that the NWD energy use is the minimum monthly electricity use during the study period, and peak (August) cooling energy use can be estimated as the net of August electricity use minus the NWD use identified. The

assumption was testified by the relational analysis between cooling/heating degree days (CDDs/HDDs) and monthly electricity use. Secondly, the detailed household NWD equipment energy use profile was estimated through referring to and adjusting the UK household electricity use profile, taking into account local socio-cultural circumstances. Thirdly, 72 (18 archetype neighbourhoods * 4 years) on-site EnergyPlus typical meteorological year (TMY) weather files were generated based on the collected city and city-districts weather data. Fourthly, archetypes' household operation parameters in zoning inputs were established though the analysis of the historical hourly households' electricity use profile, including detailed occupancy scheduling profiles of household equipment and the placement.

Finally, given the developed archetypes and the dataset analysed, modelling of archetypes' peak cooling energy was carried out to estimate the peak HVAC cooling temperature set points as an indicator of the archetypes' present (2014-17) indoor thermal conditions. The estimates showed that there were spatial (each city district's neighbourhood) and temporal (each year) variations. This was owing to differentiated responses (dwellers' cooling energy use behaviours) to the external climates (August average temperature) observed in the metred peak cooling energy uses. However, there appeared a trend that most of the highest set points occurred in 2016, the year of the largest cooling degree day (CDD) count, while the lowest set points occurred in 2014 with the lowest CDD count. This implies that there may be a certain process of indoor heat acclimatisation, which contains dwellers' adaptive opportunities associated with each archetype in the neighbourhood context.

Moreover, the estimated household's indoor thermal condition itself does not represent any details of the occupants' thermal comfort or discomfort as it only represents HVAC cooling set point temperature deduced from the history of each neighbourhood's peak cooling energy use which has been already paid by dwellers. The key part where we pay

attention to is the history which is determined by neighbourhood-specific cooling energy use behaviour responding to the external climate under the occupants' own circumstances. Therefore, the cooling temperature set point can be considered as an indicator of the maximized level of indoor heat acclimatisation (IHA).

### 7.1.3. Potential heat stress vulnerability of Seoul's dwelling stock

The indoor thermal conditions of Seoul's dwelling stock during summer months are one of the key determinants of peak cooling demand. The city's population will be subject to heat stress if the cooling demand cannot be met for reasons such as extended power outage or fuel poverty. To inform sustainable dwelling stock management, a modelling framework for estimating peak cooling demand is presented. The aim of the modelling is to obtain heat stress vulnerability (HSV) assessment of a city's dwelling stock over the timeframe of climate projections. The modelling framework is underpinned by the spatial-temporal scale of an urban microclimate boundary defined as an urban area within 1 km radius of an automatic weather station.

The modelling framework was applied to Seoul's dwelling stock drawing on the datasets available for 2014-17 as the basis for assessing the likely peak cooling demands and heat stress vulnerability in 2050s, assuming there is no stock adaptation. The assessment of the potential heat stress vulnerability of Seoul's dwelling stock in future climate is concluded as relative ranking among the neighbourhoods of six apartment archetypes in 18 city-district neighbourhoods, $CD_k(R_i/A_j)$. HSV-A is based on a fixed threshold temperature (26°C as the local statutory standard adopted in Seoul), and HSV-B is based on the historical metred energy uses reflecting households' indoor heat acclimatisation histories. Furthermore, under HSV-A and HSV-B, this study employed

two sub-methods: Cooling *Temperature* Set Points based (HSV-A$_T$, HSV-B$_T$), and Cooling *Energy* Demand based (HSV-A$_E$, HSV-B$_E$).

Taking Seoul's dwelling stock as a whole, under HSV-A$_T$, the average difference from 26°C was .81°C under RCP4.5 (2047 being the hottest year in 2050s under RCP4.5) and .88°C under RCP8.5 (2045 the hottest year in 2050s under RCP8.5), ranging from -4.68°C to 2.06°C (2047 RCP4.5), and -5.68°C to 2.48°C (2045 RCP8.5). Under HSV-B$_T$, the average difference from the present (2014-17) Max indoor temperatures (as estimated from EnergyPlus model calibration with the households' metered energy uses) was much reduced to -.42°C (RCP4.5 2047) and -.36°C (RCP8.5 2045), ranging from -4.87°C to .74°C (2047 RCP4.5), and -5.87°C to 1.22°C (RCP8.5 2045).

Looking at the neighbourhoods of housing stock individually, 14 out of 18 (77.8%) the stocks are predicted to have higher peak indoor temperatures than 26°C in future climate under HSV-A$_T$. Considering the residents' indoor heat acclimatisation histories under HSV-B$_T$, 33.3% (6/18) and 44.4% (8/18) are predicted to have higher peak indoor temperatures in 2047 RCP4.5 and 2045 RCP8.5 respectively, in comparison with the present Max indoor temperature estimated for each archetype in the neighbourhood. It should be noted that both HSV-A$_T$ and HSV-B$_T$ difference measures assume no stock adaptation and the estimated peak cooling demands will be met in the 2050s.

Also, meeting either the fixed statutory or the indoor heat acclimatisation threshold cooling temperature does not imply heat stress free absolutely. In public health research, various heat morbidity and mortality functions have been proposed recently which take measured or estimated apparent temperatures as one of the primary inputs (see among others, Kim and Joh, 2006; Kendrovski et. al., 2017; Lee et. al., 2018).

This study proposes a relative ranking of heat stress vulnerability of a city's dwelling stock based on estimated peak cooling demands in the future climate. In the HSV-A$_E$

and HSV-B$_E$ assessment of Seoul's dwelling stock, the estimated peak cooling loads required for each archetype in a neighbourhood to restore future indoor peak temperatures to the statutory 26$^o$C (HSV-A$_E$) or to the present Max cooling temperature set points calibrated for the existing stock (HSV-B$_E$) are used to establish the relative ranking (Table 6-12 and Figure 6-13). This is a more pessimistic approach to HSV assessments as it shows how each dwelling stock stands in relation to each other if the estimated peak cooling loads cannot be met in the forthcoming years. In HSV-A$_E$, the proportional difference measures show that 88.89% (16/18) and 94.44% (17/18) of the housing stock neighbourhoods will be greater than zero in RCP4.5 2047 and RCP8.5 2045. In HSV-B$_E$, the ratios reduce to 55.6% (10/18) and 83.3% (15/18) respectively. As expected, the heat acclimatisation model predicts a lower HSV level across the housing stock neighbourhoods.

Between the HSV-A$_E$ and HSV-B$_E$ paired relative rankings, some neighbourhoods cross the zero transition point from high to low: 33.3% (6/18) under RCP4.5 2047, and 11.1% (2/18) under RCP8.5 2045. There are three neighbourhoods, CD2(R3/A2), CD11(R4/A2), and CD13(R5/A2), are ranked at the top three positions persistently, which are the most vulnerable neighbourhoods if their estimated peak cooling demand cannot be met in the 2050s. Further research should focus on what and how adaptation and mitigation strategies and measures could be developed and implemented for the neighbourhoods identified, leading to significant reduction of peak cooling demands while being satisfactory to dwellers' thermal well-being as a priority.

## 7.2. Limitations and further studies

Firstly, due to the small sample size in modelling archetype-specific peak cooling energy use at micro level (section 6.2.3), the model accuracy remains uncertain, except 9 (out

of 18) archetype neighbourhoods. As the AMIS started provided an actual amount of electricity use data in 2014, the study was limited to the energy use dataset of 2014-17 (N=4). This small sample only allowed one to use a linear fit model and thus, some CDs showed a relatively weak overall relationship in bivariate linear model: i.e. CD6, 8, 11, 13 (Figure 6-6). Tracking the form of the scattered between cooling energy use and the external climates, another non-linear model may achieve a better fit in those CDs. As this study employed a parametric statistical approach to the model fit, the outcome can be sensitive to the sample size. Moreover, within the 4-year datasets, August of two years (2014 and 2016) are considered as extreme cases historically: August 2016 was reported as the warmest summer month on record since 1908, while August 2014 was one of the mildest summer months in Seoul (see also Figure 5-1). Under these small samples, such extreme cases may result in weak model reliability. However, the energy use data can be continuously collected into further years, the sample size will be large enough to implement other modelling types or fits. Therefore, the assessment of HSV in terms of dwelling's indoor thermal conditions could perform better through model improvement with an increased sample size.

Secondly, in developing archetypes, the accurate homogeneity of building typological characteristics must be further investigated even at a neighbourhood of microclimate boundary. As this study has paid much attention to residential cooling energy use characteristics in developing housing archetypes for the purpose of assessing HSV, debates in terms of all the assumptions related to building geometric configurations and thermal characteristics in archetype definitions are inevitable. For instance, there could be differentiated material assembly profiles in other ANs (from Table 5-2) and also, building regulations (Table 4-9) may be limited to entirely represent an accurate proxy for u-values to all housing stock on a city scale. Moreover, there can be a number of existing floor plans which cannot be simply unformed into a single plan (Figure 5-4).

However, the question is how sensitive are those parameters to residential peak cooling energy use? In further studies, the sensitivity analysis must be carried out in relation to data normalisation for developing archetypes.

Furthermore, in relation to the consideration of building typological characteristics in archetype developments, this study also proposes that the segmentation scale in archetype development can be further narrowed down to individual apartment neighbourhood or the building level if microclimate data is available at that spatial resolution. As pointed out in Chapter 4, the actual scale of microclimate is much smaller than 1 km and the effect of microclimate on residential cooling energy use can be much more dynamic at an individual apartment building. Solar radiation can be a good example. It is well informed that the effect of solar radiation on residential energy use varied under urban canyon geometry (Salvati et al., 2017). Although the inclusion of solar radiation can be challenging in the stock modelling (because it has to meet the temporal and spatial data homogeneity within limited data availability), the segmentation scale for developing an archetype can be classified by canyon geometry, such as the orientation of the building. However, this also remains as a further study due to the limitation of the current open residential energy use data at apartment neighbourhood level. If the data availability is extended to an individual apartment building, such detailed segmentation would be considered in developing housing archetypes.

Thirdly, this study concludes that a further study must focus on what, where and how adaptation and mitigation strategies could be developed for the neighbourhoods identified, leading to significant reduction of peak cooling demands while remaining satisfactory to dwellers' thermal well-being as a priority. Thus, it is important to identify what the main source of the increased HSV is caused by. As the microclimate was the key determinant in modelling for both indoor thermal condition and peak cooling demand of the Seoul's dwelling stock during summer months, a mitigation strategy of urban

microclimate can be considered as the possible approach to reduction of cooling loads in future years (i.e. Table 6-13).

Over the past decades, many studies have been carried out for assessing the effect of outdoor mitigation strategy in different cities and they were summarised by Salata et al. (2017). The key part can be that the effect of microclimatic variables must be considered in relation to the individual household's building geometry configuration such as orientation and glazing ratio. This represents that microclimate mitigation strategies must be effectively linked to building adaptation design.

In obtaining such microclimate data requirements at high spatial and temporal resolutions, CFD (computational fluid dynamics) based urban microclimate simulation may be essential. For instance, Ng et al. (2012) investigated the cooling effect of greening in Hong Kong context, using Envi-met, a computation intensive microclimate assessment software (developed by Bruce and Envi-met team at the University of Mainz). As a base reference model to be compared to the cooling effect of greening, they used 700 x 700 x 300 (x, y, z) model domain size of a high-density urban area, where building coverage ratio is 44% with 0% of green coverage ratio (GCR). They found that within the model domain about 33% of GRC of tree planting (20m dense crown trees) at ground level attributed to a 1°C reduction of air temperature at pedestrian level.

With further extension to building level, Yi and Peng (2014) developed outdoor and indoor coupled simulation framework for passive building adaptation design at the neighbourhood level. The key idea was to identify the main source of an indoor overheating problem through the coupling simulation framework and then, to deploy effective passive design strategy at the building to be adaptive to climate change.

In detail, one key body of knowledge in the building simulation area for assessing climate change which impacts on an existing building is how to obtain an on-site climate change

input which is specified for a target building for the future. As the scale of current climate change projections cannot be representative to a neighbourhood or building level, they introduced and application of the Envi-met microclimate simulation into generating on-site present and future (climate change) weather inputs for a building simulation. The outcome of Envi-met simulation can be considered the result of thermal interactions between air, surface of urban morphology and plants within the model domain size on the neighbourhood scale. Given the generated on-site weather inputs, they identified the main source of an indoor overheating problem in both the present and the future, (i.e. solar gain from a South facing fully-glazed wall), and suggested one passive design strategy which can cover the time frame of climate change projects. This framework can potentially be applicable into developing both building adaptation and outdoor mitigation strategies for the neighbourhoods identified.

Finally, one key area to be given further attention is how the proposed methodological framework can be refined and extended into different city contexts, e.g. the UK. In the UK, a city's housing stock is under the influence of different urban microclimatic variables on a dwelling's indoor thermal conditions due to the low-rise geometric configuration and build density. In the UK context, solar radiation was identified as a key determinant of indoor thermal environment along with air-temperature. The effects of solar radiation on the indoor thermal condition largely depends on geometric configurations (i.e. orientation, glazing-ratio) under the surrounding urban canyon geometry (i.e. low-density and low-rise). Therefore, the hypothesis can be (1) that the spatial segmentation in an archetype development can be further scaled down than the Seoul study, or (2) that several segmentations can be identified within a 1 km radius boundary. To test the hypothesis, Birmingham can be selected for further research, where 20 urban weather stations were installed and maintained across the city during 2016-17.

Moreover, the heat stress vulnerability (HSV) assessment should consider the impact of potential heat events (i.e. heatwaves) on a dwelling's indoor thermal condition owing to the dominant free-running-housing stock characteristics in the UK. This represents the temporal resolution of the UK stock modelling must be daily-based at least. To achieve it, the knowledge of a possible range of present indoor thermal conditions responding to external climates is essential. However, to obtain such knowledge of city-wide measurements through field survey would be cost-prohibitive if possible at all. Thus, empirical data modelling combined with contextual building energy simulation is required to estimate present indoor thermal condition. This is achievable as demonstrated in this thesis through the iterative EnergyPlus model calibration process. Furthermore, the HSV assessment needs to consider other factors already identified as potential determinants of heat risk on public health taking into account the compounded effects such as an inhabitant's details such as age, morbidity and domestic energy affordability. The purpose of subjecting a city's dwelling stock to the proposed HSV assessment is to establish the overall stock of neighbourhoods of higher HSV that may require urgent actions of adaptation through renovation or mitigation over the timeframe of UKCP18.

# References

# References

Aigner, D.J., Sorooshian, C. and Kerwin, P., 1984. Conditional demand analysis for estimating residential end-use load profiles. The Energy Journal, 5(3), pp.81-97.

Allegrini, J., Dorer, V. and Carmeliet, J., 2012. Influence of the urban microclimate in street canyons on the energy demand for space cooling and heating of buildings. Energy and Buildings, 55, pp.823-832.

AMIS, Apartment Management Information System, 2018a. Registered apartment stock information, Available at http://www.k-apt.go.kr/cmmn/kaptworkintro.do (accessed on 05.07.2018)

AMIS, Apartment Management Information System, 2018b. Registered apartment stock details, Available at http://www.k-apt.go.kr/kaptinfo/openkaptinfo.do (accessed on 05.07.2018)

AMIS, Apartment Management Information System, http://www.k-apt.go.kr/ (accessed on 09.08.2017)

Aniello, C., Morgan, K., Busbey, A. and Newland, L., 1995. Mapping micro-urban heat islands using Landsat TM and a GIS. Computers & Geosciences, 21(8), pp.965-969.

Aniello, C.A., 1993. Using Landsat-TM thermal data to map micro-urban heat islands in Dallas, Texas. Submitted to the Graduate Faculty of AddRan College of Arts and Sciences, Texas Christian University in partial fulfillment of the requirements for the degree of Master of Science. pp.52.

Arnfield, A.J., 2003. Two decades of urban climate research: a review of turbulence, exchanges of energy and water, and the urban heat island. International journal of climatology, 23(1), pp.1-26.

ASHRAE, 2004. Standard 90.1-2004, Energy standard for buildings except low rise residential buildings. American Society of Heating, Refrigerating and Air-Conditioning Engineers, Inc.

Asimakopoulos D.N., Assimakopoulos, V.D., Chrisomallidou, N., Klitsikas, N., Mangold, D., Michel, P., Santamouris, M. and Tsangrassoulis, A., 2001. Energy and climate in the urban built environment. M. Santamouris, University of Athens, Greece. ISBN, 1873936907.

Aydinalp, M., Ugursal, V.I. and Fung, A.S., 2002. Modeling of the appliance, lighting, and space-cooling energy consumptions in the residential sector using neural networks. Applied energy, 71(2), pp.87-110.

Aydinalp, M., Ugursal, V.I. and Fung, A.S., 2002. Modeling of the appliance, lighting, and space-cooling energy consumptions in the residential sector using neural networks. Applied energy, 71(2), pp.87-110.

Bae, C. and Chun, C., 2009. Research on seasonal indoor thermal environment and residents' control behavior of cooling and heating systems in Korea. Building and Environment, 44(11), pp.2300-2307.

Baker, N. and Standeven, M., 1995. A behavioural approach to thermal comfort assessment in naturally ventilated buildings. In Proceedings CIBSE National Conference, Eastbourne UK (pp. 76-84).

Ballarini, I., Corgnati, S.P. and Corrado, V., 2014. Use of reference buildings to assess the energy saving potentials of the residential building stock: The experience of TABULA project. Energy policy, 68, pp.273-284.

Ballarini, I., Corgnati, S.P., Corrado, V. and Talà, N., 2011. Definition of building typologies for energy investigations on residential sector by TABULA IEE-project: application to Italian case studies. Roomvent, Trondheim, pp.19-22.

Beizaee, A., Lomas, K.J. and Firth, S.K., 2013. National survey of summertime temperatures and overheating risk in English homes. Building and Environment, 65, pp.1-17.

Belcher, S.E., Hacker, J.N. and Powell, D.S., 2005. Constructing design weather data for future climates. Building services engineering research and technology, 26(1), pp.49-61.

Bentzen, J. and Engsted, T., 2001. A revival of the autoregressive distributed lag model in estimating energy demand relationships. Energy, 26(1), pp.45-55.

Boo, K.O., Kwon, W.T. and Baek, H.J., 2006. Change of extreme events of temperature and precipitation over Korea using regional projection of future climate change. Geophysical Research Letters, 33(1). pp. 1-4

Bouyer, J., Inard, C. and Musy, M., 2011. Microclimatic coupling as a solution to improve building energy simulation in an urban context. Energy and Buildings, 43(7), pp.1549-1559.

Braun, M.R., Altan, H. and Beck, S.B.M., 2014. Using regression analysis to predict the future energy consumption of a supermarket in the UK. Applied Energy, 130, pp.305-313.

Bronson, D.J., Hinchey, S.B., Haberl, J.S. and O'Neal, D.L., 1992. Procedure for calibrating the DOE-2 simulation program to non-weather-dependent measured loads. In ASHRAE Winter Meeting, Anaheim, CA, USA, 01/25-29/92 (pp. 636-652)

Brooks, N. and Adger, W.N., 2005. Assessing and enhancing adaptive capacity. Adaptation policy frameworks for climate change: Developing strategies, policies and measures, pp.165-181.

BSI, 2007. BS EN 15251: 2007. Indoor environmental input parameters for design and assessment of energy performance of buildings addressing indoor air quality, thermal environment, lighting and acoustics. (London: British Standards Institution)

Buffat, R., Froemelt, A., Heeren, N., Raubal, M. and Hellweg, S., 2017. Big data GIS analysis for novel approaches in building stock modelling. Applied Energy, 208, pp.277-290.

Catalina, T., Iordache, V. and Caracaleanu, B., 2013. Multiple regression model for fast prediction of the heating energy demand. Energy and Buildings, 57, pp.302-312.

Chan, A.L.S., 2011. Developing a modified typical meteorological year weather file for Hong Kong taking into account the urban heat island effect. Building and Environment, 46(12), pp.2434-2441.

Chan, A.L.S., 2011. Developing future hourly weather files for studying the impact of climate change on building energy performance in Hong Kong. Energy and Buildings, 43(10), pp.2860-2868.

Chappells, H. and Shove, E., 2005. Debating the future of comfort: environmental sustainability, energy consumption and the indoor environment. Building Research & Information, 33(1), pp.32-40.

Chen, J., Wang, X. and Steemers, K., 2013. A statistical analysis of a residential energy consumption survey study in Hangzhou, China. Energy and Buildings, 66, pp.193-202.

Cheng, C.S., Campbell, M., Li, Q., Li, G., Auld, H., Day, N., Pengelly, D., Gingrich, S., Klaassen, J., MacIver, D. and Comer, N., 2008. Differential and combined impacts of extreme temperatures and air pollution on human mortality in south–central Canada. Part II: future estimates. Air Quality, Atmosphere & Health, 1(4), pp.223-235.

Choi, I.Y., Cho, S.H. and Kim, J.T., 2012. Energy consumption characteristics of high-rise apartment buildings according to building shape and mixed-use development. Energy and Buildings, 46, pp.123-131.

Choi, J., Cho, H., Park, I. and Park, Y., 2004. A spatial analysis of the apartment unit plans from 1966 to 2002 in Seoul. Journal of the Architectural Institute of Korea, 20(6), pp.155-164.

Choi, J.P., Shin, J.S. and Choi, Y.J., 2013. Changes in the Planning Principles of Korean High-Rise Residential Buildings-Comparative Analysis with High-Rise Residential Buildings of America. *Journal of the architectural institute of Korea planning & design*, *29*(2), pp.123-130.

CIBSE, Guide A, 2015. Environmental design. The Chartered Institution of Building Services Engineers, London. pp. 6-2.

CIP, Climate Information Portal, 2017, http://www.climate.go.kr/index.html (accessed on 09.08.2017)

CIP, Climate Information Portal, http://www.climate.go.kr/home/ (accessed on 05.07.2018)

Collins, L., Natarajan, S. and Levermore, G., 2010. Climate change and future energy consumption in UK housing stock. Building Services Engineering Research and Technology, 31(1), pp.75-90.

Crawley, D.B., 2008. Estimating the impacts of climate change and urbanization on building performance. Journal of Building Performance Simulation, 1(2), pp.91-115.

Dascalaki, E.G., Droutsa, K.G., Balaras, C.A. and Kontoyiannidis, S., 2011. Building typologies as a tool for assessing the energy performance of residential buildings–A case study for the Hellenic building stock. Energy and Buildings, 43(12), pp.3400-3409.

De Dear, R. and Brager, G.S., 1998. Developing an adaptive model of thermal comfort and preference. ASHRAE Transactions, 104(1a), pp145-67.

De Dear, R., 2006. Adapting buildings to a changing climate: but what about the occupants?. Building Research Information, 34(1), pp. 78-81.

De La Flor, F.S. and Domınguez, S.A., 2004. Modelling microclimate in urban environments and assessing its influence on the performance of surrounding buildings. Energy and buildings, 36(5), pp.403-413.

De Wilde, P. and Coley, D., 2012. The implications of a changing climate for buildings. Building and Environment, 55 (2012), pp. 1-7.

Du, H., Underwood, C.P. and Edge, J.S., 2012. Generating design reference years from the UKCP09 projections and their application to future air-conditioning loads. Building Services Engineering Research and Technology, 33(1), pp.63-79.

Eames, M., Kershaw, T. and Coley, D., 2012. The appropriate spatial resolution of future weather files for building simulation. Journal of Building Performance Simulation, 5(6), pp.347-358.

Emery, A.F. and Kippenhan, C.J., 2006. A long term study of residential home heating consumption and the effect of occupant behavior on homes in the Pacific Northwest constructed according to improved thermal standards. Energy, 31(5), pp.677-693.

EnergPlus, 2018. Available at https://energyplus.net/ (accessed on 11.02.2019)

Famuyibo, A.A., Duffy, A. and Strachan, P., 2012. Developing archetypes for domestic dwellings—An Irish case study. Energy and Buildings, 50, pp.150-157.

Fanger, P.O., 1970. Thermal comfort. Analysis and applications in environmental engineering. Thermal comfort. Analysis and applications in environmental engineering.

Filogamo, L., Peri, G., Rizzo, G. and Giaccone, A., 2014. On the classification of large residential buildings stocks by sample typologies for energy planning purposes. Applied Energy, 135, pp.825-835.

Flynn, A., McGreevy, C. and Mulkerrin, E.C., 2005. Why do older patients die in a heatwave? Qjm, 98(3), pp.227-229.

Fouillet, A., Rey, G., Laurent, F., Pavillon, G., Bellec, S., Guihenneuc-Jouyaux, C., Clavel, J., Jougla, E. and Hémon, D., 2006. Excess mortality related to the August 2003 heat wave in France. International archives of occupational and environmental health, 80(1), pp.16-24.

Frank, T., 2005. Climate change impacts on building heating and cooling energy demand in Switzerland. Energy and buildings, 37(11), pp.1175-1185.

Frumkin, H., 2002. Urban sprawl and public health. Public Health Reports. (117), pp. 201-217.

Gaterell, M.R. and McEvoy, M.E., 2005. The impact of climate change uncertainties on the performance of energy efficiency measures applied to dwellings. Energy and buildings, 37(9), pp.982-995.

Gedzelman, S.D., Austin, S., Cermak, R., Stefano, N., Partridge, S., Quesenberry, S. and Robinson, D.A., 2003. Mesoscale aspects of the urban heat island around New York City. Theoretical and Applied Climatology, 75(1-2), pp.29-42.

Grell, G.A., Dudhia, J. and Stauffer, D.R., 1994. A description of the fifth-generation Penn State/NCAR Mesoscale Model (MM5). NCAR Tech. Note NCAR/TN-398+STR, pp.1-138

Grundy, E., 2006. Ageing and vulnerable elderly people: European perspectives. Ageing & Society, 26(1), pp.105-134.

Guan, L., 2009. Preparation of future weather data to study the impact of climate change on buildings. Building and environment, 44(4), pp.793-800.

Ha, S.K., 2010. Housing, social capital and community development in Seoul. Cities, 27, pp.S35-S42.

Hacker, J.N., Holmes, M.J., Belcher, S.E. and Davies, G., 2005. Climate change and the indoor environment: impacts and adaptation. Chartered Institution of Building Services Engineers: London.

Hajat, S., Kovats, R.S. and Lachowycz, K., 2007. Heat-related and cold-related deaths in England and Wales: who is at risk?. Occupational and environmental medicine, 64(2), pp.93-100.

Hajat, S., Kovats, R.S., Atkinson, R.W. and Haines, A., 2002. Impact of hot temperatures on death in London: a time series approach. Journal of Epidemiology & Community Health, 56(5), pp.367-372.

Hajat, S., Vardoulakis, S., Heaviside, C. and Eggen, B., 2014. Climate change effects on human health: projections of temperature-related mortality for the UK during the 2020s, 2050s and 2080s. J Epidemiol Community Health, 68(7), pp.641-648.

Hames, D. and Vardoulakis, S., 2012. CCRA Risk Assessment for the Health Sector. UK 2012 Climate Change Risk Assessment, Defra, London.

Harish, V.S.K.V. and Kumar, A., 2016. A review on modeling and simulation of building energy systems. Renewable and Sustainable Energy Reviews, 56, pp.1272-1292.

Harrison, R.M., Thornton, C.A., Lawrence, R.G., Mark, D., Kinnersley, R.P. and Ayres, J.G., 2002. Personal exposure monitoring of particulate matter, nitrogen dioxide, and carbon monoxide, including susceptible groups. Occup Environ Med, 59, pp.671-679.

He, J., Hoyano, A. and Asawa, T., 2009. A numerical simulation tool for predicting the impact of outdoor thermal environment on building energy performance. Applied Energy, 86(9), pp.1596-1605.

Hirst, E., Goeltz, R. and White, D., 1986. Determination of household energy using 'fingerprints' from energy billing data. International journal of energy research, 10(4), pp.393-405.

Hirst, E., Lin, W. and Cope, J., 1977. Residential energy use model sensitive to demographic, economic, and technological factors. Quarterly review of economics & business, 17(2), pp.7-22.

Hosni, M.H., Jones, B.W. and Xu, H., 1999. Experimental results for heat gain and radiant/convective split from equipment in buildings. ASHRAE Transactions, 105(2), pp.527-539.

Huang, C., Barnett, A.G., Wang, X., Vaneckova, P., FitzGerald, G. and Tong, S., 2011. Projecting future heat-related mortality under climate change scenarios: a systematic review. Environmental health perspectives, 119(12), p.1681-1690

Huang, Y.J. and Brodrick, J., 2000. A bottom-up engineering estimate of the aggregate heating and cooling loads of the entire US building stock. Lawrence Berkeley National Laboratory, Report LBNL-46303.

Humphreys, M. and Nicol, J.F., 1998. Understanding the adaptive approach to thermal comfort. ASHRAE transactions, 104, pp.991-1004.

Humphreys, M.A. and Hancock, M., 2007. Do people like to feel 'neutral'?: Exploring the variation of the desired thermal sensation on the ASHRAE scale. Energy and Buildings, 39(7), pp.867-874.

Humphreys, M.A. and Nicol, J.F., 2002. The validity of ISO-PMV for predicting comfort votes in every-day thermal environments. Energy and buildings, 34(6), pp.667-684.

Humphreys, M.A., Rijal, H.B. and Nicol, J.F., 2013. Updating the adaptive relation between climate and comfort indoors: new insights and an extended database. Building and Environment, 63, pp.40-55.

IES, Integrated Environmental Solutions Virtual Environment (Ver. 2017.0.2.0). http://www.iesve.com/ (accessed on 05.07.2018)

IPCC, 2013: summary for policymakers. In: Climate Change 2013: The Physical Science Basis. Contribution of Working Group I to the Fifth Assessment Report of the Intergovernmental Panel on Climate Change [Stocker, T.F., D. Qin, D, G.-K. Plattner, M. Tignor, S.K. Allen, A. Boschung, A. Nauels, Y. Xia, V. Bex, and P.M. Midgley (eds.)]. Cambridge University Press, Cambridge, United Kingdom and New York, NY, USA.

Jayamurugan, R., Kumaravel, B., Palanivelraja, S. and Chockalingam, M.P., 2013. Influence of temperature, relative humidity and seasonal variability on ambient air quality in a coastal urban area. International Journal of Atmospheric Sciences, 2013.

Jenkins, D.P., Patidar, S., Banfill, P.F.G. and Gibson, G.J., 2011. Probabilistic climate projections with dynamic building simulation: predicting overheating in dwellings. Energy and Buildings, 43(7), pp.1723-1731.

Jentsch, M.F., Bahaj, A.S. and James, P.A., 2008. Climate change future proofing of buildings—Generation and assessment of building simulation weather files. Energy and Buildings, 40(12), pp.2148-2168.

Jentsch, M.F., James, P.A., Bourikas, L. and Bahaj, A.S., 2013. Transforming existing weather data for worldwide locations to enable energy and building performance simulation under future climates. Renewable Energy, 55, pp.514-524.

Johnson, H., Kovats, R.S., McGregor, G., Stedman, J., Gibbs, M. and Walton, H., 2005. The impact of the 2003 heat wave on daily mortality in England and Wales and the use of rapid weekly mortality estimates. Euro surveillance: bulletin Europeen sur les maladies transmissibles= European communicable disease bulletin, 10(7), pp.168-171.

Jokl, M. and Kabele, K., 2007. The substitution of comfort PMV values by a new experimental operative temperature. Electronic proceedings of Clima.

Jones, G.S., Stott, P.A. and Christidis, N., 2008. Human contribution to rapidly increasing frequency of very warm Northern Hemisphere summers. J. Geophys Res., 113, D02109, doi:10.1029/2007JD008914.

Jones, L.K. and Harp, S.L., 1982. Residential energy analysis using modified degree day procedures. Transactions of the ASAE, 25(5), pp.1387-1390.

KAB, Korea Appraisal Board, 2015a, Information Service of Publicly Noticed Value of Real Estate Price. http://www.realtyprice.kr/notice/town/searchPastYear.htm (accessed on 09.08.2017)

KAB, Korea Appraisal Board, 2015b. Information Service of Publicly Noticed Value of Apartment Property Price. Available at https://www.realtyprice.kr:447/notice/town/searchPastYear.htm (accessed on 09.08.2017)

KAB, Korea Appraisal Board, 2017, http://www.kab.co.kr/kab/home/main/main.jsp (accessed on 09.08.2017)

Kavgic, M., Mavrogianni, A., Mumovic, D., Summerfield, A., Stevanovic, Z. and Djurovic-Petrovic, M., 2010. A review of bottom-up building stock models for energy consumption in the residential sector. Building and environment, 45(7), pp.1683-1697.

Kavgic, M., Mumovic, D., Summerfield, A., Stevanovic, Z. and Ecim-Djuric, O., 2013. Uncertainty and modeling energy consumption: Sensitivity analysis for a city-scale domestic energy model. Energy and Buildings, 60, pp.1-11.

Kendrovski, V., Baccini, M., Martinez, G.S., Wolf, T., Paunovic, E. and Menne, B., 2017. Quantifying projected heat mortality impacts under 21st-century warming conditions for selected European countries. International journal of environmental research and public health, 14(7), p.729-744.

KEPCO, Korea Electric Power Corporation, 2016, http://home.kepco.co.kr/kepco/main.do (accessed on 09.08.2017)

Kershaw, T., Eames, M. and Coley, D., 2011. Assessing the risk of climate change for buildings: A comparison between multi-year and probabilistic reference year simulations. Building and Environment, 46(6), pp.1303-1308.

Kim, D.W., Chung, K.S., Kim, Y.I. and Kim, S.M., 2013b. A comparative study on heating energy consumption for apartment based on the annually strengthened criteria of insulation. Journal of Energy Engineering, 22(2), pp.83-89. [In Korean]

Kim, H.M. and Han, S.S., 2012. Seoul. Cities, 29(2), pp.142-154.

Kim, K. and Park, J., 2005. Segmentation of the housing market and its determinants: Seoul and its neighbouring new towns in Korea. Australian Geographer, 36(2), pp.221-232.

Kim, M.K., Han, M.S., Jang, D.H., Baek, S.G., Lee, W.S., Kim, Y.H. and Kim, S., 2012. Production technique of observation grid data of 1 km resolution. Journal of climate research, 7(1), pp.55-68. [In Korean]

Kim, M.K., Lee, D.H. and Kim, J., 2013a. Production and validation of daily grid data with 1 km resolution in South Korea. Journal of Climate Research, 8(1), pp.13-25. [In Korean]

Kim, S.B., Park, J.H. and Yang, B.E., 2010. A study on glazing ratio of certified green building apartment. KIEAE Journal, 10. [In Korean]

Kim, S.H., 2013. Changes in urban planning policies and urban morphologies in Seoul, 1960s to 2000s. Architectural research, 15(3), pp.133-141.

Kim, S.H., 2015. Housing Site Development and a Shift in Urban Architecture at Mok-dong in Seoul. 서울학연구, (59), pp.125-162.

Kim, S.H., Kim, M.S., Lee, M.S., Park, Y.S., Lee, H.J., Kang, S.A., Lee, H.S., Lee, K.E., Yang, H.J., Kim, M.J. and Lee, Y.E., 2016. Korean diet: characteristics and historical background. Journal of Ethnic Foods, 3(1), pp.26-31.

Kim, S.H., Lee, J.G., Kim, Y.T. and Lee, K.H., 2015. Energy Load according to the Units of Apartment House. Journal of the Korea Society for Power System Engineering, 19(2), pp.78-83.

Kim, Y. and Joh, S., 2006. A vulnerability study of the low-income elderly in the context of high temperature and mortality in Seoul, Korea. Science of the total environment, 371(1-3), pp.82-88.

Klinenberg, E., 2002. Heat wave: A social autopsy of disaster in Chicago. University of Chicago Press.

KMA, Korea Meteorological Administration, 2014, Statistical analysis of climate, http://www.kma.go.kr/weather/climate/stats.jsp (accessed on 09.08.2017)

KMA, Korea Meteorological Administration, 2018, Characteristics of Seoul's climate, Available at http://www.weather.go.kr/weather/climate/average_regional.jsp (accessed on 11.02.2019)

KMA, Korea Meteorological Administration. 2016. Statistical analysis of climate, Available at http://www.weather.go.kr/weather/climate/stats.jsp (accessed on 05.07.2018)

KMA, Korea Meteorological Administration. Automatic Weather Stations (AWS). Available at http://www.weather.go.kr/weather/observation/aws_table_popup.jsp (accessed on 05.07.2018)

Knight, S., Smith, C. and Roberts, M., 2010. Mapping Manchester's urban heat island. Weather, 65(7), pp.188-193.

Kolokotroni, M., Giannitsaris, I. and Watkins, R., 2006. The effect of the London urban heat island on building summer cooling demand and night ventilation strategies. Solar Energy, 80(4), pp.383-392.

Kolokotroni, M., Ren, X., Davies, M. and Mavrogianni, A., 2012. London's urban heat island: Impact on current and future energy consumption in office buildings. Energy and buildings, 47, pp.302-311.

KOSIS, Korean Statistical Information Service, 2013, Available at http://kosis.kr/statisticsList/statisticsList_01List.jsp?vwcd=MT_ZTITLE&parentId=H#SubCont (accessed on 09.08.2017

KOSIS, Korean Statistical Information Service, 2016, Relative coefficient of hourly residential electricity profile. Available at http://kosis.kr/statHtml/statHtml.do?orgId=310&tblId=DT_3664N_1&conn_path=I3 (accessed on 05.07.2018)

KOSIS, Korean Statistical Information Service, 2017. Census for 2016 population and housing stock in South Korea. Available at http://kosis.kr/statHtml/statHtml.do?orgId=101&tblId=DT_1IN1602&conn_path=I2 (accessed on 05.07.2018)

KOSIS, Korean Statistical Information Service, 2018a. 2016 census for the number of apartment by floor area, Available at http://kosis.kr/statHtml/statHtml.do?orgId=116&tblId=DT_MLTM_688&conn_path=I3 (accessed on 05.07.2018)

KOSIS, Korean Statistical Information Service, 2018b. 2016 Regional census for the number of apartment building by building type and by top floor storey of apartment building. Available at http://kosis.kr/statHtml/statHtml.do?orgId=116&tblId=DT_MLTM_792&conn_path=I2 (accessed on 05.07.2018)

KOSIS, Korean Statistical Information Service, 2018c. Census for the regional number of apartment building by floor storey in 2016, Available at http://kosis.kr/statHtml/statHtml.do?orgId=116&tblId=DT_MLTM_722&conn_path=I2 (accessed on 05.07.2018)

Kovats, R.S. and Hajat, S., 2008. Heat stress and public health: a critical review. Annu. Rev. Public Health, 29, pp.41-55.

KPX, Korea Power Exchange, 2012, Report on home appliances penetration in 2011, Available at https://www.kpx.or.kr/www/selectBbsNttView.do?key=97&bbsNo=6&nttNo=5153 (accessed on 05.07.2018)

Kragh, J. and Wittchen, K.B., 2014. Development of two Danish building typologies for residential buildings. Energy and Buildings, 68, pp.79-86.

Kunkel, K.E., Changnon, S.A., Reinke, B.C. and Arritt, R.W., 1996. The July 1995 heat wave in the Midwest: A climatic perspective and critical weather factors. Bulletin of the American Meteorological Society, 77(7), pp.1507-1518.

Kwok, A.G. and Rajkovich, N.B., 2010. Addressing climate change in comfort standards. Building and Environment, 45(1), pp.18-22.

Lafrance, G. and Perron, D., 1994. Evolution of residential electricity demand by end-use in Quebec 1979-1989: a conditional demand analysis. Energy Studies Review, 6(2), pp.164-173.

Lai, H.K., Kendall, M., Ferrier, H., Lindup, I., Alm, S., Hänninen, O., Jantunen, M., Mathys, P., Colvile, R., Ashmore, M.R. and Cullinan, P., 2004. Personal exposures and microenvironment concentrations of PM2. 5, VOC, NO2 and CO in Oxford, UK. Atmospheric Environment, 38, pp.6399-6410.

Lane, K., Wheeler, K., Charles-Guzman, K., Ahmed, M., Blum, M., Gregory, K., Graber, N., Clark, N. and Matte, T., 2014. Extreme heat awareness and protective behaviors in New York City. Journal of urban health, 91(3), pp.403-414.

Lee, J.Y., Kim, E., Lee, W.S., Chae, Y. and Kim, H., 2018. Projection of Future Mortality Due to Temperature and Population Changes under Representative Concentration Pathways and

Shared Socioeconomic Pathways. International journal of environmental research and public health, 15(4), p.822-830.

Lee, K. and Lee, D., 2015. The Relationship Between Indoor and Outdoor Temperature in Two Types of Residence. Energy Procedia, 78, pp.2851-2856.

Lee, K., Baek, H.J. and Cho, C., 2014. The estimation of base temperature for heating and cooling degree-days for South Korea. Journal of applied meteorology and climatology, 53(2), pp.300-309.

Lee, K.H. and Levermore, G.J., 2010. Weather data for future climate change for South Korean building design: analysis for trends. Architectural Science Review, 53(2), pp.157-171.

Lee, S.H. and Baik, J.J., 2010. Statistical and dynamical characteristics of the urban heat island intensity in Seoul. Theoretical and Applied Climatology, 100(1-2), pp.227-237.

Li, D.H., Yang, L. and Lam, J.C., 2012. Impact of climate change on energy use in the built environment in different climate zones–a review. Energy, 42(1), pp.103-112.

Li, W., Zhou, Y., Cetin, K., Eom, J., Wang, Y., Chen, G. and Zhang, X., 2017. Modeling urban building energy use: A review of modeling approaches and procedures. Energy, 141, pp.2445-2457.

Lin, F.Y., Huang, K.T., Lin, T.P. and Hwang, R.L., 2019. Generating hourly local weather data with high spatially resolution and the applications in bioclimatic performance. Science of the Total Environment, 653, pp.1262-1271.

Loga, T., Stein, B. and Diefenbach, N., 2016. TABULA building typologies in 20 European countries—Making energy-related features of residential building stocks comparable. Energy and Buildings, 132, pp.4-12.

Lomas, K.J. and Porritt, S.M., 2017. Overheating in buildings: lessons from research. Building Research & Information, 45 (2017), pp. 1-18.

Lutzenhiser, L., 1992. A cultural model of household energy consumption. Energy, 17(1), pp.47-60.

Maller, C.J. and Strengers, Y., 2011. Housing, heat stress and health in a changing climate: promoting the adaptive capacity of vulnerable households, a suggested way forward. Health promotion international, 26(4), pp.492-498.

Mata, É., Kalagasidis, A.S. and Johnsson, F., 2014. Building-stock aggregation through archetype buildings: France, Germany, Spain and the UK. Building and Environment, 81, pp.270-282.

Mateus, N.M., Pinto, A. and da Graça, G.C., 2014. Validation of EnergyPlus thermal simulation of a double skin naturally and mechanically ventilated test cell. Energy and Buildings, 75, pp.511-522.

Mavrogianni, A., Taylor, J., Davies, M., Thoua, C. and Kolm-Murray, J., 2015. Urban social housing resilience to excess summer heat. Building Research & Information, 43(3), pp.316-333.

McMichael, A.J., Woodruff, R.E. and Hales, S., 2006. Climate change and human health: present and future risks. The Lancet, 367(9513), pp.859-869.

MDOP, Meteorological Data Open Portal. https://data.kma.go.kr/cmmn/main.do (accessed on 05.07.2018)

Meehl, G.A. and Tebaldi, C., 2004. More intense, more frequent, and longer lasting heat waves in the 21st century. Science, 305(5686), pp.994-997.

Met Office, UKCP09 Climate change projections, available at http://ukclimateprojections.metoffice.gov.uk/23189 (accessed on 24.08.2018)

Michelozzi, P., Bisanti, L., Russo, A., Cadum, E., DeMaria, M., D'Ovidio, M., Costa, G. and Perucci, C.A., 2005. The impact of the summer 2003 heat waves on mortality in four Italian cities. Euro surveill. 10(7), pp.161-65.

Mirchandani, H.G., McDonald, G., Hood, I.C. and Fonseca, C., 1996. Heat-related deaths in Philadelphia—1993. The American journal of forensic medicine and pathology, 17(2), pp.106-108.

MoLIT, Ministry of Land, Infrastructure and Transport in South Korea, 2009. Green Houses criteria and the Performance, Guideline for Evaluating Design and Performance.

MoLIT, Ministry of Land, Infrastructure and Transport in South Korea, 2016. Multi-family Housing Management Act. Available at http://www.law.go.kr/LSW/eng/engLsSc.do?menuId=1&query=MULTI-FAMILY+HOUSING+MANAGEMENT+ACT&x=0&y=0#liBgcolor1 (accessed on 05.07.2018)

MoLIT, Ministry of Land, Infrastructure and Transport in South Korea, 2017. Act on the certification of building energy efficiency rating and the certification criteria for zero-energy building. Available at http://www.law.go.kr/행정규칙/(국토교통부)건축물에너지효율등급인증및제로에너지건축물인증기준 (accessed on 05.07.2018)

MoLIT, Ministry of Land, Infrastructure and Transport in South Korea, 2018. Act on the energy-saving building design guideline. Available at

http://www.law.go.kr/행정규칙/건축물의에너지절약설계기준 (accessed on 05.07.2018)

Moonen, P., Defraeye, T., Dorer, V., Blocken, B. and Carmeliet, J., 2012. Urban Physics: Effect of the micro-climate on comfort, health and energy demand. Frontiers of Architectural Research, 1(3), pp.197-228.

Murphy, JM, Sexton, DM, Jenkins, GJ, Booth, BB, Brown, CC, Clark, RT, Collins, M, Harris, GR, Kendon, EJ, Betts, RA, Brown, SJ, Humphrey, KA, McCarthy, MP, McDonald, RE, Stephens, A, Wallace, C, Warren, R, Wilby, R and Wood, RA., 2009. UK Climate Projections Science Report: Climate Change projections. Working Paper. Met Office Hadley Centre, Exeter.

Nesbakken, R., 1999. Price sensitivity of residential energy consumption in Norway. Energy economics, 21(6), pp.493-515.

Ng, E., Chen, L., Wang, Y. and Yuan, C., 2012. A study on the cooling effects of greening in a high-density city: An experience from Hong Kong. Building and Environment, 47, pp.256-271.

Nicol, J.F. and Humphreys, M.A., 2002. Adaptive thermal comfort and sustainable thermal standards for buildings. Energy and buildings, 34(6), pp.563-572.

Nikolopoulou, M., 2011. Outdoor thermal comfort. Frontiers in Bioscience, S3, pp. 1552-1568.

O'Neill, M.S. and Ebi, K.L., 2009. Temperature extremes and health: impacts of climate variability and change in the United States. Journal of Occupational and Environmental Medicine, 51(1), pp.13-25.

Oke, T.R., 2004. Initial guidance to obtain representative meteorological observations at urban sites. IMO Rep. 81, WMO/TD-No. 1250, available at

http://citeseerx.ist.psu.edu/viewdoc/download?doi=10.1.1.694.2319&rep=rep1&type=pdf

Oke, T.R., 2006. Initial guidance to obtain representative meteorological observations at urban sites, IOM Rep. 81, World Meteorol. Org., Geneva.

Pallant, J., 2010. SPSS survival manual, 4th. England: McGraw-Hill Education.

Palmer, J. and Cooper, I., 2014. United Kingdom housing energy fact file 2013. Department of Energy & Climate Change, pp.33-40.

Parekh, A., 2005. Development of archetypes of building characteristics libraries for simplified energy use evaluation of houses. In Proceedings of the Ninth International Building Performance Simulation Association Conference (IBPSA), Montreal, Canada, pp 921-8.

Park, J., Choi, S., Yang, Y., Ha, J., Lee, S., Jang L., 2005. A Study on the Hillside Affordable Housing of Seoul in Late 1960s Through Early 1970s - Focusing on Jeongneung-Sky Apartment Housing and Si-Min Apartments. Journal of the Architectural Institute of Korea Planning and Design, 12, pp.47-54.

Park, K. and Kim, M., 2017. Energy Demand Reduction in the Residential Building Sector: A Case Study of Korea. Energies, 10(10), p.1506.

Parti, M. and Parti, C., 1980. The total and appliance-specific conditional demand for electricity in the household sector. The Bell Journal of Economics, pp.309-321.

Patz, J.A., Campbell-Lendrum, D., Holloway, T. and Foley, J.A., 2005. Impact of regional climate change on human health. Nature, 438(7066), pp.310-318

Pearson, E.S. and Hartley, H.O., 1958. Test for heterogeneity of variance among normally distributed observations. Biometrika tables for statisticians. Vol. I, pp.57-61.

Peeters, L., De Dear, R., Hensen, J. and D'haeseleer, W., 2009. Thermal comfort in residential buildings: Comfort values and scales for building energy simulation. Applied energy, 86(5), pp.772-780.

Perkins, S.E., Alexander, L.V. and Nairn, J.R., 2012. Increasing frequency, intensity and duration of observed global heatwaves and warm spells. Geophysical Research Letters, 39, L20714, doi:10.1029/2012GL053361.

Pittam, J., O'Sullivan, P.D. and O'Sullivan, G., 2014. Stock aggregation model and virtual archetype for large scale retrofit modelling of local authority housing in Ireland. Energy Procedia, 62, pp.704-713.

Portier, C.J., Thigpen, T.K., Carter, S.R., Dilworth, C.H., Grambsch, A.E., Gohlke, J., Hess, J., Howard, S.N., Luber, G., Lutz, J.T. and Maslak, T., 2017. A human health perspective on climate change: a report outlining the research needs on the human health effects of climate change. Environmental Health Perspectives/National Institute of Environmental Health Sciences.

Raffio, G., Isambert, O., Mertz, G., Schreier, C. and Kissock, K., 2007, January. Targeting residential energy assistance. In: Proceedings of energy sustainability conference, pp. 489-495.

Raftery, P., Keane, M. and Costa, A., 2011b. Calibrating whole building energy models: Detailed case study using hourly measured data. Energy and buildings, 43(12), pp.3666-3679.

Raftery, P., Keane, M. and O'Donnell, J., 2011a. Calibrating whole building energy models: An evidence-based methodology. Energy and Buildings, 43(9), pp.2356-2364.

Reinhart, C.F. and Davila, C.C., 2016. Urban building energy modeling–A review of a nascent field. Building and Environment, 97, pp.196-202.

Remmen, P., Lauster, M., Mans, M., Fuchs, M., Osterhage, T. and Müller, D., 2018. TEASER: an open tool for urban energy modelling of building stocks. Journal of Building Performance Simulation, 11(1), pp.84-98.

Rizwan, A.M., Dennis, L.Y. and Chunho, L.I.U., 2008. A review on the generation, determination and mitigation of Urban Heat Island. Journal of Environmental Sciences, 20(1), pp.120-128.

Robine, J.M., Cheung, S.L., Le Roy, S., Van Oyen, H. and Herrmann, F.R., 2007. Report on excess mortality in Europe during summer 2003. EU Community Action Programme for Public Health, Grant Agreement, 2005114, p.28.

Roh, S., Tae, S., Suk, S.J. and Ford, G., 2017. Evaluating the embodied environmental impacts of major building tasks and materials of apartment buildings in Korea. Renewable and Sustainable Energy Reviews, 73, pp.135-144.

Salata, F., Golasi, I., Petitti, D., de Lieto Vollaro, E., Coppi, M. and de Lieto Vollaro, A., 2017. Relating microclimate, human thermal comfort and health during heat waves: An analysis of heat island mitigation strategies through a case study in an urban outdoor environment. Sustainable cities and society, 30, pp.79-96.

Salvati, A., Roura, H.C. and Cecere, C., 2017. Assessing the urban heat island and its energy impact on residential buildings in Mediterranean climate: Barcelona case study. Energy and Buildings, 146, pp.38-54.

Sandberg, N.H., Sartori, I., Vestrum, M.I. and Brattebø, H., 2017. Using a segmented dynamic dwelling stock model for scenario analysis of future energy demand: The dwelling stock of Norway 2016–2050. Energy and Buildings, 146, pp.220-232.

Santamouris, M., Papanikolaou, N., Livada, I., Koronakis, I., Georgakis, C., Argiriou, A. and Assimakopoulos, D.N., 2001. On the impact of urban climate on the energy consumption of buildings. Solar energy, 70(3), pp.201-216.

Santin, O.G., Itard, L. and Visscher, H., 2009. The effect of occupancy and building characteristics on energy use for space and water heating in Dutch residential stock. Energy and buildings, 41(11), pp.1223-1232.

Schuler, A., Weber, C. and Fahl, U., 2000. Energy consumption for space heating of West-German households: empirical evidence, scenario projections and policy implications. Energy policy, 28(12), pp.877-894.

Schwartz, J., 2005. Who is sensitive to extremes of temperature? A case-only analysis. Epidemiology, 16, pp.67-72.

Schweizer, C., Edwards, R.D., Bayer-Oglesby, L., Gauderman, W.J., Ilacqua, V., Jantunen, M.J., Lai, H.K., Nieuwenhuijsen, M. and Künzli, N., 2007. Indoor time–microenvironment–activity patterns in seven regions of Europe. Journal of Exposure Science and Environmental Epidemiology, 17(2), p.170-181.

SERG, Sustainable Energy Research Group University of Southampton, CCWeatherGen: Climate Change Weather File Generator for the UK, available at http://www.energy.soton.ac.uk/ccweathergen/ (accessed on 26.08.2018)

SERG, Sustainable Energy Research Group University of Southampton, Climate Change World Weather File Generator for World-Wide Weather Data – CCWorldWeatherGen, available at http://www.energy.soton.ac.uk/ccworldweathergen/ (accessed on 26.08.2018)

Shin, S., Tae, S., Woo, J. and Roh, S., 2011. The development of environmental load evaluation system of a standard Korean apartment house. Renewable and Sustainable Energy Reviews, 15(2), pp.1239-1249.

Son, J.Y., Lee, J.T., Anderson, G.B. and Bell, M.L., 2012. The impact of heat waves on mortality in seven major cities in Korea. Environmental health perspectives, 120(4), p.566.

Sousa, G., Jones, B., Mirzaei, P. and Robinson, D., 2017. A review and critique of UK housing stock energy models, modelling approaches and data sources, Energy and Buildings, 151, pp.66-80.

Stafoggia, M., Forastiere, F., Agostini, D., Biggeri, A., Bisanti, L., Cadum, E., Caranci, N., de'Donato, F., De Lisio, S., De Maria, M. and Michelozzi, P., 2006. Vulnerability to heat-related mortality: a multicity, population-based, case-crossover analysis. Epidemiology, 17, pp.315-323.

Stewart, I.D, 2011. Redefining the urban heat island. Ph.D. dissertation, Department of Geography, University of British Columbia, Available at https://open.library.ubc.ca/cIRcle/collections/ubctheses/24/items/1.0072360

Stewart, I.D. and Oke, T.R., 2012. Local climate zones for urban temperature studies. Bulletin of the American Meteorological Society, 93(12), pp.1879-1900.

Stoops, J.L., 2004. A possible connection between thermal comfort and health, paper LBNL 55134. Lawrence Berkeley National Laboratory. University of California.

Suh, D. and Chang, S., 2012. An energy and water resource demand estimation model for multi-family housing complexes in Korea. Energies, 5(11), pp.4497-4516.

Summerfield, A.J., Lowe, R.J. and Oreszczyn, T., 2010. Two models for benchmarking UK domestic delivered energy. Building Research & Information, 38(1), pp.12-24.

Swan, L.G. and Ugursal, V.I., 2009. Modeling of end-use energy consumption in the residential sector: A review of modeling techniques. Renewable and sustainable energy reviews, 13(8), pp.1819-1835.

Symonds, P., Taylor, J., Mavrogianni, A., Davies, M., Shrubsole, C., Hamilton, I. and Chalabi, Z., 2017. Overheating in English dwellings: comparing modelled and monitored large-scale datasets. Building Research & Information, 45(1-2), pp.195-208.

Tabachnick, B.G. and Fidell, L.S., 2007. Using multivariate statistics, 5th. Needham Height, MA: Allyn & Bacon.

Tabares-Velasco, P.C., Christensen, C. and Bianchi, M., 2012. Verification and validation of EnergyPlus phase change material model for opaque wall assemblies. Building and Environment, 54, pp.186-196.

Tae, S., Shin, S., Woo, J. and Roh, S., 2011. The development of apartment house life cycle CO2 simple assessment system using standard apartment houses of South Korea. Renewable and Sustainable Energy Reviews, 15(3), pp.1454-1467.

Tham, Y., Muneer, T., Levermore, G.J. and Chow, D., 2011. An examination of UKCIP02 and UKCP09 solar radiation data sets for the UK climate related to their use in building design. Building Services Engineering Research and Technology, 32(3), pp.207-228.

Thomas, N.D. and Soliman, H., 2002. Preventable tragedies: Heat disaster and the elderly. Journal of Gerontological Social Work, 38(4), pp.53-66.

Tian, W. and de Wilde, P., 2011. Thermal building simulation using the UKCP09 probabilistic climate projections. Journal of Building Performance Simulation, 4(2), pp.105-124.

Tomlinson, C.J., Chapman, L., Thornes, J.E. and Baker, C.J., 2012. Derivation of Birmingham's summer surface urban heat island from MODIS satellite images. International Journal of Climatology, 32(2), pp.214-224.

Torfs, R., Brouwere, K.D., Spruyt, M., Goelen, E., Nickmilder, M. and Bernard, A., 2008. Exposure and risk assessment of air fresheners. VITO, Document No 2008/IMS/R/222; 2008.

Touchie, M.F., Binkley, C. and Pressnail, K.D., 2013. Correlating energy consumption with multi-unit residential building characteristics in the city of Toronto. Energy and Buildings, 66, pp.648-656.

Tweed, C., Dixon, D., Hinton, E. and Bickerstaff, K., 2014. Thermal comfort practices in the home and their impact on energy consumption. Architectural Engineering and Design Management, 10(1-2), pp.1-24.

University of Exeter Centre for Energy and Environment, PROMETHEUS project, available at http://emps.exeter.ac.uk/engineering/research/cee/research/prometheus/ (accessed on 24.08.2018)

Vandentorren, S., Bretin, P., Zeghnoun, A., Mandereau-Bruno, L., Croisier, A., Cochet, C., Ribéron, J., Siberan, I., Declercq, B. and Ledrans, M., 2006. August 2003 heat wave in France: risk factors for death of elderly people living at home. The European Journal of Public Health, 16(6), pp.583-591.

Vardoulakis, S., 2009. Human exposure: indoor and outdoor. In: Air Quality in Urban Environments, 28, p.85-107.

Vardoulakis, S., Dear, K., Hajat, S., Heaviside, C., Eggen, B. and McMichael, A.J., 2014. Comparative assessment of the effects of climate change on heat-and cold-related mortality in the United Kingdom and Australia. Environmental health perspectives, 122, pp.1285-1292.

Vardoulakis, S., Dimitroulopoulou, C., Thornes, J., Lai, K.M., Taylor, J., Myers, I., Heaviside, C., Mavrogianni, A., Shrubsole, C., Chalabi, Z., Davies, M., and Wilkinson, P., 2015. Impact of climate change on the domestic indoor environment and associated health risks in the UK. Environment international, 85, pp.299-313.

Vellei, M., Ramallo-González, A.P., Coley, D., Lee, J., Gabe-Thomas, E., Lovett, T. and Natarajan, S., 2017. Overheating in vulnerable and non-vulnerable households. Building Research & Information, 45(1-2), pp.102-118.

Vimmr, T., Loga, T., Diefenbach, N., Stein, B. and Bachová, L., 2013. Tabula—residential building typologies in 12 European countries—good practice example from the Czech Republic. Central Europe towards sustainable building.

Watkins, R., Palmer, J., Kolokotroni, M. and Littlefair, P., 2002. The London Heat Island--surface and air temperature measurements in a park and street gorges. ASHRAE Transactions, 108, p.419-27.

Whitman, S., Good, G., Donoghue, E.R., Benbow, N., Shou, W. and Mou, S., 1997. Mortality in Chicago attributed to the July 1995 heat wave. American Journal of public health, 87(9), pp.1515-1518.

Yang, X., Zhao, L., Bruse, M. and Meng, Q., 2012. An integrated simulation method for building energy performance assessment in urban environments. Energy and buildings, 54, pp.243-251.

Yang, Z. and Becerik-Gerber, B., 2014. The coupled effects of personalized occupancy profile based HVAC schedules and room reassignment on building energy use. Energy and Buildings, 78, pp.113-122.

Yi, C.Y. and Peng, C., 2014. Microclimate change outdoor and indoor coupled simulation for passive building adaptation design. Procedia Computer Science, 32, pp.691-698.

Yi, C.Y. and Peng, C., 2017. Correlating cooling energy use with urban microclimate data for projecting future peak cooling energy demands: Residential neighbourhoods in Seoul. Sustainable Cities and Society, 35, pp.645-659.

Yu, Z., Fung, B.C., Haghighat, F., Yoshino, H. and Morofsky, E., 2011. A systematic procedure to study the influence of occupant behavior on building energy consumption. Energy and Buildings, 43(6), pp.1409-1417.

Yun, G.Y. and Steemers, K., 2011. Behavioural, physical and socio-economic factors in household cooling energy consumption. Applied Energy, 88(6), pp.2191-2200.

Zhang, Q., 2004. Residential energy consumption in China and its comparison with Japan, Canada, and USA. Energy and buildings, 36(12), pp.1217-1225.

# Appendix

## Appendix A

- **Journal paper in peer-reviewed journals**

Yi, C.Y. and Peng, C., 2019. An archetype-in-neighbourhood framework for modelling cooling energy demand of a city's housing stock. Energy and Buildings, 196, pp.30-45.

Yi, C.Y. and Peng, C., 2017. Correlating cooling energy use with urban microclimate data for projecting future peak cooling energy demands: Residential neighbourhoods in Seoul. Sustainable Cities and Society, 35, pp.645-659.

- **Conference papers**

Yi, C.Y. and Peng, C., 2014. Microclimate change outdoor and indoor coupled simulation for passive building adaptation design. Procedia Computer Science, 32, pp.691-698.

Yi, C.Y. and Peng, C., 2015. Correlating Urban Microclimate Modelling with Energy Use Data Analysis to Inform Site-Specific Climate Change Adaptation Design. In Proc. of Architecture and Resilience on the Human, Scale Cross-Disciplinary Conference, 10-12 Sep 2015. Sheffield, UK.

## Appendix B

- **Statistical terms and tools applied in this thesis**

**Parametric statistics**: one branch of statistical techniques which makes assumptions that the underlying distribution of scores in the population from which the sample has been drawn is normal. They include *T*-test, Pearson-correlation and Analysis of Variance (ANOVA).

**Correlation analysis**: is used to describe the strength and direction of the linear relationship between two variables. Especially, Pearson correlation coefficient (r) is designed for internal level (continuous) variables. It can also be used between one continuous variable and one dichotomous variable.

**Analysis of Variance (ANOVA)**: is used in comparing the mean scores of more than two groups. One-way analysis of variance analysis involves one independent variable which has a number of different levels, which correspond to the different groups or conditions.

**Assumption of Normality**: in parametric statistics, scores on each variable should be normally distributed. It can be checked by inspecting the histograms of scores on each variable.

**Assumption of Linearity**: in parametric statistics, the relationship between the two variables should be linear. This represents that in a scatterplot of scores, a straight line (roughly) appears.

**Assumption of Homoscedasticity**: in parametric statistics, the variability in scores for X should be similar at all values of variable Y. It also can be check by the scatter plot of scores.

**Cronbach' coefficient alpha**: provides an indication of the average correlation among all of the items that make up the scale. Values ranges from 0 to 1, with higher values indicating high internal consistency. Internal consistency is the degree to which the items that make up the scale are all measuring the same underlying attribute.

**K-fold cross validation:** is one of model validation techniques. The total data "set" is split into K (number of) sets. One set is defined as a testing set while the rest of sets are defined as a training sets. The training sets are used for model fitting and a testing set is used for model evaluation through comparing the test set to results derived from the model.

**Leave-on-out cross validation (LOOCV)**: is similar to K-fold cross validation but of the total datasets, only one data remains as a test data.